BIOPHYSICAL CHARACTERIZATION OF BRANCHED AMPHIPHILIC PEPTIDE CAPSULES AND THEIR POTENTIAL APPLICATIONS IN RADIOTHERAPY

by

PINAKIN RAMCHANDRA SUKTHANKAR

M.Sc., University of Mumbai, India 2006

AN ABSTRACT OF A DISSERTATION

submitted in partial fulfillment of the requirements for the degree

DOCTOR OF PHILOSOPHY

Graduate Biochemistry and Molecular Biophysics Group
College of Arts and Sciences

KANSAS STATE UNIVERSITY
Manhattan, Kansas

2014

Abstract

Branched Amphiphilic Peptide Capsules (BAPCs) are peptide nano-spheres comprised of equimolar proportions of two branched peptide sequences bis(FLIVI)-K-KKKK and bis(FLIVIGSII)-K-KKKK that self-assemble in water to form bilayer delimited poly-cationic capsules capable of trapping solutes. We examined the lipid-like properties of this system including assembly, fusion, solute encapsulation, and resizing by membrane extrusion as well as their capability to be maintained at a specific size by storage at 4˚C. These studies along with earlier work from the lab (Gudlur et al. (2012) PLOS ONE **7**(9): e45374) demonstrated that the capsules, while sharing many properties with lipid vesicles, were much more robust. We next investigated the stability, size limitations of encapsulation, cellular localization, retention and, bio-distribution of the BAPCs. We demonstrated that the BAPCs are readily taken up by epithelial cells in culture, escape or evade the endocytotic pathway, and accumulate in the peri-nuclear region where they persist without any apparent degradation. The stability and persistence of the capsules suggested they might be useful in delivering radionuclides. The BAPCs encapsulated alpha particle emitting radionuclides without any apparent leakage, were taken up by cells and were retained for extended periods of time. Their potential in this clinical application is being currently pursued. Lastly we studied the temperature dependence of capsule formation by examining the biophysical characteristics of temperature induced conformational changes in BAPCs and examined the structural parameters within the sequences that contribute to their remarkable stability. A region in the nine-residue sequence was identified as the critical element in this process. The ability to prepare stable uniform nano-scale capsules of desired sizes makes BAPCs potentially attractive as delivery vehicles for various solutes/drugs.

BIOPHYSICAL CHARACTERIZATION OF BRANCHED AMPHIPHILIC PEPTIDE CAPSULES AND THEIR POTENTIAL APPLICATIONS IN RADIOTHERAPY

by

PINAKIN RAMCHANDRA SUKTHANKAR

M.Sc., University of Mumbai, India 2006

A DISSERTATION

submitted in partial fulfillment of the requirements for the degree

DOCTOR OF PHILOSOPHY

Graduate Biochemistry and Molecular Biophysics Group
College of Arts and Sciences

KANSAS STATE UNIVERSITY
Manhattan, Kansas

2014

Approved by:

Major Professor
Dr. John M. Tomich

Copyright

Abstract

Branched Amphiphilic Peptide Capsules (BAPCs) are peptide nano-spheres comprised of equimolar proportions of two branched peptide sequences bis(FLIVI)-K-KKKK and bis(FLIVIGSII)-K-KKKK that self-assemble in water to form bilayer delimited poly-cationic capsules capable of trapping solutes. We examined the lipid-like properties of this system including assembly, fusion, solute encapsulation, and resizing by membrane extrusion as well as their capability to be maintained at a specific size by storage at 4˚C. These studies along with earlier work from the lab (Gudlur et al. (2012) PLOS ONE **7**(9): e45374) demonstrated that the capsules, while sharing many properties with lipid vesicles, were much more robust. We next investigated the stability, size limitations of encapsulation, cellular localization, retention and, bio-distribution of the BAPCs. We demonstrated that the BAPCs are readily taken up by epithelial cells in culture, escape or evade the endocytotic pathway, and accumulate in the peri-nuclear region where they persist without any apparent degradation. The stability and persistence of the capsules suggested they might be useful in delivering radionuclides. The BAPCs encapsulated alpha particle emitting radionuclides without any apparent leakage, were taken up by cells and were retained for extended periods of time. Their potential in this clinical application is being currently pursued. Lastly we studied the temperature dependence of capsule formation by examining the biophysical characteristics of temperature induced conformational changes in BAPCs and examined the structural parameters within the sequences that contribute to their remarkable stability. A region in the nine-residue sequence was identified as the critical element in this process. The ability to prepare stable uniform nano-scale capsules of desired sizes makes BAPCs potentially attractive as delivery vehicles for various solutes/drugs.

Table of Contents

List of Figures

List of Tables

Acknowledgements

I would like to start off by acknowledging my advisor Prof. John Tomich for his patience, support and guidance through all these years. He has been a fantastic mentor, who has taught me many valuable lessons, fuelled my enthusiasm for science, encouraged me to think and act independently and provided me with the creative freedom to pursue my ideas. Without him, none of this would have been possible. I would like to thank my committee members Dr. Stefan Bossmann, Dr. Michael Kanost and Dr, Lawrence Davis for their invaluable insight, their suggestions, and for their constructive criticism of my work. I would also like to thank Dr. Ronette Gehring, my external chairperson, for dedicating her time to aid me in my academic pursuit.

A special thanks to Dr. Takeo Iwamoto for training me in peptide chemistry through my formative years in the lab - a skill that I have found rather useful. I would like to thank Dr. Jianhan Chen, Dr. Ekaterina Dadachova, Dr. Robert Hanzlik and Dr. David Moore along with others who I have had the pleasure of collaborating with over the years. I would like to acknowledge Dr. Yasuaki Hiromasa, Dr. Sushanth Gudlur, Adriana Avila, Benjamin Katz, Jammie Laymann, my remarkable undergraduate Susan Whitaker, and all other members of the Tomich lab - past and present, that have made my workplace nothing less than delightful. I thank my family and friends for the encouragement, affection and support that they have provided me during my time here as a doctoral student; and more importantly for keeping things interesting.

Finally, I would like to thank my parents Mr. Ramchandra Sukthankar and Mrs. Vaidehee Sukthankar for all this and forevermore.

Dedication

I dedicate my work to my Aai (Mrs. Tara P. Rege) and Nana (Hon. Mr. Prabhakar A. Rege).

Preface

Wenn im Unendlichen dasselbe

Sich wiederholend ewig fließt,

Das tausendfältige Gewölbe

Sich kräftig in einander schließt;

Strömt Lebenslust aus allen Dingen,

Dem kleinsten wie dem größten Stern,

Und alles Drängen, alles Ringen

Ist ewige Ruh' in Gott dem Herrn.

- Johann Wolfgang von Goethe (1749 - 1832)

Chapter 1 - Introduction

The prefix ‘nano’ in nanotechnology is derived from the Greek word ‘νάνος’, meaning dwarf. One nanometer (nm) is equal to a billionth of a meter; the width of six carbon atoms or ten molecules of water. In 1959, Richard Feynman delivered a talk at the American Physical Society entitled ‘There's Plenty of Room at the Bottom’, in which he first laid out the conceptual underpinnings of nanotechnology as he explored the possibility of directly manipulating matter on the atomic and molecular scale.[1] Nanotechnology today, is a multi-disciplinary field pertaining to the development, design, characterization and applications of materials with a functional organization on the nanometer scale.[2,3] Perhaps a stricter definition comes from the National Nanotechnology Initiative (NNI), which refers to nanotechnology as science, engineering, and technology conducted at the nanoscale, which is roughly in the size range of 1-100 nm. At this quantum-realm scale, the quantum mechanical effects gain significance and the macroscopic properties of the material become secondary to that of the individual and interacting groups of molecules.[4] More commonly, nanotechnology now refers to structures that are engineered from individual components by top-down or bottom-up modalities that can be several hundred nanometers in size.[5] While the earliest developments in nanotechnology were driven by the electronics industry in a bid to develop micro-circuitry, [6] today nanotechnology offers opportunities and insights in diverse areas of investigation such as engineering, physics, chemistry, biology and medicine. The enormous scientific and commercial importance of nanotechnology is reflected in the National Nanotechnology Initiative, a multiagency umbrella program established by President Clinton in 2000 in order to build, characterize and comprehend

nanoscale devices. The program has been budgeted to spend over $1.7 billion in the year 2014 in pursuance of its objectives.[7,8,9]

1.1 Nanotechnology in Medicine

While tremendous progress has been made in understanding fundamental biological processes over the last quarter century translation of these findings into new advanced therapies has lagged. Limitations in delivering therapeutic moieties to selective targets with minimal off-target damage have largely been held responsible for the discrepancy. [10,11] A novel molecular pharmacological agent with potential potent biological activity but limited aqueous solubility or a short circulating half-life *in vivo* is likely to face substantive physiological and commercial barriers. These delivery impediments will limit or reduce activity and disfavor potential pharmaceutically interesting compounds from entering clinical drug trials.[12] The goal of pharmaceutical research is to deliver a drug at the appropriate dosage to a target cell or tissue in a safe and reproducible manner.[3,13] Conventional modes of drug administration as pills, eye drops, intravenous solutions, ointments, inhalers etc., fall short of meeting these expectations in many ways. The oral route for example is one of the most commonly employed and preferred modes for drug administration due to its minimally-invasive nature. However the adequate delivery of peptide and protein drug candidates fuelled by the recent advances in recombinant biotechnology,[14] have not been attained via this route.[15, 16] This is the consequence of numerous factors including: the acid environment of the human stomach, proteolytic processing and the first pass effect of the liver and intestinal uptake resistance. All of these factors reduce, alter and block absorption of almost all macromolecules even before they enter systemic circulation.[17] The vast majority of experimental therapeutics are known to have poor biopharmaceutical and pharmacokinetic properties.[18] Nano-vectors have been shown to improve the pharmacological characteristics of these drug moieties. The utilization of nanotechnology for drug delivery has

been employed to enhance the delivery of poorly soluble drugs, facilitate drug targeting in a cell/tissue-specific manner and enabled the co-delivery of two or more drugs as well the intracellular delivery of larger macromolecular drugs. By enhancing the efficacy of these drugs, new candidate drugs are advancing in clinical trials with improved safety and effectivness.[12] The application of nanotechnology to drug delivery is expected to alter the landscape of pharmaceutical and biotechnology industries in the foreseeable future.[10,19,20,21,22] As of 2013, almost 250 nanotechnology based medicines had been approved or were in various stages of clinical investigation.[23]

Despite these advancements in nano-medicine; several challenges remain – 1) overcoming physicochemical and biological hurdles such as low stability, low permeability, short half-life, enzymatic susceptibility, targeting and 2) immunogenicity.[14] Although a majority of these nano-therapeutic products have improved the pharmaceutical efficacy of clinically approved drugs; nanotechnology as a whole has not yet generated entirely new therapies that would not have otherwise existed. [5] This new line of investigation portends well for future advances in nanotechnology research.

1.2 The role of nanotechnology in drug delivery

Nanomedicine can be defined as the construction, repair, monitoring and control of human biological systems at the molecular level using engineered delivery systems at the nanoscale level comprising of conjugated, adsorbed, encapsulated or dispersed drugs and imaging agents.[2,9,24,25, 26] Drug delivery using nanotechnology is a very broad and expanding area of investigation with rapidly emerging delivery modalities. This literature review will concentrate on selected prominent drug delivery systems that can be systemically administered via parenteral routes.

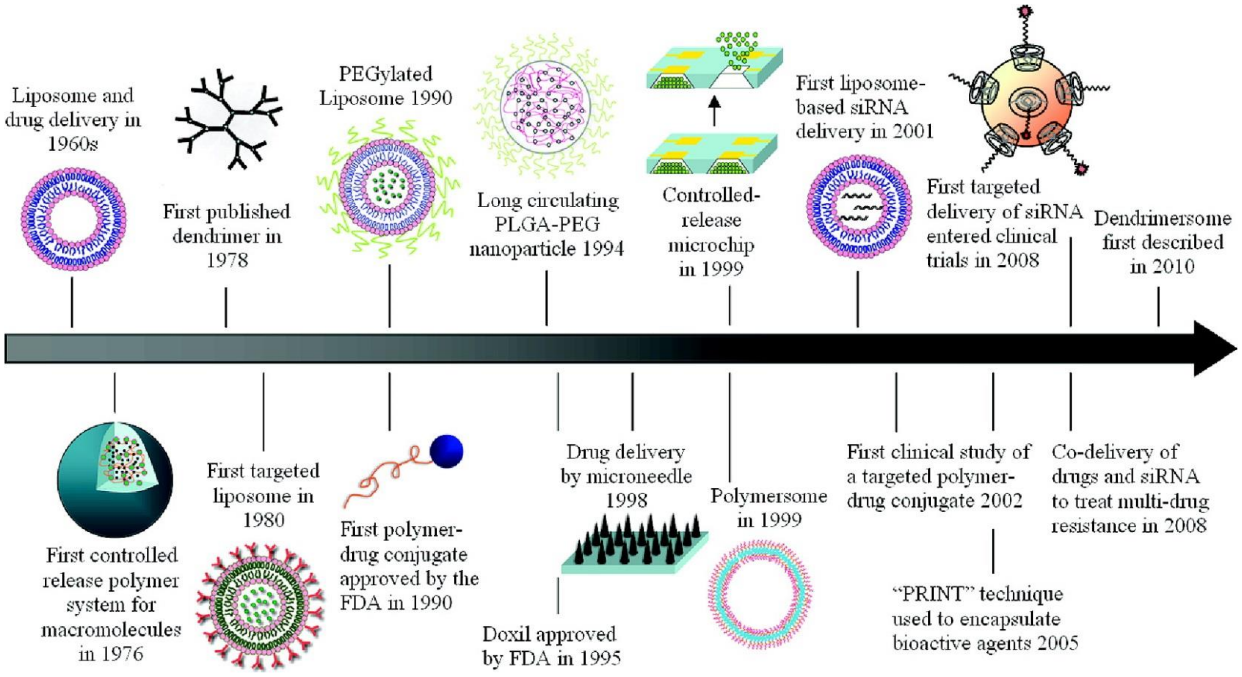

Figure 1.1. Timeline of Nanotechnology-based drug delivery.

Reprinted with permission from (Shi, J., Votruba, A.R., Farokhzad, O.C. and Langer, R. (2010) Nanotechnology in drug delivery and tissue engineering: from discovery to applications. Nano Lett. United States 10, 3223-3230). Copyright (2010) American Chemical Society

The competence of a nano-carrier is a function of its capability to safely, selectively and reliably deliver a therapeutic at the required dosage at the target site in the appropriate time

frame.[3,13,27,28] A variety of nano-materials - both organic and inorganic - have been employed for the purposes of delivery vehicles to develop new and effective therapeutic modalities. Nano-carriers in general, possess several desirable attributes. When delivered via nano-carriers; the volumes of systemic drug distribution are reduced;[29] the pharmacokinetics of biodistribution are enhanced and the ability to specifically target tissues and organs is enabled, resulting in improved therapeutic efficiency.[30,31,32,33] The preferential delivery of a drug to its target sites, along with the particle's ability to release drugs in a sustained or stimuli triggered manner will lead to reduced off-target effects and decreased toxicity. Utilization of nano-carriers also has the added advantage of improving the solubility of hydrophobic drugs in water; thus enhancing their delivery through parenteral administration. Nano-carrier based delivery systems have also been shown to improve the half-lives of a wide variety of hydrophobic moieties and peptide drugs.[34,35,36] Moreover, nanotechnology based delivery vehicles composed of biocompatible molecules[37,38,39,40] are projected as safer alternatives to existing vehicles that have been known to cause peripheral neuropathy and hypersensitivity.[41,42]

There are three fundamental factors that go into the development of a competent nano-targeting system, viz - characteristics of the diseased state, choice of therapeutics and the nature of the delivery vehicle.[5] The choice of the therapeutic and the nature of its action needs to be carefully considered during the selection of a delivery platform. The drug's site and mechanism of action define what carrier system will achieve optimal delivery. For example; drugs that require intracellular sites of action require intracellular delivery for bioactivity and therefore necessitate a delivery vehicle that enables homogenous tissue penetration.[5] Fundamental research into the nature of diseased state biomarkers and associated ligands, play vital roles in the design of functionalized delivery vehicles. Even in cases where targeting is not employed, an

understanding into the characteristics of the diseased site, tissue accumulation and cellular uptake can help us engineer more efficient non-specific drug delivery systems by modulating the biophysical properties of nano-carriers.[43,44]

1.3 The ideal nano-delivery system

The search for 'ideal nano-delivery systems' involve numerous design elements. The large repertoire of available nano-carriers, apart the ones that are in development, present nano-systems with a variety of structural, functional and physiochemical characteristics that translate into case specific advantages and/or limitations.

The selection of a nano-carrier is contingent on the pathology of the diseased state and the limitations imposed thereby; and while it would be difficult to absolutely define the ideal nanosystems, there are certain parameters generally sought out for the successful development and manufacturing of drug delivery vehicles for the purposes of targeted delivery. These include (i) biocompatibility of constituent material(s); (ii) simple and robust assembly processes; (iii) functionalization / pre-functionalization capability; (iv) intracellular stability and biodegradability; (v) long circulating half-life; (vi) suitable size, charge density, surface hydrophilicity and flexibility; and (vii) negligible immunogenicity.

It has been indicated that the complexity involved in nanoparticle fabrication and functionalization causes batch to batch variations leading to quality and purity concerns;[12] and that the development of development of targeted nano-carriers via a single step synthesis mediated by the self-assembly of pre-functionalized biomaterials would serve to alleviate these concerns by simplifying the optimization and the scalable manufacture of these systems.[21,45,46,47,48]

1.4 Targeted drug delivery

Generally speaking, increasing target selectivity[49] and improving a drug's ability to overcome biological barriers thereby increasing the per dose efficacy of a therapeutic are typical goals of the medicinal chemist [20, 50].

1.4.1 Passive Targeting

Diseased tissues tend to exhibit numerous alterations in their physiology as compared to healthy tissues. Passive targeting seeks to take advantage of the differences between normal and diseased tissues to effect site specific targeted drug delivery.[3] Passive drug targeting proceeds via the extravasation of the nanoparticle at the target site by exploiting the distinct pathophysiological features of tumorous and inflamed tissues which exhibit leaky vasculature.[13] Needless to say, this mode of drug targeting is widely employed clinically in cancer therapy. The leakiness of tumor vasculature is a consequence of angiogenesis, and the presence of permeability enhancing cytokines and vasoactive factors.[51] A majority of tumors show a vascular pore cut-off sizes of 380-780 nm as opposed to 2-4 nm for normal vasculature.[29,52,53,54] Tumor angiogenesis is characterized by undefined, branching in blood vessels with irregular diameters as well as with other vascular structures viz venules, arterioles and capillaries. This increased vascular permeability coupled with an impaired lymphatic system in tumors enhances permeability and the retention (EPR) effect of the nano-carriers in tumorous and inflamed tissues.[55,56]

Nano-carrier systems also have another distinct advantage. Their larger size compared to free drug molecules results in accumulation at higher concentrations in the target tissues; and their tendency to localize specifically in the Reticulo-Endothelial System (RES) makes them particularly well suited for passive targeting of macrophages in the spleen and liver thus enabling passive targeting as a modality for treating intracellular infections. [57] The long circulating times needed for the successful administration of passively targeted drugs via nano-carriers are greatly inhibited due to opsonization by the mononuclear phagocytic system. To this end, hydrophilic polymers such as polyethylene glycol (PEG) have been successfully utilized as surface modifying agents, to generate chemically inert, low immunogenic and low antigenic nano-carriers,. Also derivatization of their free hydroxyl groups on the polymer backbone offers sites for the addition of other adducts.[58] 'Stealth' liposomes comprised of distearoyl phosphatidylethanolamine (DSPE) or dipalmitoyl phosphatidylethanolamine grafted with 3-7% methoxy-PEG-2000 showed circulation half-lives of up to 45 h in humans[59,60,61] as opposed to the 2 h half-lives seen with their non-PEGylated variants.[62]

The tight segregation of the blood from the brain by the blood-brain barrier membrane[63] greatly diminishes the therapeutic potential of numerous drugs designed to treat neurological disorders.[64] Drug loading into nanoparticles leads to greater selectivity in targeting of biologically active compounds by modifying cell and tissue distribution, thus enhancing the efficacy and ameliorating the toxicity of the drug. [65,66,67,68] Moreover, the blood-brain barrier has been shown to exhibit increased permeability in instances of ischemic hypoxia induced by stroke; and during the course of HIV-induced dementia, stroke, septic encephalopathy, multiple sclerosis and Alzheimer's disease.[69,70,71,72] This permeability change enables improved uptake of nanotechnology mediated drug delivery to the brain and central nervous system.

1.4.2 Active Targeting

The majority of the two dozen or so nano-materials clinically approved by the Food and Drug Administration (as of 2010) were derivatives of first generation nanosystems such as liposomes and polymersomes.[73] These nanosystems provide numerous advantages such as enhanced drug activity, improved solubility of hydrophobic drugs, longer half-lives, reduced immunogenicity, reduced peripheral drug toxicity, sustained and stimulated drug release etc., [12] in comparison to conventional modes of drug delivery. However, the ability to specifically target cells rather than tissues in localized diseases and to facilitate drug uptake via receptor mediated endocytosis and other associated modalities was found to be lacking in these systems. It is believed that 'Active Targeting' facilitated by the modification and/or conjugation of nanoparticles with ligands has the potential to bridge this gap.[74]

While the accumulation of nanoparticles in tumors is largely determined by the physiochemical characteristics of the nanoparticles, the addition of ligands can improve retention and uptake via endocytotic mechanisms.[74;75] Higher intracellular drug concentrations facilitated by this modality resulted in improved therapeutic activity. [76] Cancerous tissue - apart from having altered vasculatures - also overexpresses certain receptors and epitopes such as transferrin, FOLR, TfR, $\alpha_V\beta_3$, MUC1, BCL-2, GNRHR, VPAC, PACAP, VEGFR2, CEA etc. that could be exploited as targets.[77,78,79,80,81,82,83,84,85,86,87,88,89,90,91] Active targeting of nanodrugs is especially relevant for bioactive molecules that require intracellular delivery for optimal activity.[74] Active targeting has been considered in resistant cancer cells,[92] and it is speculated that long-circulating targeted nanodrugs might be able to locate and kill migrating metastatic cancer cells.[12] Active targeting is used in therapies where cellular uptake of a drug would benefit from facilitated processes that can access active sites on or in cell.[93] This is important in immune

and endothelial cell targeting for cardiovascular disorders, where localization is directed by ligand-receptor interactions rather than EPR effects.[5] Moreover, active ligand-mediated targeting has been found to be valuable in facilitating transcytosis of drugs across endothelial barriers.[94]

Ligands can be coupled to nano-carriers either covalently or non-covalently. Covalent coupling methodologies employ reactive sites on both the carrier and ligand. Commonly employed chemistries include disulfide bond formation, reactions between-- primary amines and carboxylic acids, maleimides and thiols, primary amines and free aldehydes and aldehydes and hydrazide.[92,127] The physical associations involved in non-covalent bonding (hydrophobic or electrostatic) eliminates the need for harsher chemistries and reagents at the expense of random ligand orientations, weak binding leading to loss of the ligand and poor control of the reaction leading to batch to batch variations in degrees of complexation.

1.5 Classification of Nanoscale systems for drug delivery

The classification of nano-carriers is a difficult exercise owing to the wide spectrum of available nano-systems currently in use as well as in development. Another challenge involves the realization that in many instances a description of the nanocarrier might be a function of its intended application and not its composition. For example, multifunctional nanocarriers are used to describe a variety of organic and/or inorganic nanoparticles that have been selectively modified and re-engineered to perform various therapeutic and diagnostic functions by 1) improving stability, 2) lengthening circulatory half-life and biodistribution, 3) incorporating passive and active targeting capabilities, 4) tuning responsiveness to pH and/or temperature and other pathological and physiological variations, 5) incorporating various contrast agents and imaging modalities (*viz* - magnetic resonance imaging, gamma-scintigraphy, ultra sonography, computed tomography etc.) and 6) including magnetic sensitivity.[95,96,97,98] Some of the magnetic particles have been tried as magnetic contrast agents,[99] hyperthermia agents for thermal ablation of tumors,[100] and magnetic vectors for drug targeting[101] amongst other applications.[102,103] As such, the nomenclature of these systems refers to the modality of operation and function of these nano-particles; not their architecture and constituents.

The specific nano-delivery agents that will be presented provide a brief overview of the major carriers employed for drug delivery. They will be classified based on their composition and assembly characteristics.

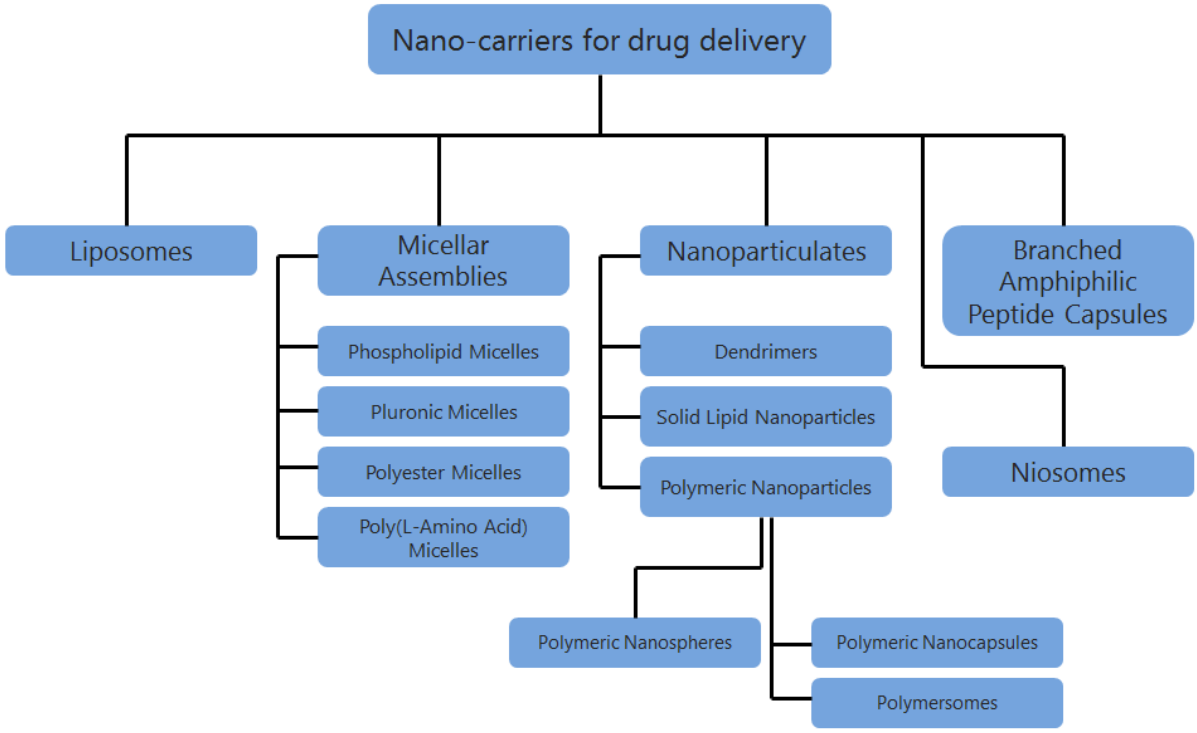

Figure 1.2 Classification of Nanocarrier Systems for Drug Delivery

1.5.1 Liposomes

Liposomes are possibly the oldest and most widely studied drug delivery systems and have been in use since the 1960s.[104] These artificially produced vesicles range from 30 nm to several micrometers in size and consist of an aqueous core surrounded by uni- or multi-lamellar membranes comprised of phospholipids and cholesterol.[105] Their utility lies in their ability to fuse with cellular membranes[106] and lipid bilayers membranes or to enter cells through clathrin mediated endocytosis.[107,108109] The properties of liposomes have been extensively investigated and have been modulated to express a great deal of variation in size, lipid composition, surface charge and other characteristics.[110] The aqueous core of the liposomes is known to be able to encapsulate a large payload of hydrophilic and moderately hydrophobic drugs; and their ability to naturally associate with tumors and the EPR effect has led to the development of numerous FDA approved drugs based on the liposome platform.[111,112]

Numerous studies have been conducted to surface modify classical liposomes in an effort to increase their targeting capabilities and circulating half-lives. These include incorporation of linear dextrans,[113] gangliosides containing sialic acid,[114] lipid derivatives of hydrophilic polymers such as polyvinyl alcohol,[115] polyethylene glycol[116,117] and poly-N-vinylpyrrolidones[118] for stabilization and protection from uptake by the mononuclear phagocytic system (MPS). Targeted therapy has also been demonstrated using liposomes conjugated with a monoclonal antibody via a PEG linker,[119] and protease-sensitive polymer-caged liposomes have been developed to enable selective targeting and drug release at the cancerous site by exploiting the

natural tendency of affected cells to produce cancer associated proteases to destabilize the liposome resulting in drug extravasation.[120]

Liposomes also appear to be the preferred carriers for purposes of radionuclide based targeting for cancer therapy. A variety of liposomes such as multi-vesicular liposomes (MUVEL) - small vesicles containing radionuclides trapped into large liposomes, polymer coated long

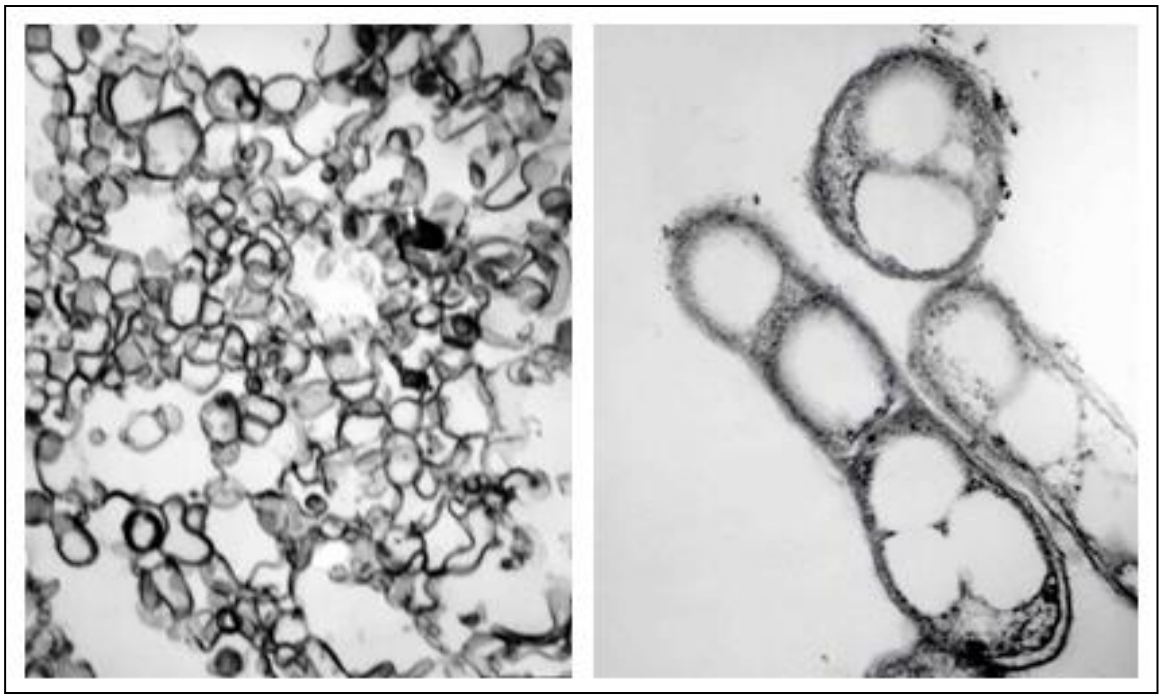

Figure 1.3 Electron microscopy pictures of POPC:POPE (6:4) liposomes made using extrusion.
Seabra, M.B. (2006) Studies of a Channel-Forming Peptide Inserted into Liposomes formed by POPC:POPS and POPC:POPE, Kansas State University.

circulating liposomes - with low bilayer permeability and low lipid exchange, sterically stabilized liposomes (SSL) - with high load capacity and tumor affinity, etc. have been developed exclusively for this purpose.[121,122,123,124,125] The therapeutic efficacy of targeted radiotherapy is due to the tumor's absorption of alpha (α) or beta (β) radiation emitted by the radionuclide. β-emitters such as ^{90}Y, ^{32}P, ^{166}Ho, ^{89}Sr, ^{188}Re and ^{186}Re are by far the most widely utilized radionuclides. β-electrons have low linear energy transfer (LET) values and long path-lengths. They can pass through tissue, and interact with atoms via energy loss causing ionization,

generating free radicals thus causing DNA damage by inducing single strand breaks. On the other hand α-particles have high LET values and shorter path lengths, and are used to generate more localized cellular effects with high chromosomal damage during mitosis and irreparable double strand DNA breaks. Short half-life α-particles emitters ^{225}Ac, ^{211}At and ^{213}Bi are commonly employed for targeted alpha particle therapy (TAT).[126] Naturally varying considerations exist in the selection of liposomal carriers based on whether they are employed for beta - or alpha - radiation therapy. For instance studies relating to the effect of surface charge of the liposomes on the radionuclide delivery demonstrated that the use of neutral lipids such as DMPC-Cholesterol in liposomal preparation substantially increased the effective maximum absorbed dosage of beta emitters such as ^{32}P, ^{67}Cu, ^{90}Y and ^{131}I at the tumor site as opposed to cationic DC-cholesterol lipids. On the other hand a study performed on cholesterol stabilized PEGylated liposomes with ^{225}Ac and ^{213}Bi showed high retention of the radionuclide and daughter isotopes where large (> 650 nm) cationic liposomes were involved.[126]

Generally speaking, due to the low LET values exhibited by beta electrons, considerations of liposomal rupture due to beta-emissions are not as critical as in the case of alpha emitters where the high LET values of alpha particles coupled with the high energy recoil generated during the formation of daughter nuclides can damage and rupture the liposomal membrane. Moreover, the greater availability of beta-emitters for radiotherapy enables a greater choice in the selection of radionuclides as opposed to those employed in alpha particle therapy. The chemistry of the parent ^{225}Ac used in most alpha particle therapies has a chemistry that is not well understood; and that precludes the effective utilization of these emitters in chelate complexes and from integration in larger compounds for the purposes of liposomal encapsulation. Time is yet another factor to be considered in case of radiotherapy. Unlike

conventional drugs, radioactive moieties decay over time, thus losing treatment potency. This is especially true in cases of radionuclides such as ^{213}Bi ($t_{1/2}$ = 45.7 min), where the long times taken for liposomal preparation come at the expense of therapeutic efficacy. Discussion of problems associated with alpha particle delivery will be detailed in chapter 3.

Despite their versatility, biocompatibility, relative non-toxicity and wide application platform, liposome preparation is lengthy and tedious, and preparation steps have to be very carefully monitored to ensure reproducibility in size and entrapment efficiency.[127] Moreover, liposomes have been demonstrated to alter the pharmacokinetic properties of the drugs and are prone to systemic leakage.[128] All of these parameters must be factored in while selecting liposomes as candidates for therapeutic delivery.

1.5.2 Micellar Assemblies

Micelles are self-assemblies of amphiphilic macromolecules - with distinct hydrophobic and hydrophilic block domains - that form supramolecular core-shell structures in aqueous environments.[129] Amphiphilic molecules tend to accumulate at the boundary of two phases with the hydrophobic blocks oriented away from the aqueous environment to achieve a state of minimum free energy. Hydrophobic interactions are the main driving force behind micellar assembly above a specific concentration termed the 'Critical Micellar Concentration' (CMC). Each amphiphile has a unique CMC in distilled water, which can increase or decrease depending on the presence of various solutes.[130] Micelles maintain their assembly as long as their concentrations in solution exist above the CMC. However, in some cases they can resist disassembly below their CMC, if physical interactions between chains in the micellar core can out-compete the thermodynamic forces involved in micellar destabilization.[131] Micelles usually range from 10-100 nm in diameter and exhibit a core-shell architecture, in which the inner core - comprised of the hydrophobic regions of the amphiphiles serve as an environment that can entrap lipophilic drugs.[132] The CMC and morphological features exhibited by micelles are a function of the nature of their hydrophilic and hydrophobic block constituents. Eisenberg et al. have demonstrated the formation of a variety of micellar structures such as, spheres, rods, vesicles, tubules and lamellae depending on solvent conditions and the relative size of hydrophobic and hydrophilic segments, resulting in varied pharmacokinetic properties.[133,134,135,136] Numerous copolymers can be used for the production of micelles, but constraints of biocompatibility and biodegradability limits this choice therapeutic applications.[120] Usually, the preferred choice for

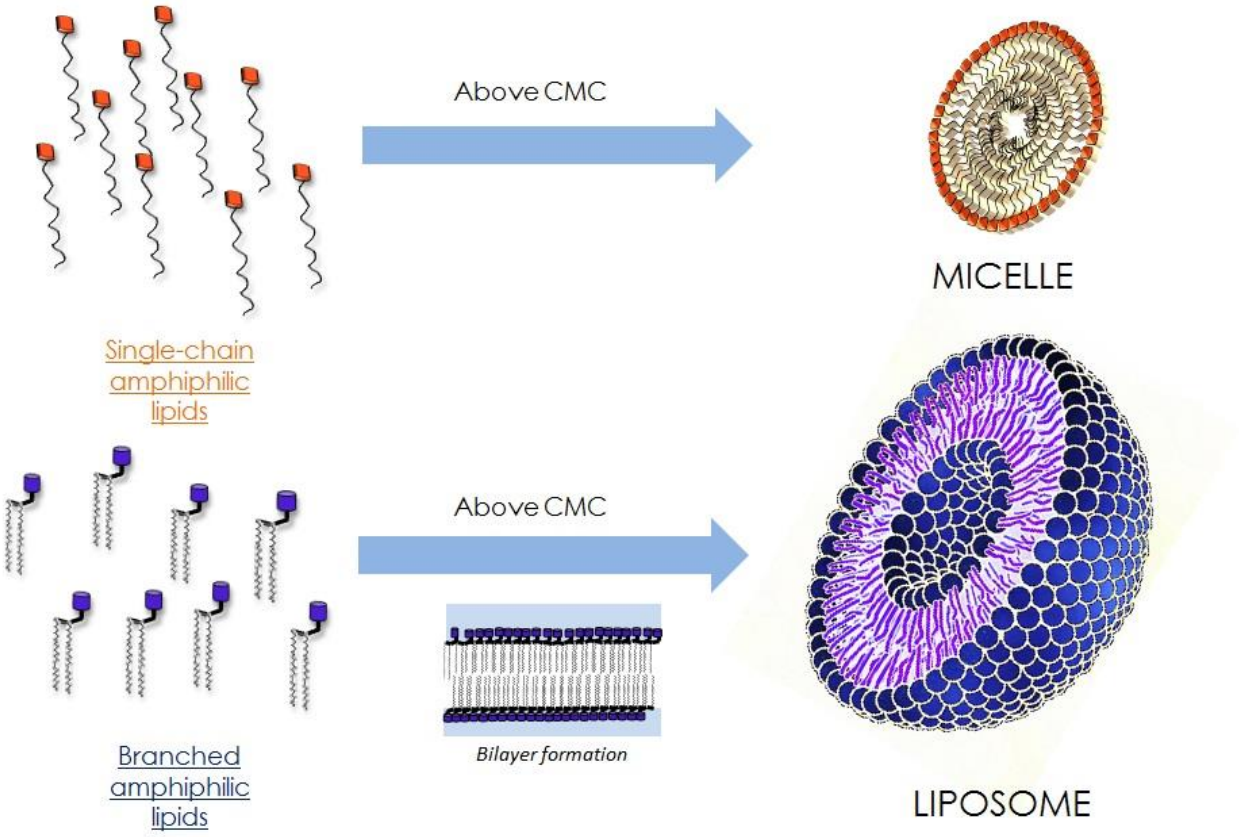

Figure 1.4 . Formation of Liposomes and Micelles above the Critical Micellar Concentration

the hydrophilic block has been PEG. In most micellar assemblies, the molecular weight of PEG tends to exceed that of the hydrophobic core forming block.[137] This outer hydrophilic corona region tends to become highly water bound resulting in a splayed appearance giving rise to various conformations, such as a polymer brush.[138] These conformations give micelles new characteristics that suppress binding to serum proteins and phagocytic attack in blood thereby decreasing clearance by the RES.[129] PEGylated co-polymer micelles also have lower CMC than traditional surfactants resulting in lower cellular toxicity.[129] The highly hydrated corona and the hydrophobic core generate a polarity gradient which aids in the solubilization of a range of hydrophobic compounds of varied polarities, by mere physical association without the need for any drug modification.[119] Using micellar delivery system, the biodistribution and

pharmacokinetics of many drugs are positively altered by means of increased circulatory half-life and tumor accumulation.[139]

Based on their shared molecular architecture, micelles can be divided into four general categories.

1.5.2.1 Phospholipid Micelles

Typical membrane phospholipids are branched and assemble into bilayers, and are used for the generation of liposomes. An interesting exception is the phospholipid 1,2-distearoylphosphatidylethanolamine (DSPE), which when conjugated with PEG assembles into nano-sized micellar structures. These DSPE-PEG micelle cores are stable due to the low CMC of the DSPE with the PEG forms the outer hydrophilic shell. PEGylated phospholipid micelles avoid MPS uptake, exhibit extended circulatory half-lives,[140,141] and are described as sterically stabilized micelles (SSM).[59,60,61] These nano-carrier constructs have PEGs with molecular weights ranging from 1000-5000 Da and are biocompatible, easy to produce and non-toxic.[142,143] The CMC of these phospholipid micelles is a function of PEG chain length, with lower CMCs for shorter chains. However, SSMs with PEG molecular weights less than 1000 Da failed to provide the necessary polarity to form

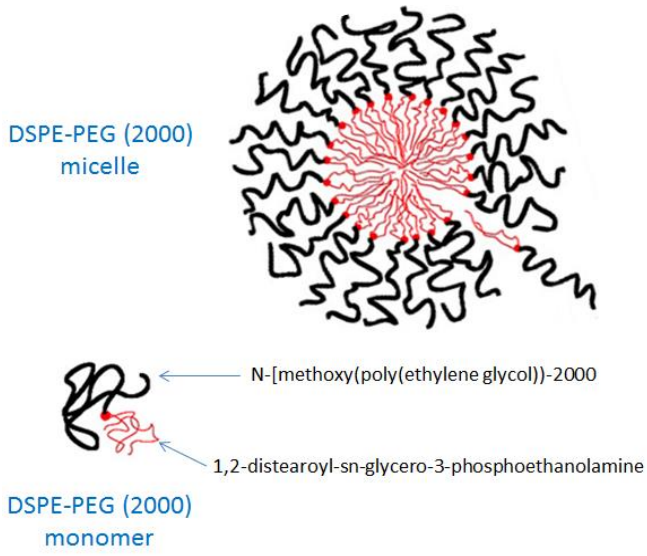

Figure 1.5. Representation of a DSPE-PEG(2000) Micelle. Adapted with permission from (Kastantin, M., Ananthanarayanan, B., Karmali, P., Ruoslahti, E. and Tirrell, M. (2009) Effect of the lipid chain melting transition on the stability of DSPE-PEG(2000) micelles. Langmuir. United States 25, 7279-7286). Copyright (2009) American Chemical Society.

micelles whereas the ones with weights greater than 5000 Da made the moieties excessively soluble to maintain functionality.[144] A number of therapeutic agents have been used for delivery with SSM, *viz* diazepam,[142] campothecin,[34] paclitaxel[40] and vasoactive intestinal peptide (VIP).[145] The incorporation of a water insoluble phospholipid molecule such as phosphatidylcholine to increase the solubilization potential of phospholipid micelles had led to the development sterically stabilized mixed micelles (SSMM) with differences in size and solubility depending on variations in phosphatidylcholine composition and PEG chain length.[40,142] Phospholipid micelles are stable and can be reconstituted upon freeze drying without the need for cryo - and/or lyo-protecting agents.[34] However, they exhibit limited stability in water when compared to other types of micelles.[119]

1.5.2.2 Pluronic Micelles

These are block copolymer micelles where polyethylene oxide (PEO) forms the hydrophilic block and polypropylene oxide (PPO)provides the hydrophobic block. These blocks are arranged in structural variations of the basic pattern PEO_x-PPO_y-PEO_x , where *x* and *y*

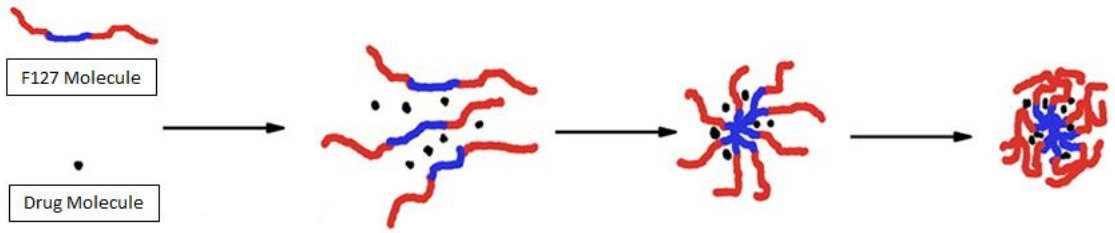

Figure 1.6. Drug Encapsulation in encapsulated in spherical Pluronic F127 micelles.
Adapted with permission from (Basak, R. and Bandyopadhyay, R. (2013) Encapsulation of hydrophobic drugs in Pluronic F127 micelles: effects of drug hydrophobicity, solution temperature, and pH. Langmuir. United States 29, 4350-4356). Copyright 2013

represent the number of time a PEO or a PPO block is repeated. They are characterized by their core-shell architecture where, in water, the hydrophilic segments form a palisade surrounding the

segregated hydrophobic core. The toxicity of the pluronic micelles have been correlated to their hydrophobicity while their biological distribution has been correlated with their charge and surface properties.[146,147] Pluronic micelles are formulated by combining two or more types of blocks generating a wide range of hydrophobicities and have also been used in vitro in chemotherapy to overcome multi drug resistance.[148] Pluronics have been modified by covalent chemical conjugation to generate new polymers. A case in point would be pluronics conjugated with polyacrylic acid (PAA) to generate nano-micellar systems incorporating the solubility capabilities of poloaxamers with the bio-adhesive and pH sensitivities of the PAA.[119]

1.5.2.3 Polyester Micelles

Polyester micelles are made up of FDA approved, biocompatible and biodegradable amphiphilic polymer conjugates such as, PEG-poly(lactic acid) (PLA), PEG-poly(lactic-co-glycolic acid) (PLGA) and PEG-poly(caprolactone).[135] An increase in the poly(lactone) chain length resulted in increased hydrophobicity and subsequently increased loading efficiency of the model drug indomethacin. Alternatively, the use of PLA - a more hydrophilic lactone, resulted in a more rapid release of the drug due to weaker interactions between the drug and the poly(lactide) core. Similarly, shorter chain length PEG increased drug loading and decreased rate of release compared to longer chain length PEG.[149] Drug loading efficiency and release in these systems is a function of the nature of the hydrophobic core as well as the PEG chain length and the ratio between them. Although these micelles have been investigated for delivery of paclitaxel and doxorubicin, concerns regarding the acid metabolites generated during the hydrolytic breakdown of polyester lactones *in vivo* remain to be addressed.[119]

1.5.2.4 Poly(L-amino acid) Micelles

Poly(L-amino acid) micelles are Poly(L-Histidine)-PEG block co-polymers blended in with poly(L-lactic acid)-PEG micellar systems (PLLA-PEG) that have been investigated as pH sensitive drug carriers for cancer therapy.[150,151,152] Cancerous cells - due to a higher rate of aerobic and anaerobic glycolysis compared to normal cells - tends to have pH < 7.2. [148,153,154] The imidazole side-chain of histidine has a pKa in this range; which leads to an increase in histidine hydrophobicity, destabilization of the micelle and subsequent drug release. The pH sensitivity of Poly(L-amino acid) micelles has been modulated by varying the %wt. of the poly(L-lactic acid)-PEG composition. Moreover, Poly(L-histidine) (PLHS) has been indicated to demonstrate fusogenic activity in endosomes facilitating cytosolic drug release in cancer cells.[148] PLHS-PEG/DSPE-PEG as well as PLHS-PEG/PLLA-PEG co-polymer micelles have been developed as pH sensitive nanocarriers for the purposes of cytosolic drug delivery.[155] Drugs have been conjugated to these poly(amino acid) copolymers via chemical modifications of the drugs, but not without concerns relating to drug decoupling at the target site.[156,157,158] Also, immunogenicity is a potential concern with these systems upon the increase in the number and diversity of amino acids used.[135] However, the use of D-amino acids might help to alleviate that concern.

1.5.3 Nanoparticulates in drug delivery

Nanoparticulates are colloidal macromolecular nanocarrier systems ranging from 10-100 nm and deemed as potentially attractive candidates for the entrapment and encapsulation of hydrophobic drugs. Solid nanoparticulates can either be defined as nanocapsules - where the active drug molecule is encapsulated within the carrier; or matrix based nanospheres - where the drug molecules are adsorbed and dispersed throughout the nanomaterial.[159] Nanoparticulates can be engineered using 'top down' or 'bottom up' methods.[160] In the former, the larger material is broken down into smaller particles whereas the bottom up approach involves the thermodynamically regulated, molecule by molecule synthesis of the nanomaterial in a controlled environment.[161] Based on their composition; nanoparticulates are classified into the following categories:

1.5.3.1 Polymeric Nanoparticles

These nanoparticles are engineered from synthetic polymeric constituents such as PLA, PGA, PLGA, poly-ε-caprolactone, poly(methyl methacrylate), etc.[3] and formulated to be biocompatible and biodegradable; maximize tissue compatibility and minimize cyto-toxicity.[119] Based on the methods of assembly and function, they fall into two categories;

1.5.3.1.1 Polymeric Nanospheres

A polymeric nanosphere is defined as polymer matrix colloidal nanoparticulate that entraps, encapsulates, chemically binds to, or adsorbs a drug molecule. [130] These particles are between 100-200 nm and demonstrate poly-dispersity. [130] The hydrophobic surfaces of these

particles however make them susceptible to clearance by the RES and efforts have been made to alter the surface characteristics of these by absorbing various surfactants and moieties like poloxamine, poloxamer and Brij to their surface.[162,163,164,165] Nanospheres prepared using amphiphilic co-polymers such as methoxypolyethylene glycol - poly(lactic acid) (MePEG-b-PLA) and high molecular weight hydrophobic blocks, not only demonstrated higher stability, but also provided sites for functionalization and conjugation.[166,167] The presence of di- block copolymers in nanospheres resulted in a phase separated structure consisting of a solid core.[164] It was observed in case of methoxypolyethylene glycol - poly(D,L- Lactic acid) (MePEG-b-PDLLA) copolymers, that the aggregation behavior was and the physiochemical properties were strongly dependent on copolymer composition.[168],[169] An increase in PDLLA molecular mass resulted in the central core of the nanocapsules becoming more solid like and a decrease resulted in nanoparticles which were defined as micelle-like assemblies.

1.5.3.1.2 Polymeric Nanocapsules / Polymersomes

These are colloidal vesicular systems in which the drug is confined within a cavity or

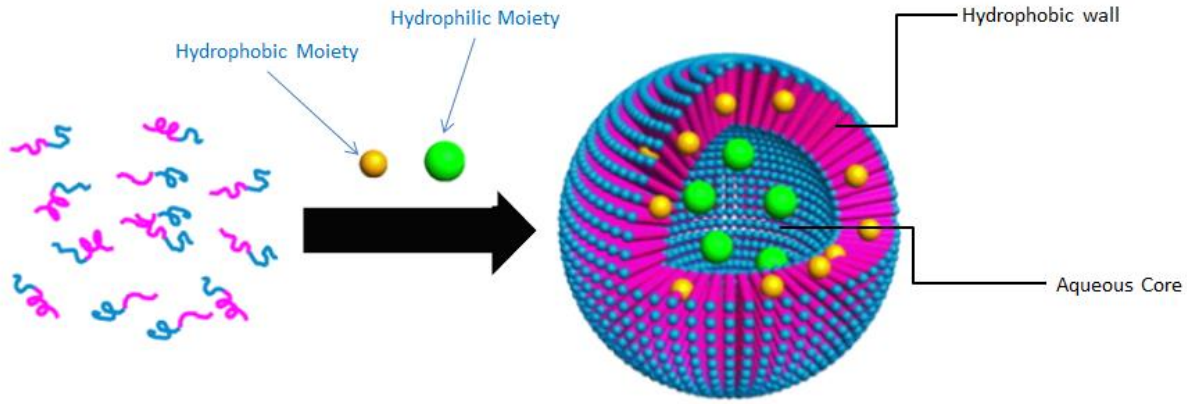

Figure 1.7.Assembly and Encapsulation in Polymersomes.

Adapted with permission from (Qiao, Z.Y., Ji, R., Huang, X.N., Du, F.S., Zhang, R., Liang, D.H. and Li, Z.C. (2013) Polymersomes from dual responsive block copolymers: drug encapsulation by heating and acid-triggered release. Biomacromolecules. United States 14, 1555-1563). Copyright (2013) American Chemical Society.

reservoir surrounded by a polymer coating or membrane.[130,170] If the central cavity consists of an oily liquid surrounded by a single layer of polymer, the resulting structure is a nanocapsule.[168] Nanocapsules are have been indicated for the encapsulation and delivery of hydrophobic drugs such as methotrexate, xanthone, Ru 58668 and 3-methylxanthone, and nanocapsules comprising of PEG copolymers and chitosan are suitable for oral delivery.[171,172,173,174] On the other hand, if the aqueous reservoir is encapsulated by a polymeric bilayer, the resulting structure is termed as a polymersome.[175] Polymersomes are essentially the polymer equivalents of liposomes, the difference being that the external bilayer is constituted of amphiphilic di-block copolymers such as PEG-b-PBD (poly(butadiene)) and PEG-b-PEE (poly(ethylethylene)).[176,177] Polymersomes are particularly suited for the targeting of water soluble drugs. PEGylated variants have a greater PEG surface density and consequently exhibit longer circulation times compared to stealth liposomes.[178]

1.5.3.2 Dendrimers

Dendrimers are 1-10 nm sized synthetic hyper-branched polymeric macromolecules that comprise of a series of well-defined branches around a central inner core[179,180.181] Dendrimers are synthesized by convergent or divergent approaches.[178] The former approach capitalizes on the symmetric nature of the dendrimer with synthesis commencing at the periphery and terminating at the core; while the divergent approaches commences at the core upon which each successive layer is built.[182] Dendrimers are structurally well-defined and display low poly-dispersity despite their large molecular mass. The branching of the dendrimers generates semi-globular / globular structures which are available for functionalization.[177] Consequently glycol-dendrimers, peptide-dendrimers and silicon-dendrimers have been synthesized using carbohydrates, peptides and

silicon as functionalities. [178,183] Drugs are associated with the dendrimers by physical encapsulation in the void spaces or by attachment of the pro-drug to the dendrimer surface.[181] Dendrimers have been studied for the delivery of fluorouracil[184] and indomethacin.[185] Dendrimer size has been exponentially correlated with the duration of extravasation across the endothelium, with larger dendrimers indicating faster extravasations.[186] The positive charges on the polyamine and/or polyamide linkages used for dendrimer construction indicate potential for cellular toxicity and immunogenicity. However, partial derivatization of the dendrimer surface with PEG and/or fatty acids has been shown to mitigate these concerns significantly by shielding the positive charge on the surface.[187,188]

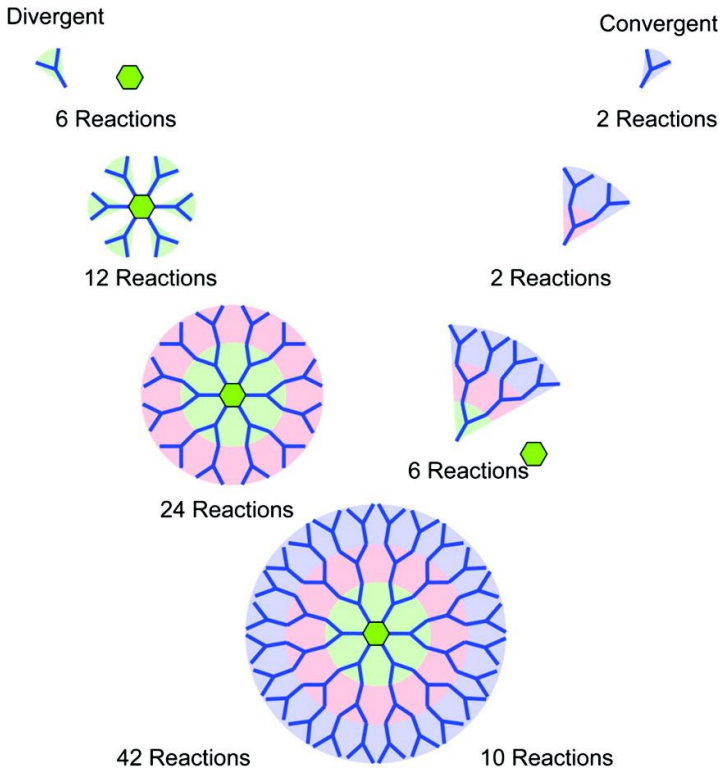

Figure 1.8. Convergent and divergent synthesis of dendrimers and dendrons.

Reprinted with permission from (Rosen, B.M., Wilson, C.J., Wilson, D.A., Peterca, M., Imam, M.R. and Percec, V. (2009) Dendron-mediated self-assembly, disassembly, and self-organization of complex systems. Chem.Rev. United States 109, 6275-6540). Copyright (2009) American Chemical Society.

1.5.3.3 Solid Lipid Nanoparticles

Solid Lipid Nanoparticles (SLN) constitute a class of nanoscale carriers where a central solid hydrophobic core comprised of physiological lipid/s are dispersed in an aqueous surfactant

by micro-emulsification or high pressure homogenization.[189] The drugs in this case are dissolved and dispersed in the solid hydrophobic core.[190] These nanoparticles due to their narrow size range (100 - 200 nm) evade the RES and also cross the tight endothelial cells of the blood-brain barrier to be taken up by the brain.[191] The biodegradable nature of the non-toxic constituent physiological lipids makes them very safe to use. SLN also demonstrate higher stable drug entrapment, especially in case of very hydrophobic drugs and provide controlled release lasting several weeks. SLN are conjugated hydrophilic polymers and/or surfactants to minimize their hepatic uptake and improve bioavailability.[119] SLN can be stabilized by the incorporation of stearic acid - PEG 2000, however cytotoxic effects due to the release of free stearic acid, upon degradation needs to be factored in as a cost of stabilization.[192] The loading efficiency of SLN can be modulated by employing complex lipids with varying chain lengths. Overall, SLN are a safe delivery system for hydrophobic drugs especially to the brain and production is scalable with excellent reproducibility.[157,193]

1.5.4 Niosomes

Niosomes or Non-ionic surfactant vesicles (NSV) are nanoscopic lamellar structures that self-assemble into closed bilayers upon hydrating a preparation of non-ionic surfactants such as alkyl or dialkyl polyglycerol ethers; cholesterol and a charge inducing agent.[194] In many ways Niosomes are liposomal analogs and are prepared much like liposomes through non-spontaneous processes involving the input of energy in the form of heat, ultrasound, physical agitation, application of pressure or a combination thereof.[195] Consequently, just like liposomes, most NSV preparation methods involve some hydration of the non-ionic surfactant at an elevated temperature followed by an optional size reduction to obtain a colloidal suspension.[196] However,

there are some fundamental distinctions. While liposomes are made up of neutral or charged double chained phospholipids; niosomes are made up of uncharged single chain surfactants. And since non-ionic surfactants are more stable than, and more resistant to air-oxidation than phospholipids, niosome preparation is usually much easier than that of their liposomal counterparts.[195] Liposomes are expensive and difficult to prepare, require special storage and handling and the constituent phospholipids have a predisposition to become oxidized. The interest in ninosomes as potential nano-carriers is a result of their versatility, cost-efficacy, stability and ability to surmount some of the drawbacks associated with liposomes.[197]

Niosomes are essentially comprised of three different constituents; i) Non-ionic surfactant, ii) Cholesterol and, iii) Charged molecule.

1.5.4.1 Non-ionic surfactants are amphiphilic or amphipathic, non-ionic molecules and are the basic component of niosomes. Non-ionic surfactants are preferred due to their diversity, stability, non-toxic nature and biocompatibility.[198] The hydrophobic and hydrophilic segments in these amphipathic molecules are bonded by esters, amides or ethers. Non-ionic surfactants such as alkyl ethers, alkyl glyceryl ethers, sorbitan fatty acid ethers, Brij 30 (polyoxyethylene 4 lauryl ether), Brij 58 (polyoxyethylene acetyl ether), Span 60, Tween 40 etc. have been used for the preparation of niosomes, with polyglycerol monoalkyl ethers and their polyoxylate analogs being the most widely employed single chain surfactants.[195, 196] Moreover, Gemini surfactants - two hydrophobic chains linked with two hydrophobic head groups via spacers,[199,200] and bolasurfactants - two identical polar azacrown ethers linked together with a long alkyl chain,[201] have been used to develop novel NSVs. The diversity available surfactants and numerous permutations thereof, make NSV a highly tunable system.

1.5.4.2--Cholesterol - due to its interaction with non-ionic surfactants greatly influences the physical and structural properties of niosomes, and numerous surfactants form NSV only after addition of anywhere between 30 - 50 mol% of cholesterol.[202] Cholesterol modulates the cohesion of the NSVs, their mechanical strength and permeation to water. The rigidity imparted by cholesterol is vital to the stability of the NSV in conditions of stress.[203] When surfactants with hydrophilic-lipophilic balance (HLB) values greater than 10 are involved in NSV formation, the incorporation of cholesterol is a structurally critical compensation for the presence of larger hydrophilic head groups.[204] Nevertheless, the concentration of cholesterol in NSVs is much less than that typically found in liposomes resulting in higher niosomal drug entrapment efficiency.[195]

1.5.4.3 Charged Molecules - Negatively charged molecules such as Dicetyl phosphate (DCP) and phosphatidic acid, or positively charged molecules such as cetylpyridinium chloride and sterylamine (SA) are added (2.5 - 5 mol%) to prevent aggregation and stabilize the niosomal bilayer.[196]

When a water soluble carrier such as sorbitol, sucrose stearate, maltodextrin etc. is coated with a thin film of dry non-ionic surfactant, the resulting preparation is termed 'Proniosomes'.[205] These proniosomes can be reconstituted via hydration to generate Niosomes. Since proniosomes are obtained as a dry powder; they can be formulated to make beads, capsules or tablets with convenient unit dosing and demonstrate reduced aggregation, fusion, leakage and increased drug entrapment efficiency.[196, 206]

Niosomes, due to the presence of amphiphilic, lipophilic and hydrophilic moieties can incorporate drugs with a wide range of solubility, and indicate potential applications for the delivery of numerous pharmacological agents.[195] Niosomal preparations have been investigated for the purposes of drug, gene and vaccine delivery through parenteral, oral, ocular, pulmonary

and transdermal routes. The breadth of these studies precludes them from comment in this thesis. Marianecci et al. (2013)[196] provides an excellent and comprehensive review on the numerous potential applications of niosomes. A worthwhile mention however is the ability of niosomes to deliver drugs via topical application. Dermal / transdermal drug delivery is an alternative route for therapeutic administration that enables localized delivery of high concentrations of the drug, while bypassing the limitations associated with systemic circulation and/or gastrointestinal degradation. The *stratum cornuem* of the epidermis works as a barrier for permeation and consequently severely restricts the administration of most drugs through transdermal routes.[196] Niosomes loaded with drugs demonstrate enhanced permeation characteristics and niosomes formulations demonstrated greater skin permeation of enoxacin and higher stability of tretinoin when compared to their respective liposomal counterparts.[207, 208] pH sensitive niosomes generated with Span 60, cholesterol and cholesteryl hemisuccinate (CHEMS) were proposed for the topical delivery of ibuprofen and demonstrated a significant increase in drug permeation through the skin.[209]

Despite the numerous advantages proffered by niosomes over liposomes, niosomal preparation is generally exhaustive, utilizes numerous moieties, involves the application of non-spontaneous energy consuming processes and takes considerable time. Niosomes have yet to be (as of 2013) employed as a clinical therapeutic, and no specific, long term studies to study the toxicity of niosomes *in vivo* are available.[196]

1.5.5 Branched Amphiphilic Peptide Capsules

Branched Amphiphilic Peptide Capsules represent a novel class of nanocarriers. First described by Gudlur et al.[210] in 2012, they are self-assembling structures where a water filled cavity is surrounded by an amphiphilic branched peptide bilayer. They are essentially stable, non-immunogenic, biocompatible and biodegradable nanocarriers that are structurally similar to liposomes and polymersomes. The properties, applications and biophysical characterization of these carrier systems will be discussed at length in the proceeding chapters.

1.6 Other Peptide Based Carriers

Apart from realm of nano-carriers; it is worthwhile to mention cell penetrating peptide based modalities for drug delivery into the cells. Cell penetrating peptides (CPP) are short cationic sequences of natural derivation, or synthetic constructs that function as vectors to promote cellular uptake.[211] The 'Tat' peptide sequence derived from the HIV transactivator transcription protein was discovered in 1998 and demonstrated to gain intracellular access by translocating the cellular membrane.[212,213] The number of CPPs has grown ever since and commonly used sequences such as penetratin, polyarginine, transportan and Tat are used to deliver a diverse cargo such as small molecule therapeutics,[214] proteins,[215] and nucleic acids[216] into the cell; with high translocation and minimal toxicity in a variety of cell lines.[217]

Table 1 Examples of cell-penetrating peptides, their sequences, structures and proposed mechanisms of cellular uptake.
Adapted from Koren et al (2012)[218] and Fonseca et al (2009)[219]

Cell Penetrating Peptide	Amino Acid Sequence	Structure	Proposed Mechanism
$Tat_{(49-57)}$	RKKRRQRRR	Random Coil / PPII helix	Pore formation, direct penetration
Pep-1	KETWWETWWTEWSQPKKKRKV	Amphipathic, α-helical	Pore formation, direct penetration
Penetratin (pAntp)	RQIKIWFQNRRMKWKK	Amphipathic, α-helical, β-sheet(high concentration)	Endocytosis, direct penetration
pVEC	LLIILRRRRIRKQAHAHSK	Amphipathic, β-sheet	Transporter mediated, direct penetration

The mechanism of CPP uptake across the plasma membrane remains unresolved. The length of the molecule, the sequence of amino acids, charge delocalization on the peptide, and the properties of the associated cargo have all been held as determining factors.[219] However, it has become apparent that a single CPP could employ multiple pathways of entry into the cell.[220] CPPs have not only demonstrated energy independent direct-translocation into the cell; but also

have been seen to exploit the energy dependent endocytotic modes of entry such as macropinocytosis, clathrin mediated endocytosis, caveolae/lipd-raft mediated endocytosis and clathrin/caveolae independent endocytosis.[221] The major advantage of CPP is their ability to transport cargo into the intracellular compartments of the cell such as the nucleus, mitochondria, lysosome and cytoplasm.[221] Pep-1 (Chariot™ Protein Delivery Reagent, Active Motif, USA), an amphipathic 21-residue sequence, became the first commercially available peptide carrier for the non-covalent delivery of proteins into cells.[222,223] Subsequently, a number of nano-carriers such as liposomes, micelles, nanocapsules, polymeric nanospheres, dendrimers, solid-lipid nanoparticles, etc. have been conjugated, encapsulated or physically adsorbed to CPPs to facilitate their intracellular transport; and have been shown to mediate the intracellular transport of a variety of pharmacologically relevant and biologically active agents in a non-cell-type-specific manner.[224,225,226]

1.7 References

[1] Feynman, R. P. There's plenty of room at the bottom. (Caltech, February, 1960) *Engineering and Science* **23**(5), 22–36

[2] Emerich, D.F. and Thanos, C.G. (2003) Nanotechnology and medicine. *Expert Opin. Biol. Ther.***3**, 655-663

[3] Sahoo, S.K. and Labhasetwar, V. (2003) Nanotech approaches to drug delivery and imaging. *Drug Discov. Today.* **8**, 1112-1120

[4] Silva, G.A. (2004) Introduction to nanotechnology and its applications to medicine. *Surg. Neurol.* **61**, 216-220

[5] Farokhzad, O.C. and Langer, R. (2009) Impact of Nanotechnology on Drug Delivery. *ACS Nano*. **3**, 16-20

[6] Whitesides, G.M. (2003) The 'right' size in nanobiotechnology. *Nat.Biotechnol.* **21**, 1161-1165

[7] Roco, M.C. (2003) Nanotechnology: convergence with modern biology and medicine. *Curr. Opin. Biotechnol.* **14**, 337-346

[8] Roco, M.C. and Bainbridge, W.S. (2002) Converging Technologies for Improving Human Performance: Integrating From the Nanoscale. *Journal of Nanoparticle Research.* 4, 281-295

[9] National Science and Technology Council Committee on Technology, sub-committee on Nanoscale Science, Engineering and Technology. The National Nanotechnology Initiative Supplement to the President's 2014 budget. Washington (DC): Office of Science and Technology Policy; 2013

[10] Langer, R. (1998) Drug delivery and targeting. *Nature.* **392**, 5-10

[11] Duncan, R. (2003) The dawning era of polymer therapeutics. *Nat. Rev. Drug Discov.* **2**, 347-360

[12] Shi, J., Votruba, A.R., Farokhzad, O.C. and Langer, R. (2010) Nanotechnology in drug delivery and tissue engineering: from discovery to applications. *ACS Nano Lett.* **10**, 3223-3230

[13] Vasir, J.K. and Labhasetwar, V. (2005) Targeted drug delivery in cancer therapy. *Technol. Cancer. Res. Treat.* **4**,363-374

[14] Kim, J.K., Kim, H.J., Chung, J.Y., Lee, J.H., Young, S.B. and Kim, Y.H. (2014) Natural and synthetic biomaterials for controlled drug delivery. *Arch. Pharm. Res.* **37**, 60-68

[15] Hamman, J.H., Enslin, G.M. and Kotze, A.F. (2005) Oral delivery of peptide drugs: barriers and developments. *Bio. Drugs.* **19**, 165-177

[16] Pawar, R., Ben-Ari, A. and Domb, A.J. (2004) Protein and peptide parenteral controlled delivery. *Expert Opin. Biol. Ther.* **4**, 1203-1212

[17] Sahoo, S.K., Parveen, S. and Panda, J.J. (2007) The present and future of nanotechnology in human health care. *Nanomedicine: Nanotechnology, Biology and Medicine.* **3**, 20-31

[18] Brayden, D.J. (2003) Controlled release technologies for drug delivery. *Drug Discov.Today.* **8**, 976-978

[19] LaVan, D.A., McGuire, T. and Langer, R. (2003) Small-scale systems for in vivo drug delivery. *Nat Biotech.* **21**, 1184-1191

[20] Ferrari, M. (2005) Cancer nanotechnology: opportunities and challenges. *Nat.Rev.Cancer.* **5**, 161-171

[21] Zhang, L., Gu, F.X., Chan, J.M., Wang, A.Z., Langer, R.S. and Farokhzad, O.C. (2008) Nanoparticles in medicine: therapeutic applications and developments. *Clin. Pharmacol. Ther.* **83**, 761-769

[22] Langer, R. (1990) New methods of drug delivery. *Science.* **249**, 1527-1533

[23] Etheridge, M.L., Campbell, S.A., Erdman, A.G., Haynes, C.L., Wolf, S.M. and McCullough, J. (2013) The big picture on nanomedicine: the state of investigational and approved nanomedicine products. *Nanomedicine: Nanotechnology, Biology and Medicine.* **9**, 1-14

[24] Moghimi, S.M., Hunter, A.C. and Murray, J.C. (2005) Nanomedicine: current status and future prospects. *FASEB J.* **19**, 311-330

[25] Emerich, D.F. (2005) Nanomedicine--prospective therapeutic and diagnostic applications. *Expert Opin. Biol. Ther.* **5**,1-5

[26] Jain, K.K. (2003) Nanodiagnostics: application of nanotechnology in molecular diagnostics. *Expert Rev. Mol. Diagn.* **3**, 153-161

[27] Kubik, T., Bogunia-Kubik, K. and Sugisaka, M. (2005) Nanotechnology on duty in medical applications.*Curr.Pharm.Biotechnol.* **6**, 17-33

[28] Kayser, O., Lemke, A. and Hernandez-Trejo, N. (2005) The impact of nanobiotechnology on the development of new drug delivery systems. *Curr. Pharm. Biotechnol.* **6**, 3-5

[29] Drummond, D.C., Meyer, O., Hong, K., Kirpotin, D.B. and Papahadjopoulos, D. (1999) Optimizing liposomes for delivery of chemotherapeutic agents to solid tumors. *Pharmacol. Rev.* **51**, 691-743

[30] Au, J.L., Jang, S.H., Zheng, J., Chen, C.T., Song, S., Hu, L. and Wientjes, M.G. (2001) Determinants of drug delivery and transport to solid tumors. *J. Control. Release.* **74**, 31-46

[31] Fetterly, G.J. and Straubinger, R.M. (2003) Pharmacokinetics of paclitaxel-containing liposomes in rats. *AAPS Pharm. Sci.* **5**, E32

[32] Hoarau, D., Delmas, P., David, S., Roux, E. and Leroux, J.C. (2004) Novel long-circulating lipid nanocapsules. *Pharm. Res.* **21**, 1783-1789

[33] Moghimi, S.M. and Szebeni, J. (2003) Stealth liposomes and long circulating nanoparticles: critical issues in pharmacokinetics, opsonization and protein-binding properties. *Prog. Lipid Res.* **42**, 463-478

[34] Koo, O.M., Rubinstein, I. and Onyuksel, H. (2005) Camptothecin in sterically stabilized phospholipid micelles: a novel nanomedicine. *Nanomedicine.* **1**, 77-84

[35] Kristl, J., Volk, B., Gasperlin, M., Sentjurc, M. and Jurkovic, P. (2003) Effect of colloidal carriers on ascorbyl palmitate stability. *Eur. J. Pharm. Sci.* **19**, 181-189

[36] Arnedo, A., Irache, J.M., Merodio, M. and Espuelas Millan, M.S. (2004) Albumin nanoparticles improved the stability, nuclear accumulation and anticytomegaloviral activity of a phosphodiester oligonucleotide. *J. Control. Release.* **94**, 217-227

[37] Zhang, J.A., Anyarambhatla, G., Ma, L., Ugwu, S., Xuan, T., Sardone, T. and Ahmad, I. (2005) Development and characterization of a novel Cremophor EL free liposome-based paclitaxel (LEP-ETU) formulation. *Eur. J. Pharm. Biopharm.* **59**, 177-187

[38] Ibrahim, N.K., Desai, N., Legha, S., Soon-Shiong, P., Theriault, R.L., Rivera, E., Esmaeli, B., Ring, S.E., Bedikian, A., Hortobagyi, G.N. and Ellerhorst, J.A. (2002) Phase I and pharmacokinetic study of ABI-007, a Cremophor-free, protein-stabilized, nanoparticle formulation of paclitaxel. *Clin. Cancer Res.* **8**, 1038-1044

[39] Kim, T.Y., Kim, D.W., Chung, J.Y., Shin, S.G., Kim, S.C., Heo, D.S., Kim, N.K. and Bang, Y.J. (2004) Phase I and pharmacokinetic study of Genexol-PM, a Cremophor-free, polymeric micelle-formulated paclitaxel, in patients with advanced malignancies. *Clin. Cancer Res.***10**, 3708-3716

[40] Krishnadas, A., Rubinstein, I. and Onyuksel, H. (2003) Sterically stabilized phospholipid mixed micelles: in vitro evaluation as a novel carrier for water-insoluble drugs. *Pharm. Res.* **20**, 297-302

[41] Gelderblom, H., Verweij, J., Nooter, K. and Sparreboom, A. (2001) Cremophor EL: the drawbacks and advantages of vehicle selection for drug formulation. *Eur. J. Cancer.* **37**, 1590-1598

[42] ten Tije, A.J., Verweij, J., Loos, W.J. and Sparreboom, A. (2003) Pharmacological effects of formulation vehicles : implications for cancer chemotherapy. *Clin. Pharmacokinet.* **42**, 665-685

[43] Verma, A., Uzun, O., Hu, Y., Hu, Y., Han, H.S., Watson, N., Chen, S., Irvine, D.J. and Stellacci, F. (2008) Surface-structure-regulated cell-membrane penetration by monolayer-protected nanoparticles. *Nat. Mater.* **7**, 588-595

[44] Gratton, S.E., Ropp, P.A., Pohlhaus, P.D., Luft, J.C., Madden, V.J., Napier, M.E. and DeSimone, J.M. (2008) The effect of particle design on cellular internalization pathways. *Proc.Natl.Acad.Sci.U.S.A.* **105**, 11613-11618

[45] Davis, M.E. (2009) The first targeted delivery of siRNA in humans via a self-assembling, cyclodextrin polymer-based nanoparticle: from concept to clinic. *Mol. Pharm* **6**, 659-668

[46] Decuzzi, P., Pasqualini, R., Arap, W. and Ferrari, M. (2009) Intravascular delivery of particulate systems: does geometry really matter? *Pharm. Res.* **26**, 235-243

[47] Patil, Y.B., Toti, U.S., Khdair, A., Ma, L. and Panyam, J. (2009) Single-step surface functionalization of polymeric nanoparticles for targeted drug delivery. *Biomaterials.* **30**, 859-866

[48] Kim, B.S., Park, S.W. and Hammond, P.T. (2008) Hydrogen-bonding layer-by-layer-assembled biodegradable polymeric micelles as drug delivery vehicles from surfaces. *ACS Nano.* **2**, 386-392

[49] Allen, T.M. (2002) Ligand-targeted therapeutics in anticancer therapy. *Nat. Rev. Cancer.* **2**, 750-763

[50] Jain, R.K. (1998) The next frontier of molecular medicine: delivery of therapeutics. *Nat. Med.* **4**, 655-657

[51] Oeffinger, B.E. and Wheatley, M.A. (2004) Development and characterization of a nano-scale contrast agent. *Ultrasonics.* **42**, 343-347

[52] Fu, B.M., Adamson, R.H. and Curry, F.E. (1998) Test of a two-pathway model for small-solute exchange across the capillary wall. *Am. J. Physiol.* **274**, H2062-73

[53] Firth, J.A. (2002) Endothelial barriers: from hypothetical pores to membrane proteins. *J. Anat.* **200**, 541-548

[54] Hobbs, S.K., Monsky, W.L., Yuan, F., Roberts, W.G., Griffith, L., Torchilin, V.P. and Jain, R.K. (1998) Regulation of transport pathways in tumor vessels: role of tumor type and microenvironment. *Proc. Natl. Acad. Sci. U.S.A.* **95**, 4607-4612

[55] Maeda, H., Wu, J., Sawa, T., Matsumura, Y. and Hori, K. (2000) Tumor vascular permeability and the EPR effect in macromolecular therapeutics: a review. *J. Control. Release.* **65**, 271-284

[56] Matsumura, Y. and Maeda, H. (1986) A new concept for macromolecular therapeutics in cancer chemotherapy: mechanism of tumoritropic accumulation of proteins and the antitumor agent smancs. *Cancer Res.* **46**, 6387-6392

[57] Vasir JK, Labhasetwar V. (2005) Targeted drug delivery in cancer therapy. *Technol. Cancer Res Treat* **4**:363- 74.

[58] Moghimi, S.M., Hunter, A.C. and Murray, J.C. (2001) Long-circulating and target-specific nanoparticles: theory to practice. *Pharmacol. Rev.* **53**, 283-318

[59] Klibanov, A.L., Maruyama, K., Torchilin, V.P. and Huang, L. (1990) Amphipathic polyethyleneglycols effectively prolong the circulation time of liposomes. *FEBS Lett.* **268**, 235-237

[60] Allen, T.M., Hansen, C., Martin, F., Redemann, C. and Yau-Young, A. (1991) Liposomes containing synthetic lipid derivatives of poly(ethylene glycol) show prolonged circulation half-lives in vivo. *Biochimica et Biophysica Acta (BBA) - Biomembranes.***1066**, 29-36

[61] Woodle, M.C. (1993) Surface-modified liposomes: assessment and characterization for increased stability and prolonged blood circulation. *Chem. Phys. Lipids.* **64**, 249-262

[62] llen, T.M. and Everest, J.M. (1983) Effect of liposome size and drug release properties on pharmacokinetics of encapsulated drug in rats. *J. Pharmacol. Exp. Ther.* **226**, 539-544

[63] Pardridge, W.M. (1999) Vector-mediated drug delivery to the brain. *Adv. Drug Deliv. Rev.* **36**, 299-321

[64] Calvo, P., Gouritin, B., Chacun, H., Desmaele, D., D'Angelo, J., Noel, J.P., Georgin, D., Fattal, E., Andreux, J.P. and Couvreur, P. (2001) Long-circulating PEGylated polycyanoacrylate nanoparticles as new drug carrier for brain delivery. *Pharm. Res.* **18**, 1157-1166

[65] Alyautdin, R.N., Tezikov, E.B., Ramge, P., Kharkevich, D.A., Begley, D.J. and Kreuter, J. (1998) Significant entry of tubocurarine into the brain of rats by adsorption to polysorbate 80-coated polybutylcyanoacrylate nanoparticles: an in situ brain perfusion study. *J. Microencapsul.* **15**, 67-74

[66] Garcia-Garcia, E., Gil, S., Andrieux, K., Desmaele, D., Nicolas, V., Taran, F., Georgin, D., Andreux, J.P., Roux, F. and Couvreur, P. (2005) A relevant in vitro rat model for the evaluation of blood-brain barrier translocation of nanoparticles. *Cell Mol. Life Sci.* **62**, 1400-1408

[67] Feng, S.S., Mu, L., Win, K.Y. and Huang, G. (2004) Nanoparticles of biodegradable polymers for clinical administration of paclitaxel. *Curr. Med. Chem.* **11**, 413-424

[68] de Kozak, Y., Andrieux, K., Villarroya, H., Klein, C., Thillaye-Goldenberg, B., Naud, M.C., Garcia, E. and Couvreur, P. (2004) Intraocular injection of tamoxifen-loaded

nanoparticles: a new treatment of experimental autoimmune uveoretinitis.*Eur. J. Immunol.* **34**, 3702-3712

[69] Ballabh, P., Braun, A. and Nedergaard, M. (2004) The blood-brain barrier: an overview: structure, regulation, and clinical implications. *Neurobiol. Dis.* **16**, 1-13

[70] Oki, T., Takahashi, S., Kuwabara, S., Yoshiyama, Y., Mori, M., Hattori, T. and Suzuki, N. (2004) Increased ability of peripheral blood lymphocytes to degrade laminin in multiple sclerosis. *J. Neurol. Sci.* **222**, 7-11

[71] Inoue, S. (2001) Basement membrane and beta amyloid fibrillogenesis in Alzheimer's disease. *Int. Rev. Cytol.* ***210***, 121-161

[72] Cornford, E.M. and Cornford, M.E. (2002) New systems for delivery of drugs to the brain in neurological disease. *Lancet. Neurol.* **1**, 306-315

[73] Riehemann, K., Schneider, S.W., Luger, T.A., Godin, B., Ferrari, M. and Fuchs, H. (2009) Nanomedicine--challenge and perspectives. *Angew.Chem.Int.Ed Engl.* **48**, 872-897

[74] Bartlett, D.W., Su, H., Hildebrandt, I.J., Weber, W.A. and Davis, M.E. (2007) Impact of tumor-specific targeting on the biodistribution and efficacy of siRNA nanoparticles measured by multimodality in vivo imaging. *Proc. Natl. Acad. Sci.U.S.A.* **104**, 15549-15554

[75] Pirollo, K.F. and Chang, E.H. (2008) Does a targeting ligand influence nanoparticle tumor localization or uptake? *Trends. Biotechnol.* **26**, 552-558

[76] Davis, M.E., Chen, Z.G. and Shin, D.M. (2008) Nanoparticle therapeutics: an emerging treatment modality for cancer. *Nat. Rev. Drug Discov.* **7**, 771-782

[77] Ishida, O., Maruyama, K., Tanahashi, H., Iwatsuru, M., Sasaki, K., Eriguchi, M. and Yanagie, H. (2001) Liposomes bearing polyethyleneglycol-coupled transferrin with intracellular targeting property to the solid tumors in vivo. *Pharm. Res.***18**, 1042-1048

[78]Omori, N., Maruyama, K., Jin, G., Li, F., Wang, S.J., Hamakawa, Y., Sato, K., Nagano, I., Shoji, M. and Abe, K. (2003) Targeting of post-ischemic cerebral endothelium in rat by liposomes bearing polyethylene glycol-coupled transferrin. *Neurol. Res.* **25**, 275-279

[79] Maruyama, K., Ishida, O., Kasaoka, S., Takizawa, T., Utoguchi, N., Shinohara, A., Chiba, M., Kobayashi, H., Eriguchi, M. and Yanagie, H. (2004) Intracellular targeting of sodium mercaptoundecahydrododecaborate (BSH) to solid tumors by transferrin-PEG liposomes, for boron neutron-capture therapy (BNCT). *J. Control. Release.* **98**, 195-207

[80] Missailidis, S., Thomaidou, D., Borbas, K.E. and Price, M.R. (2005) Selection of aptamers with high affinity and high specificity against C595, an anti-MUC1 IgG3 monoclonal antibody, for antibody targeting. *J. Immunol. Methods.* **296**, 45-62

[81] Mitra, A., Mulholland, J., Nan, A., McNeill, E., Ghandehari, H. and Line, B.R. (2005) Targeting tumor angiogenic vasculature using polymer-RGD conjugates. *J. Control. Release.* **102**, 191-201

[82] Schiffelers, R.M., Ansari, A., Xu, J., Zhou, Q., Tang, Q., Storm, G., Molema, G., Lu, P.Y., Scaria, P.V. and Woodle, M.C. (2004) Cancer siRNA therapy by tumor selective delivery with ligand-targeted sterically stabilized nanoparticle. *Nucleic Acids Res.* **32**, e149

[83] Gosk, S., Vermehren, C., Storm, G. and Moos, T. (2004) Targeting anti-transferrin receptor antibody (OX26) and OX26-conjugated liposomes to brain capillary endothelial cells using in situ perfusion. *J. Cereb. Blood Flow Metab.* **24**,1193-1204

[84] Ni, S., Stephenson, S.M. and Lee, R.J. (2002) Folate receptor targeted delivery of liposomal daunorubicin into tumor cells. *Anticancer Res.* **22**, 2131-2135

[85] Moody, T.W., Leyton, J., Gozes, I., Lang, L. and Eckelman, W.C. (1998) VIP and Breast Cancer. *Ann. N.Y. Acad. Sci.* **865**,290-296

[86] Li, L., Wartchow, C.A., Danthi, S.N., Shen, Z., Dechene, N., Pease, J., Choi, H.S., Doede, T., Chu, P., Ning, S., Lee, D.Y., Bednarski, M.D. and Knox, S.J. (2004) A novel

antiangiogenesis therapy using an integrin antagonist or anti-Flk-1 antibody coated 90Y-labeled nanoparticles. *Int. J. Radiat. Oncol. Biol. Phys.* **58**, 1215-1227

[87] Fonseca, M.J., Jagtenberg, J.C., Haisma, H.J. and Storm, G. (2003) Liposome-mediated targeting of enzymes to cancer cells for site-specific activation of prodrugs: comparison with the corresponding antibody-enzyme conjugate. *Pharm. Res.* **20**, 423-428

[88] Dharap, S.S., Qiu, B., Williams, G.C., Sinko, P., Stein, S. and Minko, T. (2003) Molecular targeting of drug delivery systems to ovarian cancer by BH3 and LHRH peptides. *J. Control. Release.* **91**, 61-73

[89] Medina, O.P., Kairemo, K., Valtanen, H., Kangasniemi, A., Kaukinen, S., Ahonen, I., Permi, P., Annila, A., Sneck, M., Holopainen, J.M., Karonen, S.L., Kinnunen, P.K. and Koivunen, E. (2005) Radionuclide imaging of tumor xenografts in mice using a gelatinase-targeting peptide. *Anticancer Res.* **25**, 33-42

[90] Pastorino, F., Brignole, C., Marimpietri, D., Cilli, M., Gambini, C., Ribatti, D., Longhi, R., Allen, T.M., Corti, A. and Ponzoni, M. (2003) Vascular damage and anti-angiogenic effects of tumor vessel-targeted liposomal chemotherapy. *Cancer Res.* **63**, 7400-7409

[91] Farokhzad, O.C., Jon, S., Khademhosseini, A., Tran, T.N., Lavan, D.A. and Langer, R. (2004) Nanoparticle-aptamer bioconjugates: a new approach for targeting prostate cancer cells. *Cancer Res.* **64**, 7668-7672

[92] Sapra, P. and Allen, T.M. (2003) Ligand-targeted liposomal anticancer drugs. Prog. Lipid Res. **42**, 439-462

[93] Forssen, E. and Willis, M. (1998) Ligand-targeted liposomes. *Adv.Drug Deliv.Rev.* **29**, 249-271

[94] Gabathuler, R. (2010) Approaches to transport therapeutic drugs across the blood-brain barrier to treat brain diseases.*Neurobiol.Dis.* **37**, 48-57

[95] Torchilin, V.P. (2012) Multifunctional nanocarriers. *Adv.Drug Deliv.Rev.* **64**, Supplement, 302-315

[96] Liong, M., Lu, J., Kovochich, M., Xia, T., Ruehm, S.G., Nel, A.E., Tamanoi, F. and Zink, J.I. (2008) Multifunctional inorganic nanoparticles for imaging, targeting, and drug delivery. *ACS Nano.* **2**, 889-896

[97] Cheng, Z., Al Zaki, A., Hui, J.Z., Muzykantov, V.R. and Tsourkas, A. (2012) Multifunctional Nanoparticles: Cost Versus Benefit of Adding Targeting and Imaging Capabilities. *Science.* **338**, 903-910

[98] Cheng, Z., Al Zaki, A., Hui, J.Z., Muzykantov, V.R. and Tsourkas, A. (2012) Multifunctional Nanoparticles: Cost Versus Benefit of Adding Targeting and Imaging Capabilities. *Science.* **338**, 903-910

[99] Cunningham, C.H., Arai, T., Yang, P.C., McConnell, M.V., Pauly, J.M. and Conolly, S.M. (2005) Positive contrast magnetic resonance imaging of cells labeled with magnetic nanoparticles. *Magn. Reson. Med.* **53**, 999-1005

[100] Johannsen, M., Gneveckow, U., Eckelt, L., Feussner, A., Waldofner, N., Scholz, R., Deger, S., Wust, P., Loening, S.A. and Jordan, A. (2005) Clinical hyperthermia of prostate cancer using magnetic nanoparticles: presentation of a new interstitial technique. *Int. J. Hyperthermia.* **21**, 637-647

[101] Alexiou, C., Tietze, R., Schreiber, E., Jurgons, R., Richter, H., Trahms, L., Rahn, H., Odenbach, S. and Lyer, S. (2011) Cancer therapy with drug loaded magnetic nanoparticles—magnetic drug targeting. *J. Magn. Magn. Mater.* **323**, 1404-1407

[102] Chomoucka, J., Drbohlavova, J., Huska, D., Adam, V., Kizek, R. and Hubalek, J. (2010) Magnetic nanoparticles and targeted drug delivering. *Pharmacological Research.* **62**, 144-149

[103] Chomoucka, J., Drbohlavova, J., Huska, D., Adam, V., Kizek, R. and Hubalek, J. (2010) Magnetic nanoparticles and targeted drug delivering. *Pharmacological Research.* **62**, 144-149

[104] Bangham, A.D., Standish, M.M. and Watkins, J.C. (1965) Diffusion of univalent ions across the lamellae of swollen phospholipids. *J. Mol. Biol.* **13**, 238-252

[105] Samad, A., Sultana, Y. and Aqil, M. (2007) Liposomal drug delivery systems: an update review. *Curr. Drug Deliv.* **4**, 297-305

[106] Marsden, H.R., Tomatsua, I., Kros, A. (2011) Model systems for membrane fusion. *Chem. Soc. Rev.* **40**, 1572-1585.

[107] Hart, S.L. (2005) Lipid carriers for gene therapy. *Curr. Drug Deliv.* **2**, 423-428

[108] Ewert, K., Evans, H.M., Ahmad, A., Slack, N.L., Lin, A.J., Martin-Herranz, A. and Safinya, C.R. (2005) Lipoplex structures and their distinct cellular pathways. *Adv. Genet* **53**, 119-155

[109] Pollock, S., Antrobus,R., Newton,R., Kampa,B., Rossa,J., Latham, S. Nichita,N.B., Dwek,R.A., Zitzmann, N. (2010) Uptake and trafficking of liposomes to the endoplasmic reticulum. *FASEB J.* **24**(6):1866-1878.

[110] Sethi, V., Onyuksel, H. and Rubinstein, I. (2005) Liposomal vasoactive intestinal peptide. *Methods Enzymol.* United States 391, 377-395

[111] Moses, M.A., Brem, H. and Langer, R. (2003) Advancing the field of drug delivery: taking aim at cancer. *Cancer. Cell.* **4**, 337-341

[112] Allen, T.M. and Cullis, P.R. (2004) Drug delivery systems: entering the mainstream. *Science.* **303**, 1818-1822

[113] Pain, D., Das, P.K., Ghosh, P.C., and Bachhawat, B.K. (1984) Increased circulatory half-life of liposomes after conjunction with dextran. *J. Biosci.* **6**:811–816. 32

[114] Allen, T.M. and Chonn, A. (1987) Large unilamellar liposomes with low uptake into the reticuloendothelial system. *FEBS Lett.* **223**, 42-46

[115] Takeuchi, H., Kojima, H., Yamamoto, H. and Kawashima, Y. (2001) Evaluation of circulation profiles of liposomes coated with hydrophilic polymers having different molecular weights in rats. *J. Control. Release.* **75**, 83-91

[116] Papahadjopoulos, D., Allen, T.M., Gabizon, A., Mayhew, E., Matthay, K., Huang, S.K., Lee, K.D., Woodle, M.C., Lasic, D.D. and Redemann, C. (1991) Sterically stabilized liposomes: improvements in pharmacokinetics and antitumor therapeutic efficacy. *Proc. Natl. Acad. Sci. U.S.A.* **88**, 11460-11464

[117] Lasic, D.D., Martin, F.J., Gabizon, A., Huang, S.K. and Papahadjopoulos, D. (1991) Sterically stabilized liposomes: a hypothesis on the molecular origin of the extended circulation times. *Biochim. Biophys. Acta.* **1070**, 187-192

[118] Torchilin, V.P., Levchenko, T.S., Whiteman, K.R., Yaroslavov, A.A., Tsatsakis, A.M., Rizos, A.K., Michailova, E.V. and Shtilman, M.I. (2001) Amphiphilic poly-N-vinylpyrrolidones: synthesis, properties and liposome surface modification. *Biomaterials.* **22**, 3035-3044

[119] Zhang, Y., Schlachetzki, F., Li, J.Y., Boado, R.J. and Pardridge, W.M. (2003) Organ-specific gene expression in the rhesus monkey eye following intravenous non-viral gene transfer. *Mol. Vis.* **9**, 465-472

[120] Basel, M.T., Shrestha, T.B., Troyer, D.L. and Bossmann, S.H. (2011) Protease-sensitive, polymer-caged liposomes: a method for making highly targeted liposomes using triggered release. *ACS Nano.* **5**, 2162-2175

[121] Miederer, M., Scheinberg, D.A. and McDevitt, M.R. (2008) Realizing the potential of the Actinium-225 radionuclide generator in targeted alpha particle therapy applications. *Adv. Drug Deliv. Rev.* **60**, 1371-1382

[122] Kim, Y.S. and Brechbiel, M.W. (2012) An overview of targeted alpha therapy. *Tumour Biol.* **33**, 573-590

[123] Sofou, S., Thomas, J.L., Lin, H.Y., McDevitt, M.R., Scheinberg, D.A. and Sgouros, G. (2004) Engineered liposomes for potential alpha-particle therapy of metastatic cancer. *J. Nucl. Med.* **45**, 253-260

[124] Sofou, S., Kappel, B.J., Jaggi, J.S., McDevitt, M.R., Scheinberg, D.A. and Sgouros, G. (2007) Enhanced retention of the alpha-particle-emitting daughters of Actinium-225 by liposome carriers. *Bioconjug. Chem.* **18**, 2061-2067

[125] Henriksen, G., Schoultz, B.W., Michaelsen, T.E., Bruland, Ø.S. and Larsen, R.H. (2004) Sterically stabilized liposomes as a carrier for α-emitting radium and actinium radionuclides. *Nucl. Med. Biol.* **31**, 441-449

[126] Hamoudeh, M., Kamleh, M.A., Diab, R. and Fessi, H. (2008) Radionuclides delivery systems for nuclear imaging and radiotherapy of cancer. *Adv. Drug Deliv. Rev.* **60**, 1329-1346

[127] Koo, O.M., Rubinstein, I. and Onyuksel, H. (2005) Role of nanotechnology in targeted drug delivery and imaging: a concise review. *Nanomedicine: Nanotechnology, Biology and Medicine.* **1**, 193-212

[128] Gabizon, A.A., Shmeeda, H. and Zalipsky, S. (2006) Pros and cons of the liposome platform in cancer drug targeting.*J.Liposome Res.* **16**, 175-183

[129] Sutton, D., Nasongkla, N., Blanco, E. and Gao, J. (2007) Functionalized micellar systems for cancer targeted drug delivery. *Pharm. Res.* **24**, 1029-1046

[130] Krimm, S. (1980) The hydrophobic effect: Formation of micelles and biological membranes, Charles Tanford, Wiley-Interscience, New York, 1980, 233 pp. *Journal of Polymer Science: Polymer Letters Edition.* **18**, 687-687

[131] Allen, C., Maysinger, D. and Eisenberg, A. (1999) Nano-engineering block copolymer aggregates for drug delivery. *Colloids and Surfaces B: Biointerfaces.***16**, 3-27

[132] Letchford, K. and Burt, H. (2007) A review of the formation and classification of amphiphilic block copolymer nanoparticulate structures: micelles, nanospheres, nanocapsules and polymersomes. *European Journal of Pharmaceutics and Biopharmaceutics.* **65**, 259-269

[133] Yu, Y., Zhang, L. and Eisenberg, A. (1998) Morphogenic Effect of Solvent on Crew-Cut Aggregates of Apmphiphilic Diblock Copolymers. *Macromolecules.* **31**, 1144-1154

[134] Shen, H., Zhang, L. and Eisenberg, A. (1999) Multiple pH-Induced Morphological Changes in Aggregates of Polystyrene-block-poly(4-vinylpyridine) in DMF/H2O Mixtures. *J.Am.Chem.Soc.* **121**, 2728-2740

[135] Choucair, A. and Eisenberg, A. (2003) Interfacial solubilization of model amphiphilic molecules in block copolymer micelles. *J.Am.Chem.Soc.* **125**, 11993-12000

[136] Choucair, A. and Eisenberg, A. (2003) Control of amphiphilic block copolymer morphologies using solution conditions. *Eur.Phys.J.E.Soft Matter.* **10**, 37-44

[137] Kwon, G.S. (2003) Polymeric micelles for delivery of poorly water-soluble compounds. *Crit.Rev.Ther.Drug Carrier Syst.* **20**, 357-403

[138] Vonarbourg, A., Passirani, C., Saulnier, P. and Benoit, J.P. (2006) Parameters influencing the stealthiness of colloidal drug delivery systems. *Biomaterials.* **27**, 4356-4373

[139] Garrec, D., Ranger, M. and Leroux, J. (2004) Micelles in anticancer drug delivery. *American Journal of Drug Delivery*. **2**, 15-42

[140] Sethi V, Onyuksel H, Rubinstein I. (2003) Enhanced circulation half-life and reduced clearance of vasoactive intestinal peptide (VIP) loaded in sterically stabilized phospholipid micelles (SSM) in mice with collagen-induced arthritis (CIA) AAPS PharmSci.;5 (Suppl 1):M1045.

[141] Lukyanov, A., Gao, Z., Mazzola, L. and Torchilin, V. (2002) Polyethylene Glycol-Diacyllipid Micelles Demonstrate Increased Accumulation in Subcutaneous Tumors in Mice. *Pharm. Res.* **19**, 1424-1429

[142] Working, P.K. and Dayan, A.D. (1996) Pharmacological-toxicological expert report. CAELYX. (Stealth liposomal doxorubicin HCl). *Hum. Exp. Toxicol.* 15, 751-785

[143] Wade A, Weller PJ. (1994) Handbook of pharmaceutical excipients. Washington (DC): American Pharmaceutical Association and Pharmaceutical Press.

[144] Ashok, B., Arleth, L., Hjelm, R.P., Rubinstein, I. and Onyuksel, H. (2004) In vitro characterization of PEGylated phospholipid micelles for improved drug solubilization: effects of PEG chain length and PC incorporation. *J. Pharm. Sci.* **93**,2476-2487

[145] Onyuksel, H., Ikezaki, H., Patel, M., Gao, X.P. and Rubinstein, I. (1999) A novel formulation of VIP in sterically stabilized micelles amplifies vasodilation in vivo. *Pharm. Res.* **16**, 155-160

[146] Kataoka, K., Harada, A. and Nagasaki, Y. (2001) Block copolymer micelles for drug delivery: design, characterization and biological significance. *Adv. Drug Deliv. Rev.* **47**, 113-131

[147] Johnston, T.P. and Miller, S.C. (1985) Toxicological evaluation of poloxamer vehicles for intramuscular use.*J. Parenter. Sci. Technol.* **39**, 83-89

[148] Kabanov, A.V., Batrakova, E.V. and Alakhov, V.Y. (2002) Pluronic block copolymers for overcoming drug resistance in cancer.*Adv. Drug Deliv. Rev.* **54**, 759-779

[149] Lin, W.J., Juang, L.W. and Lin, C.C. (2003) Stability and release performance of a series of pegylated copolymeric micelles. *Pharm. Res.* **20**, 668-673

[150] Lee, E.S., Na, K. and Bae, Y.H. (2003) Polymeric micelle for tumor pH and folate-mediated targeting. *J. Control. Release.* **91**, 103-113

[151] Lee, E.S., Na, K. and Bae, Y.H. (2005) Doxorubicin loaded pH-sensitive polymeric micelles for reversal of resistant MCF-7 tumor. *J. Control. Release.* **103**, 405-418

[152] Matsumura, Y., Hamaguchi, T., Ura, T., Muro, K., Yamada, Y., Shimada, Y., Shirao, K., Okusaka, T., Ueno, H., Ikeda, M. and Watanabe, N. (2004) Phase I clinical trial and pharmacokinetic evaluation of NK911, a micelle-encapsulated doxorubicin. *Br. J. Cancer.* **91**, 1775-1781

[153] Ojugo, A.S., McSheehy, P.M., McIntyre, D.J., McCoy, C., Stubbs, M., Leach, M.O., Judson, I.R. and Griffiths, J.R. (1999) Measurement of the extracellular pH of solid tumours in mice by magnetic resonance spectroscopy: a comparison of exogenous (19)F and (31)P probes. *NMR Biomed.* **12**, 495-504

[154] Engin, K., Leeper, D.B., Cater, J.R., Thistlethwaite, A.J., Tupchong, L. and McFarlane, J.D. (1995) Extracellular pH distribution in human tumours. *Int. J. Hyperthermia.* **11**, 211-216

[155] Wu, H., Zhu, L. and Torchilin, V.P. (2013) pH-sensitive poly(histidine)-PEG/DSPE-PEG co-polymer micelles for cytosolic drug delivery. *Biomaterials*. **34**, 1213-1222

[156] Lavasanifar, A., Samuel, J. and Kwon, G.S. (2002) Poly(ethylene oxide)-block-poly(L-amino acid) micelles for drug delivery. *Adv. Drug Deliv. Rev.* **54**, 169-190

[157] Li, Y. and Kwon, G.S. (2000) Methotrexate esters of poly(ethylene oxide)-block-poly(2-hydroxyethyl-L-aspartamide). Part I: Effects of the level of methotrexate conjugation on the stability of micelles and on drug release. *Pharm. Res.* **17**, 607-611

[158] Bae, Y., Nishiyama, N., Fukushima, S., Koyama, H., Yasuhiro, M. and Kataoka, K. (2005) Preparation and biological characterization of polymeric micelle drug carriers with intracellular pH-triggered drug release property: tumor permeability, controlled subcellular drug distribution, and enhanced in vivo antitumor efficacy. *Bioconjug. Chem.* **16**, 122-130

[159] Mishra, B., Patel, B.B. and Tiwari, S. (2010) Colloidal nanocarriers: a review on formulation technology, types and applications toward targeted drug delivery. *Nanomedicine: Nanotechnology, Biology and Medicine.* **6**, 9-24

[160] Alexis, F., Rhee, J.W., Richie, J.P., Radovic-Moreno, A.F., Langer, R. and Farokhzad, O.C. (2008) New frontiers in nanotechnology for cancer treatment. *Urol. Oncol.* **26**, 74-85

[161] Keck C, Kobierski S, Mauludin R, Muller RH. (2008) Second generation of drug nanocrystals for delivery of poorly soluble drugs: smart crystals technology. DSOIS; **24**:124-8.

[162] Illum, L. and Davis, S.S. (1984) The organ uptake of intravenously administered colloidal particles can be altered using a non-ionic surfactant (Poloxamer 338). *FEBS Lett.* **167**, 79-82

[163] Troster, S.D. and Kreuter, J. (1992) Influence of the surface properties of low contact angle surfactants on the body distribution of 14C-poly(methyl methacrylate) nanoparticles. *J. Microencapsul.* **9**, 19-28

[164] Müller, R.H. and Wallis, K.H. (1993) Surface modification of i.v. injectable biodegradable nanoparticles with poloxamer polymers and poloxamine 908. *Int. J. Pharm.* **89**, 25-31

[165] Müller, R.H. and Wallis, K.H. (1993) Surface modification of i.v. injectable biodegradable nanoparticles with poloxamer polymers and poloxamine 908. *Int. J. Pharm.* **89**, 25-31

[166] Gref, R., Minamitake, Y., Peracchia, M.T., Trubetskoy, V., Torchilin, V. and Langer, R. (1994) Biodegradable long-circulating polymeric nanospheres. *Science.* **263**, 1600-1603

[167] Peracchia, M.T., Gref, R., Minamitake, Y., Domb, A., Lotan, N. and Langer, R. (1997) PEG-coated nanospheres from amphiphilic diblock and multiblock copolymers: Investigation of their drug encapsulation and release characteristics. *J. Controlled Release.* **46**, 223-231

[168] Riley, T., Stolnik, S., Heald, C.R., Xiong, C.D., Garnett, M.C., Illum, L., Davis, S.S., Purkiss, S.C., Barlow, R.J. and Gellert, P.R. (2001) Physicochemical Evaluation of Nanoparticles Assembled from Poly(lactic acid)−Poly(ethylene glycol) (PLA−PEG) Block Copolymers as Drug Delivery Vehicles. *Langmuir.* **17**, 3168-3174

[169] Heald, C.R., Stolnik, S., Kujawinski, K.S., De Matteis, C., Garnett, M.C., Illum, L., Davis, S.S., Purkiss, S.C., Barlow, R.J. and Gellert, P.R. (2002) Poly(lactic acid)−Poly(ethylene

oxide) (PLA−PEG) Nanoparticles: NMR Studies of the Central Solidlike PLA Core and the Liquid PEG Corona. *Langmuir.* **18**, 3669-3675

[170] Soppimath, K.S., Aminabhavi, T.M., Kulkarni, A.R. and Rudzinski, W.E. (2001) Biodegradable polymeric nanoparticles as drug delivery devices. *J. Controlled Release.***70**, 1-20

[171] Ameller, T., Marsaud, V., Legrand, P., Gref, R., Barratt, G. and Renoir, J.M. (2003) Polyester-poly(ethylene glycol) nanoparticles loaded with the pure antiestrogen RU 58668: physicochemical and opsonization properties. *Pharm. Res.* **20**,1063-1070

[172] de Faria, T.J., Machado de Campos, A. and Lemos Senna, E. (2005) Preparation and Characterization of Poly(D,L-Lactide) (PLA) and Poly(D,L-Lactide)-Poly(Ethylene Glycol) (PLA-PEG) Nanocapsules Containing Antitumoral Agent Methotrexate. *Macromolecular Symposia.* **229**, 228-233

[173] Teixeira, M., Alonso, M.J., Pinto, M.M. and Barbosa, C.M. (2005) Development and characterization of PLGA nanospheres and nanocapsules containing xanthone and 3-methoxyxanthone. *Eur.J.Pharm.Biopharm.* **59**, 491-500

[174] Prego, C., Torres, D., Fernandez-Megia, E., Novoa-Carballal, R., Quinoa, E. and Alonso, M.J. (2006) Chitosan-PEG nanocapsules as new carriers for oral peptide delivery. Effect of chitosan pegylation degree. *J.Control.Release.* **111**, 299-308

[175] Discher, D.E. and Eisenberg, A. (2002) Polymer vesicles. *Science.* **297**, 967-973

[176] Discher, B.M., Won, Y.Y., Ege, D.S., Lee, J.C., Bates, F.S., Discher, D.E. and Hammer, D.A. (1999) Polymersomes: tough vesicles made from diblock copolymers. *Science.* **284**, 1143-1146

[177] Discher, B.M., Won, Y.Y., Ege, D.S., Lee, J.C., Bates, F.S., Discher, D.E. and Hammer, D.A. (1999) Polymersomes: tough vesicles made from diblock copolymers. *Science.* **284**, 1143-1146

[178] Photos, P.J., Bacakova, L., Discher, B., Bates, F.S. and Discher, D.E. (2003) Polymer vesicles in vivo: correlations with PEG molecular weight. *J. Control. Release.* **90**, 323-334

[179] Quintana, A., Raczka, E., Piehler, L., Lee, I., Myc, A., Majoros, I., Patri, A.K., Thomas, T., Mule, J. and Baker, J.R.,Jr (2002) Design and function of a dendrimer-based therapeutic nanodevice targeted to tumor cells through the folate receptor. *Pharm. Res* **19**, 1310-1316

[180] Boas, U. and Heegaard, P.M. (2004) Dendrimers in drug research. *Chem. Soc. Rev.* **33**, 43-63

[181] Mainardes, R.M. and Silva, L.P. (2004) Drug delivery systems: past, present, and future. *Curr. Drug Targets.* **5**,449-455

[182] Hawker, C.J. and Frechet, J.M.J. (1990) Preparation of polymers with controlled molecular architecture. A new convergent approach to dendritic macromolecules. *J. Am. Chem. Soc.* **112**, 7638-7647

[183] Cloninger, M.J. (2002) Biological applications of dendrimers. *Curr. Opin. Chem. Biol.* **6**, 742-748

[184] Tripathi, P.K., Khopade, A.J., Nagaich, S., Shrivastava, S., Jain, S. and Jain, N.K. (2002) Dendrimer grafts for delivery of 5-fluorouracil. *Pharmazie.* **57**, 261-264

[185] Chauhan, A.S., Jain, N.K., Diwan, P.V. and Khopade, A.J. (2004) Solubility enhancement of indomethacin with poly(amidoamine) dendrimers and targeting to inflammatory regions of arthritic rats. *J. Drug Target.* **12**, 575-583

[186] El-Sayed, M., Kiani, M.F., Naimark, M.D., Hikal, A.H. and Ghandehari, H. (2001) Extravasation of poly(amidoamine) (PAMAM) dendrimers across microvascular network endothelium. *Pharm. Res.* **18**, 23-28

[187] Jevprasesphant, R., Penny, J., Jalal, R., Attwood, D., McKeown, N.B. and D'Emanuele, A. (2003) The influence of surface modification on the cytotoxicity of PAMAM dendrimers. *Int. J. Pharm.* **252**, 263-266

[188] Nigavekar, S.S., Sung, L.Y., Llanes, M., El-Jawahri, A., Lawrence, T.S., Becker, C.W., Balogh, L. and Khan, M.K. (2004) 3H dendrimer nanoparticle organ/tumor distribution. *Pharm. Res.* **21**, 476-483

[189] Müller, R.H., Mäder, K. and Gohla, S. (2000) Solid lipid nanoparticles (SLN) for controlled drug delivery – a review of the state of the art. *European Journal of Pharmaceutics and Biopharmaceutics.* **50**, 161-177

[190] Kaur, I.P., Bhandari, R., Bhandari, S. and Kakkar, V. (2008) Potential of solid lipid nanoparticles in brain targeting. *J. Control. Release.* **127**, 97-109

[191] Blasi, P., Giovagnoli, S., Schoubben, A., Ricci, M. and Rossi, C. (2007) Solid lipid nanoparticles for targeted brain drug delivery. *Adv. Drug Deliv. Rev.* **59**, 454-477

[192] Zara, G.P., Cavalli, R., Bargoni, A., Fundaro, A., Vighetto, D. and Gasco, M.R. (2002) Intravenous administration to rabbits of non-stealth and stealth doxorubicin-loaded solid lipid nanoparticles at increasing concentrations of stealth agent: pharmacokinetics and distribution of doxorubicin in brain and other tissues. *J. Drug Target.* **10**, 327-335

[193] Wissing, S.A., Kayser, O. and Muller, R.H. (2004) Solid lipid nanoparticles for parenteral drug delivery. *Adv. Drug Deliv. Rev.* **56**, 1257-1272

[194] Uchegbu, I.F. and Vyas, S.P. (1998) Non-ionic surfactant based vesicles (niosomes) in drug delivery. *Int. J. Pharm.* **172**, 33-70

[195] Kazi, K.M., Mandal, A.S., Biswas, N., Guha, A., Chatterjee, S., Behera, M. and Kuotsu, K. (2010) Niosome: A future of targeted drug delivery systems. *J. Adv. Pharm. Technol. Res.* **1**, 374-380

[196] Marianecci, C., Di Marzio, L., Rinaldi, F., Celia, C., Paolino, D., Alhaique, F., Esposito, S. and Carafa, M. (2013) Niosomes from 80s to present: The state of the art. *Adv. Colloid Interface Sci.* **205** C:187-206

[197] Azeem, A., Anwer, M.K. and Talegaonkar, S. (2009) Niosomes in sustained and targeted drug delivery: some recent advances. *J. Drug Target.* **17**, 671-689

[198] Rajera, R., Nagpal, K., Singh, S.K. and Mishra, D.N. (2011) Niosomes: a controlled and novel drug delivery system. *Biol. Pharm. Bull.* **34**, 945-953

[199] Hait S.K., Maulik S.P. (2002) Gemini surfactants: a distinct class of self-assembling molecules. *Curr Sci*; **82**:1101-11.

[200] Silva, S.G., Alves, C., Cardoso, A.M.S., Jurado, A.S., Pedroso de Lima, M.C., Vale, M.L.C. and Marques, E.F. (2013) Synthesis of Gemini Surfactants and Evaluation of Their Interfacial and Cytotoxic Properties: Exploring the Multifunctionality of Serine as Headgroup. *European Journal of Organic Chemistry.* 1758-1769

[201] Yan, Y., Lu, T. and Huang, J. (2009) Recent advances in the mixed systems of bolaamphiphiles and oppositely charged conventional surfactants. *J. Colloid Interface Sci.* **337**, 1-10

[202] Liu, T., Guo, R., Hua, W. and Qiu, J. (2007) Structure behaviors of hemoglobin in PEG 6000/Tween 80/Span 80/H2O niosome system. *Colloids Surf. Physicochem. Eng. Aspects.***293**, 255-261

[203] Mahale, N.B., Thakkar, P.D., Mali, R.G., Walunj, D.R. and Chaudhari, S.R. (2012) Niosomes: Novel sustained release nonionic stable vesicular systems — An overview. *Adv. Colloid Interface Sci.* 183–184, 46-54

[204] Talsma H, Steenbergen Mv, Borchert J, Crommelin D.(1994) A novel technique for the one-step preparation of liposomes and nonionic surfactant vesicles without the use of organic solvents. Liposome formation in a continuous gas stream: the 'bubble' method. *J Pharm Sci;* **83**:276-80.

[205] Hu, C. and Rhodes, D.G. (1999) Proniosomes: a novel drug carrier preparation. *Int. J. Pharm.* **185**, 23-35

[206] Yasam, V.R., Jakki, S.L., Natarajan, J. and Kuppusamy, G. (2013) A review on novel vesicular drug delivery: proniosomes. *Drug Deliv.* [Epub ahead of print]

[207] Fang, J.Y., Hong, C.T., Chiu, W.T. and Wang, Y.Y. (2001) Effect of liposomes and niosomes on skin permeation of enoxacin.*Int. J. Pharm.* **219**, 61-72

[208] Manconi, M., Sinico, C., Valenti, D., Lai, F. and Fadda, A.M. (2006) Niosomes as carriers for tretinoin. III. A study into the in vitro cutaneous delivery of vesicle-incorporated tretinoin. *Int.J.Pharm.* **311**, 11-19

[209] Carafa, M., Marianecci, C., Rinaldi, F., Santucci, E., Tampucci, S. and Monti, D. (2009) Span and Tween neutral and pH-sensitive vesicles: characterization and in vitro skin permeation. *J. Liposome Res.* **19**, 332-340

[210] Gudlur, S., Sukthankar, P., Gao, J., Avila, L.A., Hiromasa, Y., Chen, J., Iwamoto, T. and Tomich, J.M. (2012) Peptide nanovesicles formed by the self-assembly of branched amphiphilic peptides. *PLoS One.* **7**, e45374

[211] Fischer, R., Fotin-Mleczek, M., Hufnagel, H. and Brock, R. (2005) Break on through to the other side-biophysics and cell biology shed light on cell-penetrating peptides. *Chembiochem.* **6**, 2126-2142

[212] Frankel, A.D. and Pabo, C.O. (1988) Cellular uptake of the tat protein from human immunodeficiency virus. *Cell.* **55**, 1189-1193

[213] Green, M. and Loewenstein, P.M. (1988) Autonomous functional domains of chemically synthesized human immunodeficiency virus tat trans-activator protein. *Cell.* **55**, 1179-1188

[214] Rothbard, J.B., Garlington, S., Lin, Q., Kirschberg, T., Kreider, E., McGrane, P.L., Wender, P.A. and Khavari, P.A. (2000) Conjugation of arginine oligomers to cyclosporin A facilitates topical delivery and inhibition of inflammation. *Nat. Med* **6**, 1253-1257

[215] Fawell, S., Seery, J., Daikh, Y., Moore, C., Chen, L.L., Pepinsky, B. and Barsoum, J. (1994) Tat-mediated delivery of heterologous proteins into cells. *Proc. Natl. Acad. Sci. U.S.A.* **91**, 664-668

[216] Chiu, Y.L., Ali, A., Chu, C.Y., Cao, H. and Rana, T.M. (2004) Visualizing a correlation between siRNA localization, cellular uptake, and RNAi in living cells. *Chem. Biol.* **11**, 1165-1175

[217] Nagahara, H., Vocero-Akbani, A.M., Snyder, E.L., Ho, A., Latham, D.G., Lissy, N.A., Becker-Hapak, M., Ezhevsky, S.A. and Dowdy, S.F. (1998) Transduction of full-length TAT fusion proteins into mammalian cells: TAT-p27Kip1 induces cell migration.*Nat. Med.***4**, 1449-1452

[218] Koren, E. and Torchilin, V.P. (2012) Cell-penetrating peptides: breaking through to the other side. *Trends. Mol. Med.***18**, 385-393

[219] Mueller, J., Kretzschmar, I., Volkmer, R. and Boisguerin, P. (2008) Comparison of cellular uptake using 22 CPPs in 4 different cell lines. *Bioconjug. Chem.* **19**, 2363-2374

[220] Fonseca, S.B., Pereira, M.P. and Kelley, S.O. (2009) Recent advances in the use of cell-penetrating peptides for medical and biological applications. *Adv. Drug Deliv.Rev.* **61**, 953-964

[221] Conner, S.D. and Schmid, S.L. (2003) Regulated portals of entry into the cell. *Nature.* **422**, 37-44

[222] Henriques, S.T. and Castanho, M.A. (2008) Translocation or membrane disintegration? Implication of peptide-membrane interactions in pep-1 activity. *J. Pept. Sci.* **14,** 482-487

[223] Morris, M.C., Depollier, J., Mery, J., Heitz, F. and Divita, G. (2001) A peptide carrier for the delivery of biologically active proteins into mammalian cells. *Nat. Biotechnol.* **19,** 1173-1176

[224] Gupta, B., Levchenko, T.S. and Torchilin, V.P. (2005) Intracellular delivery of large molecules and small particles by cell-penetrating proteins and peptides. *Adv. Drug Deliv. Rev.* **57,** 637-651

[225] Torchilin, V.P. (2008) Cell penetrating peptide-modified pharmaceutical nanocarriers for intracellular drug and gene delivery. *Biopolymers.* **90,** 604-610

[226] Lindberg, S., Copolovici, D.M. and Langel, U. (2011) Therapeutic delivery opportunities, obstacles and applications for cell-penetrating peptides. *Ther. Deliv.* **2,** 71-82

Chapter 2 - Branched Oligopeptides Form Nano-Capsules with Lipid Vesicle Characteristics

This chapter has been reproduced in its current format with permission from 'Sukthankar, P., Gudlur, S., Avila, L.A., Whitaker, S.K., Katz, B.B., Hiromasa, Y., Gao, J., Thapa, P., Moore, D., Iwamoto, T., Chen, J. and Tomich, J.M. (2013) Branched Oligopeptides Form Nanocapsules with Lipid Vesicle Characteristics. Langmuir. 29 (47), 14648-14654' © 2013 American Chemical Society

2.1 Introduction

There is a need for new safe drug delivery vehicles that can better target specific tissues or organs and minimize off-target accumulation[1]. In Gudlur et al.[2], we described, for the first time, a drug delivery system in which two peptides of different lengths; and designed to mimic diacyl glycerols (**Fig. 2.1**) form water filled vesicles. In that paper we referred to these constructs as vesicles. Owing to the heuristic association of lipids with vesicles; we have introduced the term 'capsule' in an effort to negate the confusion between our peptidic nano-spheres and traditional lipid vesicles. The branch point lysine orients the two peptide segments at a 90˚ angle, similar to the geometry of diacyl phospholipids. The bis(FLIVI)-K-KKKK and bis(FLIVIGSII)-K-KKKK peptides together self-assemble with beta-like secondary structure to form a new class of capsules that are readily taken up by cells in culture while retaining trapped solutes. Since neither peptide alone forms stable capsules, we hypothesized that two sizes are required to accommodate the curvature of assembled capsules.

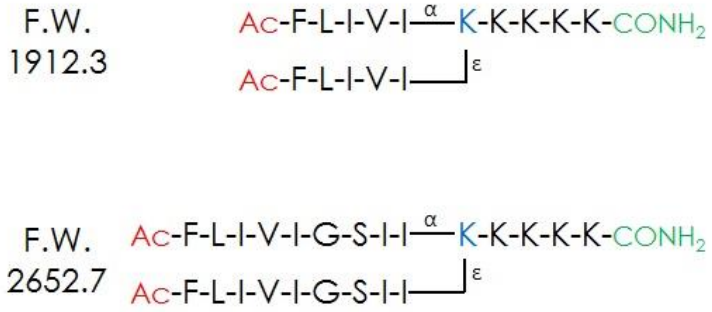

Figure 2.1. Branched Bilayer Forming Sequences

The fact that they undergo self-assembly gives us the ability to modify individual peptides with various ligands or markers that can then be incorporated into the aggregate. In the first paper we adducted the C-terminal lysine with fluorescent dyes and in another case included a cysteine residue at the C-terminus that was used to attach methyl mercury[2]. The labeled peptides are usually incorporated at 30 mole percent with unlabeled peptides, without affecting assembly or cellular uptake. The peptide capsules were also tested for thermal stability using Differential Scanning Calorimetry up to 95˚C and were found to maintain their structural and functional integrity at all studied temperatures. In this study we report on the phospholipid vesicle-like characteristics of our assemblies. The peptides are mixed and dried as monomers. Within minutes of adding water to the dried peptides, fibrils form, which soon coalesce into 20 nm capsules. It is during this phase that solutes become entrapped. Thereafter, the capsules begin fusing, and by 24 h appear as much larger structures (up to 1 μm, with most having diameters of 50-200 nm) (see **Fig. 2.2**). We were able to follow the fusion process by observing the dilution of a self-quenching fluorescent dye. Since cell and tissue uptake is size dependent, we also examined the effects of extruding the larger capsules through membranes with various pore sizes. Dropping the temperature to 4° C suspends the fusion process allowing for storage of the uniform sized material. These studies

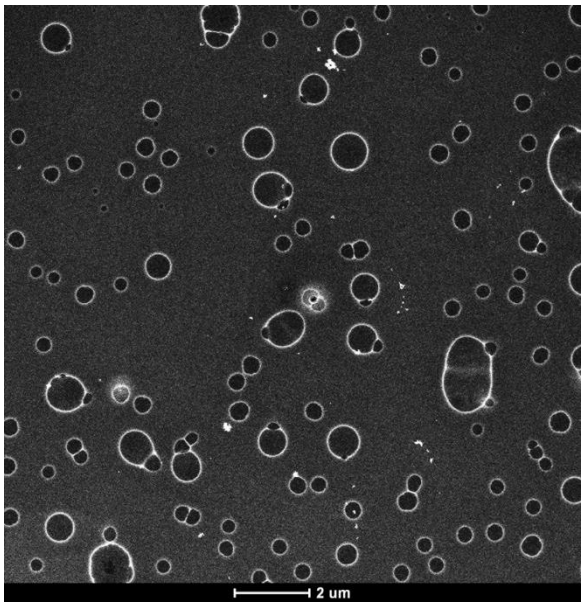

Figure 2.2. Scanning Transmission Electron Micrograph (STEM) Hg-Labeled Peptides 24 hr after mixing.
Capsules were prepared with 30% Me-Hg label in both peptides at 0.1 mM. The images were captured using annular dark field mode and then inverted to produce the final image.

together provide further evidence supporting the hypothesis that these branched sequences self-assemble into bilayers and form capsules in an aqueous environment.

2.2 Materials and Methods

2.2.1 Peptide Synthesis

Peptides were synthesized by solid phase peptide chemistry on 4-(2,4-Dimethoxyphenyl-Fmoc-aminomethyl) phenoxyacetyl-norleucyl-cross-Linked Ethoxylate Acrylate Resin[3] (Peptides International Inc; Louisville, Kentucky) on a 0.1 mmol scale using Fmoc (N-(9-fluorenyl) methoxycarbonyl)/tert-butyl chemistry on an ABI Model 431 peptide synthesizer (Applied Biosystems; Foster City, CA). The Fmoc amino acids were obtained from Anaspec, Inc (Fremont, CA). The branch point was introduced by incorporating $N^{\alpha,\varepsilon}$ di-Fmoc-L-Lysine in the fifth position from the C-terminus. De-protection of this moiety leads to the generation of two reactive amino sites that subsequently and simultaneous generate the bifurcated peptide branch point. This enables the addition of the hydrophobic tail segments FLIVI and FLIVIGSII to the common hydrophilic oligo-Lysine segment by the stepwise addition of Fmoc amino acids[4]. The N-terminal ends of the peptide were acetylated on the resin using Acetic Anhydride / N, N-Diisopropylethylamine / 1-Hydroxybenzotriazole prior to cleavage. The peptide was cleaved from the resin using TFA/water (98:2, v/v) for 90 min at RT to generate C-terminal carboxamide. The peptide product was washed 3x with diethyl ether and re-dissolved in water prior to lyophilization. The water used throughout this study is deionized, reverse osmosis treated and then distilled. The RP-HPLC purified peptides were dried in vacuo and characterized on a Bruker Ultraflex III matrix-assisted laser desorption ionization time of flight mass spectrometer (MALDI TOF/TOF) (Bruker Daltonics, Billerica, MA) using 2,5-dihydroxybenzoic

acid matrix (Sigma-Aldrich Corp., St. Louis, MO). The dried peptides were stored at room temperature.

2.2.2 Peptide Modifications (Me-Hg-Cys)

The synthesis of the cysteine modified peptides were effected on a 0.1mmol scale with standard Fmoc(N-(9-fluorenyl)methoxycarbonyl)/tert-butyl chemistry on CLEAR-Amide Resin (Peptides International Inc; Louisville, Kentucky) by means of N-α-Fmoc-S-p-methoxytrityl-L–cysteine (Anaspec, Inc; Fremont, CA) coupled to the resin at C-terminus. The remainder of the synthesis, cleavage, post cleavage processing and characterization was performed as previously described, to generate bis(FLIVI)-K-KKKK-C-$CONH_2$ and bis(FLIVIGSII)-K-KKKK-C-$CONH_2$ respectively[2]. Both cysteine adducted peptides were solubilized in water and reacted with 1 equivalent of Methylmercury(II) iodide (Sigma-Aldrich Corp., St. Louis, MO) at pH 9.8 for 6 h at RT[5, 6]. The resulting solution was reduced in vacuo and subsequently lyophilized to generate the desired product. The percent methyl mercury incorporated was determined by measuring the concentration of free cysteine remaining after the coupling reaction. Unlabeled peptides of equal concentration served as the control. Samples were treated with 4 mg/mL 5, 5'-Dithiobis-(2-nitrobenzoic acid) (Sigma-Aldrich Corp., St. Louis, MO) in pH 8.2, 0.1 M phosphate buffer. The fully reacted sample absorbance values were measured at 412 nm on a CARY 50 Bio UV/Vis spectrophotometer (Varian Inc., Palo Alto, CA) using a 0.3 cm path length quartz cuvette (Starna Cells Inc., Atascadero, CA)[7]. The concentrations of the peptides were calculated using the molar extinction coefficient (ε) of phenylalanine residues (two per sequence) at 257.5 nm (195 cm^{-1} M^{-1})[8, 9].

2.2.3 Capsule Formation and Encapsulation

The bis(FLIVI)-K-KKKK and bis(FLIVIGSII)-K-KKKK peptides were dissolved individually in neat 2,2,2-Trifluoroethanol. In this solvent the peptides are helical and monomeric thereby ensuring complete mixing when combined. Concentrations were determined as diluted samples in water using the absorbance of phenylalanine as previously described. The bis(FLIVI)-K-KKKK and bis(FLIVIGSII)-K-KKKK peptide samples were mixed in equimolar ratios to generate a final concentration of 0.1 mM, then dried *in vacuo*. The dried peptide samples were then hydrated to form capsules of desired concentration by the drop-wise addition of water.

2.2.4 S/TEM Sample Preparation

The 30% Me-Hg capsules were prepared in a manner similar to that previously detailed, by co-dissolving 0.7 mole equivalents of bis(FLIVI)-K-KKKK and bis(FLIVIGSII)-K-KKKK with 0.3 mole equivalents of their respective cysteine containing Me-Hg labeled variants in water, to a final concentration containing 0.1 mM each of bis(FLIVI)-K-KKKK and bis(FLIVIGSII)-K-KKKK. The dried peptide mixture was hydrated and allowed to stand for the indicted time intervals. Carbon Type A (15-25 nm) on 300 mesh support film grids with removable Formvar (Ted Pella Inc., Redding, CA) were immersed in chloroform to strip off the Formvar. These were subsequently negatively (hydrophilic) glow discharged[10] at 5 mA for 20 s using a EMS 150 ES Turbo-Pumped Sputter Coater/Carbon Coater (Electron Microscopy Sciences, Hatfield, PA) - the carbon end of the grids being exposed to the plasma discharge making the carbon film hydrophilic and negatively charged, thus allowing easy spreading of aqueous suspensions. Capsule sample solutions (6 μL) were spotted on to grids and allowed to stand for 5 min, after which, excess solution was wicked off the grid with a Kimwipe™ tissue (Kimberly-Clark

Worldwide Inc., Roswell, GA) and allowed to air dry before loading it into the FEI Tecnai F20XT Field Emission Transmission Electron Microscope (FEI North America, Hillsboro, Oregon) with a 0.18 nm STEM HAADF resolution and a 150X – 2306 x 106 X range of magnification[11]. Scanning transmission electron microscopy was carried out in the annular dark field mode with a single tilt of 17°.

2.2.5 Capsule Assembly Time Course Experiment

For the purposes of the time course experiment, 30% Me-Hg labeled 0.1mM, bis(FLIVIGSII)-K-KKKK:bis(FLIVI)-K-KKKK peptide capsules were prepared as before and spotted on negative glow discharged TEM grids at 0, 5, 25, 55 and 115 min post hydration to account for different time points (5,10, 30, 60 and 120 min respectively) during the process of assembly and fusion. For the purposes of the '0' min time point; separate 2.5 μL 0.1mM bis(FLIVIGSII)-K-KKKK and 2.5 μL 0.1 mM bis(FLIVI)-K-KKKK peptide samples were co-spotted on to the grid immediately upon hydration. After letting the sample stand on the grid for 5 min, the excess solution was wicked off, and the sample stained with 5 μL of an aqueous solution of 2% multi-isotope Uranyl Acetate (Uranium bis(acetato-o)dioxo-dihydrate). This was then allowed to stand for 5 min, after which the excess stain was wicked off and the sample allowed to air dry before studying it under a FEI Tecnai F20XT Field Emission Transmission Electron Microscope in the previously specified manner.

2.2.6 Coarse-grained Modeling

A modified MARTINI force field[2, 12-14] was used to describe the peptide and water molecules. The peptide backbone was represented by particle types for β secondary structure in the

hydrophobic segments, and coil particle types for the poly-lysine C-termini. The thickness of the bilayer membrane and the average area of each peptide were calculated by performing 100 ns molecular dynamics (MD) simulations of pure model bilayers[2]. In order for the bilayer to maintain the capsule curvature restriction, the outside leaflet requires a greater amount of the longer peptide (2:1= bis(FLIVIGSII)-K-KKKK:bis(FLIVI) -K-KKKK) than the inside leaflet (1:2 = bis(FLIVIGSII)-K-KKKK:bis(FLIVI)-K-KKKK). This ratio was based on preliminary results obtained using a titration assay that measured the solvent exposed thiols of added C-terminal cysteines in the assembled capsules (data not shown). To avoid overlap of peptides, the initial diameter (~28 nm) of the capsule is built larger than the experimentally observed 20nm. After 200 steps of energy minimization, a total of ~2 ns equilibrium simulations were carried out at 298K by incorporating several steps, in which harmonic potentials with gradually increasing strength was imposed on the peptides. All simulations were performed in CHARMM[14, 15] on the Beocat Research Cluster at Kansas State University. VMD[16] was used for preparation of the snapshots presented in this work.

2.2.7 Eosin Self-Quenching Curve

The fluorescence self-quenching of eosin was recorded by exciting 0, 10, 20, 40, 80, 90, 100, 125, 150, 175, 200, 400, 600, 800, 1000, 1500 and 2126 μM aqueous concentrations of eosin Y (Sigma-Aldrich Corp., St. Louis, MO) at 490 nm and scanning for observed emissions from 495-800 nm with a CARY Eclipse Fluorescence spectrophotometer (Varian Inc., Palo Alto, CA) (Scan rate: 600 nm/min; PMT detector voltage: 600 V; Excitation slit: 5 nm; Emission slit: 5 nm) using a 0.3 cm path length quartz cuvette. The resulting data was plotted as change in fluorescence intensity as well as change in λ_{max} as a function of increasing eosin concentration.

Fluorescence intensity was seen to increase with eosin Y concentration until about 100 μM after which the trend was reversed, and the intensity of fluorescence proceeded to decrease such that the fluorescence intensity of 1.13 mM eosin Y solution was lower than that of a 10 μM solution of the same. A consistent red shift of λ_{max} towards higher wavelengths was witnessed as a function of increasing concentrations of eosin Y – all consistent with the phenomenon of fluorescence self-quenching[17].

2.2.8 Salt Wash Study

The bis(FLIVIGSII)-K-KKKK:bis(FLIVI)-K-KKKK peptide capsules (1.0 mM) were prepared using the protocol described earlier. One hour post hydration, the capsule containing solution was centrifuged at 14,000 x g in Amicon ultra- 0.5 mL, 30K molecular weight cut-off (MWCO) centrifugal units with regenerated cellulose filters (Millipore, Billerica, MA) using a Thermo Electron Legend 14 personal micro-centrifuge (Thermo Fisher Scientific Inc., Waltham, MA). At the conclusion of the spin, the removable-filter unit was inverted and placed in a fresh tube and spun at 2000 x g for 5 min to recover the remaining volume containing the capsules. The filtered preformed capsules were then incubated in a 2.13 mM aqueous eosin Y solution for 30 min to coat the exterior surface. The capsule-eosin solution was filtered as described above to remove the excess eosin. This solution was used as a control and its fluorescence measured by excitation at 490 nm and scanning for observed emissions from 495-800 nm with a CARY Eclipse Fluorescence spectrophotometer as previously described. The samples were split into two aliquots – the first aliquot was washed with water prior to centrifugal MWCO filtration and the other with an equal volume of 200 mM Sodium Trifluoroacetate (Na-TFA, Sigma-Aldrich Corp., St. Louis, MO) - and simultaneously subjected to the MWCO centrifugation process along with

isolation and re-solvation of the capsule containing solution. The samples were rescanned with the spectrometer. Subsequently both samples were washed and centrifuged with just water multiple times and measured for eosin fluorescence after each centrifugal cycle. A cycle by cycle comparison between water washed capsules versus Na-TFA salt-water washed capsules demonstrated a significant decrease in the eosin fluorescence signal.

2.2.9 Capsule Fusion Study

1.0 mM and 20.0 mM dried samples of bis(FLIVIGSII)-K-KKKK:bis(FLIVI)-K-KKKK peptide capsules were made in a manner analogous to the one previously described. Both these samples were simultaneously solvated; the 1 mM sample with aqueous 2.13 mM eosin Y and the 20.0 mM sample with water, and then allowed to stand for 30 min. All samples were subjected to three 30 kDa MWCO centrifugation process cycles starting with a 5 min incubation with 200 mM Na-TFA salt, and then spin filtered. For the second and third centrifugation cycles, the eosin encapsulating capsules were washed with water prior to centrifugation. At the end, both the 1.0 mM and 20.0 mM capsules were suspended in water; then immediately mixed in equal volumes; an aliquot of which was stored at 4˚C and the other placed in a 0.3 cm quartz cuvette and scanned for observed emission from 495-800 nm for 4 h with a scan every 5 min, upon excitation at 490 nm, with a CARY Eclipse Fluorescence spectrophotometer (Scan rate: 600 nm/min; PMT detector voltage: 800 V; Excitation slit: 5 nm; Emission slit: 5 nm). The 4˚C aliquot was scanned for change in fluorescence intensity at 6 h and 24 h intervals post mixing. The resulting data was plotted as change in intensity and change in λ_{max} as a function of capsule fusion over time.

2.2.10 Resizing the Capsules

A 0.1 mM solution of bis(FLIVIGSII)-K-KKKK:bis(FLIVI)-K-KKKK peptide capsules with 30% Me-Hg label was prepared in a manner as described previously and allowed to stand for 24 h. A 6 µL aliquot was then loaded on a negatively glow discharged TEM grid, allowed to dry for 5 min, with the excess solution wicked off and then air dried as previously described. The 24 h capsule solution was divided into two parts and then individually loaded in gas-tight syringes and extruded respectively through 0.1 µm and 0.03 µm 19 mm Whatman® Nuclepore™ Track-Etched Polycarbonate Membranes using the Avanti® Mini-Extruder (Avanti Polar Lipids, Inc., Alabaster, AL); with at least 40 passes through the membrane per sample. The extruded samples were immediately spotted on negatively glow discharged TEM grids as with the 24 h sample and observed using a FEI Tecnai F20XT Field Emission Transmission Electron Microscope as before.

2.2.11 Beta Amyloid Test

Due to the speed at which these peptides adopt beta-structure in water we tested the sequences to see if they were amyloids using the Thioflavin T assay[13]. In the presence of amyloid proteins the fluorescence excitation and emission spectra of the dye are right shifted and enhanced emission at the new wavelength.

2.3 Results and Discussion

For this system to find utility as a drug delivery vehicle, there are numerous parameters requiring definition and control. These issues include — understanding capsule formation, controlling their size and tuning their stability. The work presented here addresses the first two of these properties. As shown in **Fig. 2.2**, at 24 h post hydration of the peptide mixture, we always observe a heterogeneous population of capsules. Preparing a defined and uniform size for these nano-capsules can be highly useful since size is known to play a key role in where these materials segregate when used in vivo[19-22]. Studies were performed to track capsule formation by following the time course for the appearance of the smallest observable capsules. Knowing this size provides guidance regarding the size of molecules capable of being entrapped. Even though larger capsules ultimately form due to fusion, this initial size likely limits the size of the trapped solutes added during the initial hydration step.

To begin, the four peptides— bis(FLIVI)-K-KKKK, bis(FLIVIGSII)-K-KKKK, bis(FLIVI)-K-KKKK-C-Hg-Me and bis(FLIVIGSII)-K-KKKK-C-Hg-Me are dissolved in 100% trifluoroethanol (TFE). A ratio of 1:1 is set for all of the FLIVI and FLIVIGSII peptides. The methyl mercury peptides are present at a 30 mole percent and provide an electron dense heavy metal for visualizing the structures in S/TEM. In the electron beam, the irradiated Hg emits an X-ray at a specific energy that can be detected and is visualized as a white glow in the S/TEM images. In TFE, the peptides adopt a helical conformation, indicating a monomeric state where they can mix completely. When the solvent is removed *in vacuo*, the helical conformation is preserved as judged by the FTIR wave number for the Amide I band at 1650 cm^{-1} (data not

shown). Water is added to the dry material and mixed. In water, the peptides begin to adopt a beta (extended) conformation and start assembling. Aliquots were removed at the indicated times and dried on copper grids for imaging. Representative images at various time points are shown in **Fig 2.3.** At t = 0, the peptides (glowing elements) appear as amorphous structures.

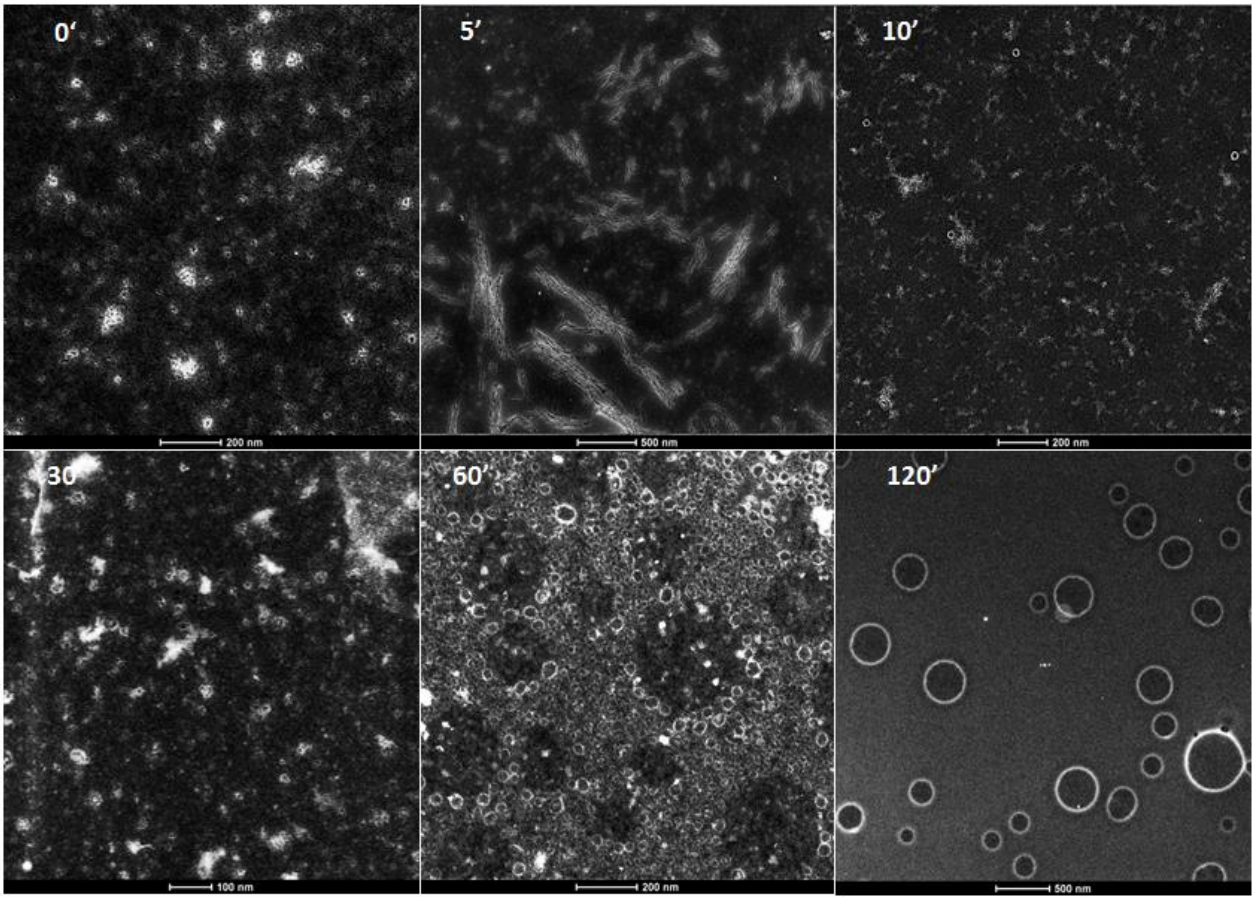

Figure 2.3. Time course of capsule formation. S/TEM images of Hg-Labeled peptides taken at the indicated times. Capsules contain 30% Me-Hg label in both the bis(FLIVI) and bis(FLIVIGSII) peptides at 0.1 mM. The images were captured using annular dark field mode and then inverted to produce the final image. The scale bars at the bottom of the micrographs, in nm, are 200, 500, 200, 100, 200, and 500, for the 0, 5, 10, 30, 60 and 120 min time points, respectively.

However by 5 min, the peptides appear as long micron length nano fibrils that occur in clusters. Incubation of the nano fibrils with Thioflavin T did not result in any spectral shift, suggesting that an absence of amyloid structure in these fibrils[23]. The fibril structures appear to be transient

and quickly break down by 10 min, when the first capsules also start to appear. Small and relatively uniform capsules of ~20 nm in diameter begin to accumulate by 30 min. By 60 min, the small capsules begin to associate and form what appears to be, 'spheres of spheres'. The associations lead to spheres with different diameters as judged by the dark centers associated with the alignment of the 20 nm capsules. By 120 min the small capsules are no longer visible and appear to have all fused to make well-defined capsules of the sizes ranging from 100 nm to

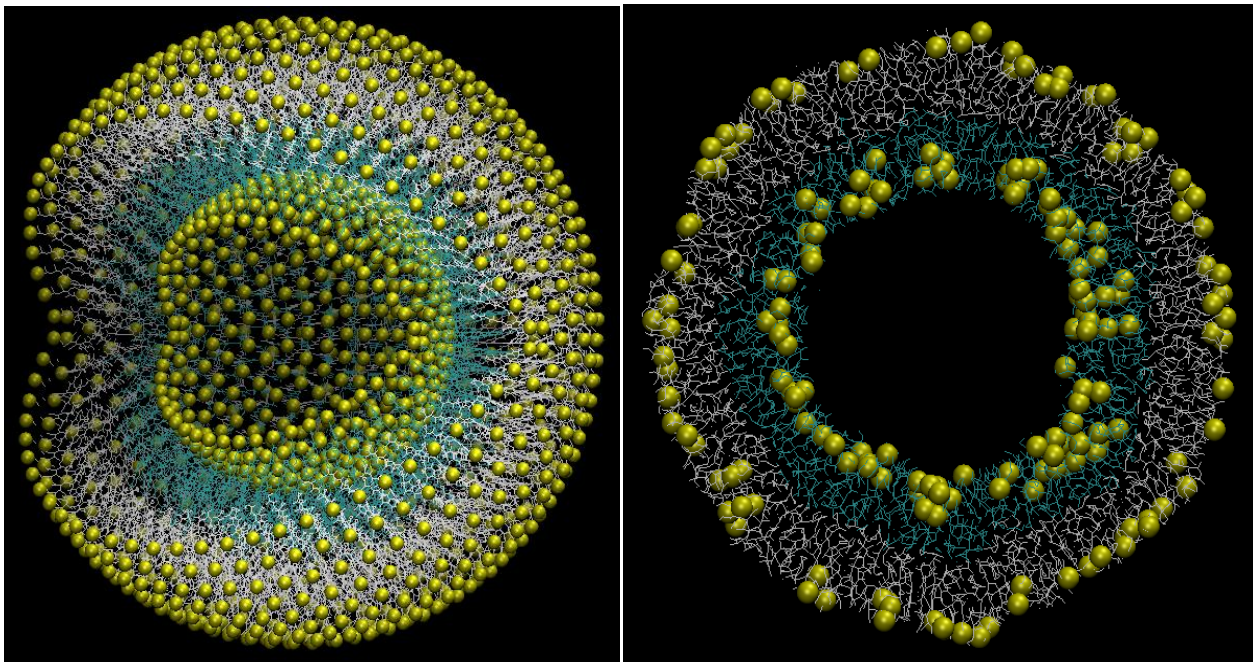

Figure 2.4. Snapshots of initial and equilibrated structures of capsule coarse-grained model.
The C-terminus group is represented by a yellow sphere; outside peptides are shown as light grey lines, with inside shown as cyan lines. The outside diameter of capsule is ~22nm

greater than 500 nm. These results illustrate the dynamic nature of the self-assembly process of the capsules. Based on the observation that 20 nm-sized capsules are the first to appear, we built a similarly sized capsule *in silico* using coarse-grained modeling to assess whether the peptide could be assembled into a bilayer that formed a stable capsule structure, and to illustrate a plausible three dimensional structure of the same. The system was modeled using a modified

version of the MARTINI coarse-grained (CG) force field[2, 12, 13, 24] that was implemented in CHARMM[14, 15]. The model capsule, shown in **Fig. 2.4** left panel, contains a total of 1680 peptides, of which 1080 and 600 peptides are on the outside and the inside leaflet, respectively. To overcome strain due to curvature, the outer leaflet contains 66.7% of the larger peptide while the inner leaflet contains only 33.3%. After energy minimization and equilibration simulation, the capsule slightly contracted but well retained the overall structure. The thickness of the outside leaflet is somewhat longer than that of the inside leaflet, due to higher ratio of the longer peptide. The inside volume of the capsule is about 760 nm^3. The cross section of capsule (**Fig. 2.4**, right panel) shows that the two peptide leaflets have minimal inter-digitation, which is consistent with earlier IR results showing parallel beta-sheets[2]. Inter-digitated strands would result in anti-parallel IR signatures.

As shown in **Fig. 2. 2** the capsules continually grow in size at room temperature and reach sizes in excess of a micron by 24 h. To further establish that the growth is through direct fusion of small capsules, we measured the dilution of the self-quenching fluorescent dye eosin Y (2 mM) as a function of the loaded capsules fusing with a large excess of capsules containing just water. The surface of the capsules is highly cationic due to the presence of all the lysine residues and it adsorbs anionic compounds such as 5,6-Carboxyfluorescein in a saturable manner[2]. Eosin Y is also anionic at neutral pH and can interact strongly with the outer surface of the capsules. The following protocol was developed to displace any surface-bound anionic molecules without compromising the integrity of the capsules or releasing their contents. This protocol involves first washing the eosin Y loaded capsules with 200 mM Na-TFA at neutral pH, followed by two water washes. The TFA^- salt is a strong counter ion and easily displaces most of the dye in the first wash. Water alone was also effective but required 5 washes to reach the

1% residual bound level. Each wash takes additional time that, in turn, affects the size of the capsules as shown in the next set of experiments. Use of the strong counter ion will also allow us to wash capsules free of negatively charged endotoxin (LPS), which can elicit innate immune responses in vivo. Eosin bound to the outer surface of preformed capsules shows an emission maximum at 535 nm, which corresponds to free eosin, indicating that its bound concentration is sufficiently low to prevent self-quenching. After filtering the capsules containing 30% Me-Hg with the 0.22 μ polycarbonate filter and the previously described washing steps, a sample was removed for imaging by TEM, with a representative image shown in **Fig. 2.5**. Most of the capsules are in the 20-30 nm in size with several beginning to associate to form larger structures.

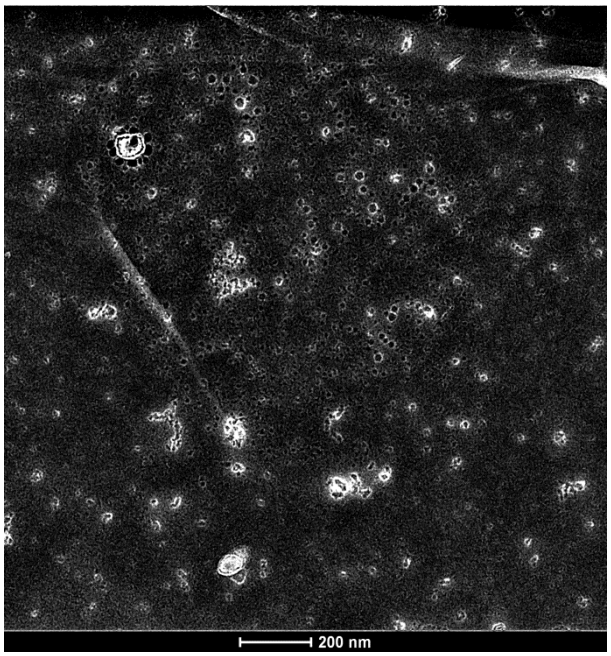

Figure 2.5. TEM image of Me-Hg labeled washed capsules just prior to fusion experiment.

Being able to wash the surface clean of the anionic eosin Y allows us to assess the behavior of encapsulated material. At 2.0 mM the self-quenching dye has a λ_{max} of 522 nm with an intensity just 22% of its maximum unquenched concentration, which has a red shifted λ_{max} of 550 nm. By mixing a small percentage of the salt/water washed eosin filled capsules with an excess of water filled capsules (1:20), the initial fusions lead to a rapid dilution of the dye. As shown in **Fig. 2.6A** fluorescence intensity increases with a concomitant red shift at the earliest times. The fluorescence intensity increases as a consequence of the decreased self-quenching

associated with each fusion event. The reaction was allowed to proceed for 235 min. At the end of the reaction the sample was salt washed and passed through a 30 kDa filter to measure any released dye. No significant fluorescence was observed, indicating that the capsules remained intact throughout the experiment. Another control with all eosin-loaded capsules and no water capsules showed no increase in fluorescence over the same time frame. **Fig. 2.6B** is a derivative plot that shows the percent fluorescence increase at a given time point relative to the maximal fluorescence intensity observed. Because of the red shift that occurs during this process, the plotted intensity values were taken at the individual λ_{max} values for each time point. An apparent equilibrium is reached around 3 h. This endpoint represents the time where all the capsules have attained equivalent entrapped concentrations. Further fusions will continue as judged by EM studies; however there is no discernible change in the entrapped concentration of the larger structures.

The insert to **Fig. 2.6A** shows the fluorescence for an aliquot of the fusion sample stored for 6.5 h at 4° C. Note that the fluorescence spectrum is similar to that of the earliest time point in **Fig. 2.6A**. The 6.5 h time window is well beyond the duration needed for the capsules to reach a maximum fluorescent intensity at room temperature. This result suggests that lowering the temperature to 4° C is sufficient to prevent the capsules from changing size through fusion; thus providing for a convenient means to control the capsule size. The cessation of fusion at the lower temperature is most likely a kinetic effect, with the process slowed down enough to afford better size control. The fusion experiment also provides further evidence that the capsules are hollow and water filled. Given the amphiphilic nature of the peptides, the most reasonable explanation of how a water-filled capsule could form is that they behave like diacyl phospholipids and assemble into bilayers thereby creating a hydrophilic lined hollow space (see **Fig. 2.4**). The

capsule's propensity to fuse at room temperature tends to result in a heterogeneous population with a significant range of sizes on the order of microns. This property is undesirable for

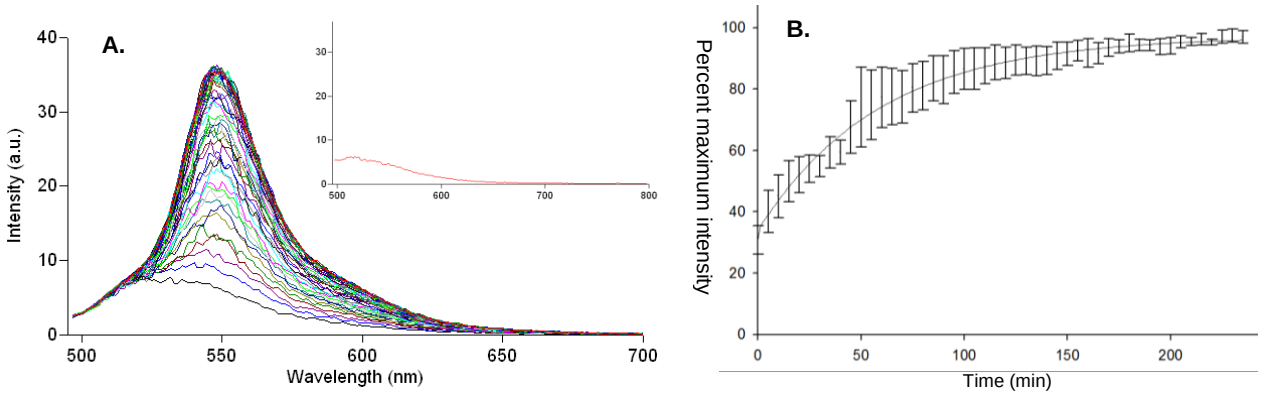

Figure 2.6 Capsule Fusion Study.

Salt washed eosin Y trapped capsules were mixed with water filled capsules in the ratio of 1:20 at RT. A) Five min fluorescence scans of eosin encapsulated vesicles spectra were taken at 5 min intervals for 235 min. The inset shows spectrum of sample stored at 4° C for 6.5 h. The units shown are identical to those in panel A. B) Measured maximum eosin fluorescence intensity as a function of time during the fusion reaction. The t = 0 represents quenched value of salt washed eosin encapsulate in the capsules (2.0 mM). The data was fitted to a second order exponential with the error bars representing the SEM with n = 3.

potential applications as drug delivery vehicles due to strict size dependent cellular uptake in vivo. Liposomes made from diacyl phospholipids are easily resized to uniform diameters using membrane extrusion filters. Given the behavioral similarities of the peptide capsules to lipid vesicles, applying membrane extrusion to resize the peptide capsules seems appropriate. In the resizing experiment the Me-Hg labeled peptides were mixed and allowed to fuse for 24 h at RT. The size distribution observed is typical for a 24 h sample. At that point an aliquot of the peptide capsule solution was extruded back and forth numerous times through a 100 nm membrane filter followed by a final extrusion using a 30 nm membrane filter. Immediately after repeated extrusions through each membrane, a small volume was spread on a TEM grid and dried. The 24

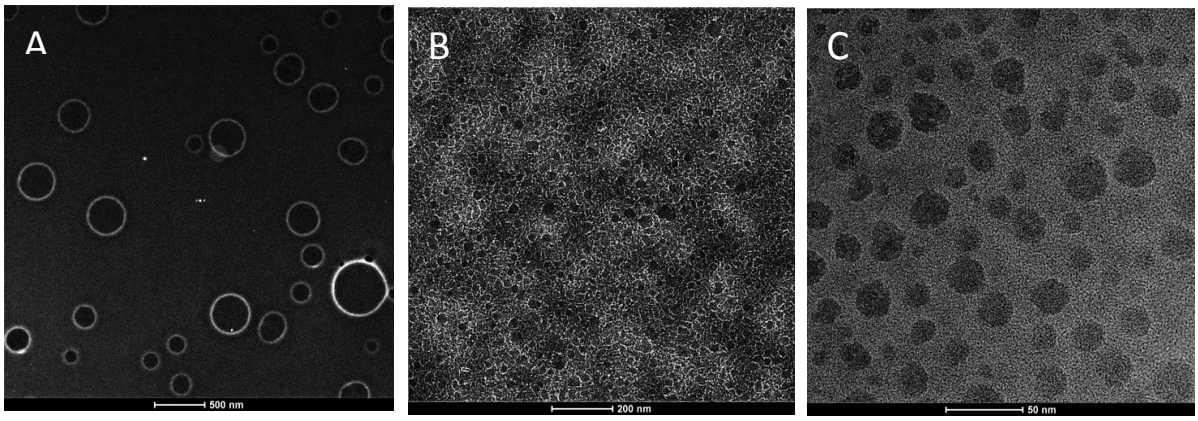

Figure 2.7 Filter Resizing Study.

TEM images are shown for the A) 24 h control. B) 100 nm membrane extruded material and C) 30 nm membrane extruded material. All figures are displayed as inverse images

hr sample (**Fig. 2.7A**) shows the larger peptide capsules normally seen at this time point. The 100 nm, extruded sample (**Fig. 2.7B**) shows a mixed population of heterogeneous capsules that range in size from 20 to 60 nm in diameter. Few if any 100 nm capsules have ever been observed using this technique suggesting that this size is disfavored over smaller ones. The 30 nm filter extruded capsules (**Fig. 2.7C**) are observed as a relatively homogeneous population with most capsules ranging in diameter from 20-30 nm. The 30 nm pore size is the smallest available through our vendor and attempting to go even smaller may not be feasible since our capsules assemble as 20 nm structures. After extruding, if the capsules are allowed to sit for any appreciable time at RT they rapidly begin re-fusing (data not shown). In the absence of refrigeration, we envision using the samples immediately after the extrusion process to ensure size uniformity. Upon dilution in the blood stream or tissues, the likelihood of fusion is remote. This study clearly shows that regulating the size of the capsules is straightforward.

2.4 Conclusion

In this report we characterized several properties of peptide capsules that form through the self-assembly of two branched peptides, bis(FLIVI)-K-KKKK and bis(FLIVIGSII)-K-KKKK (**Fig. 1**). The assembly process is initiated with the formation of nano-fibrils that condense into 20 nm water filled spheres. It is during this phase that solutes can be encapsulated. Washes with strong counter-ions followed by water washes remove any surface bound materials without disrupting the loaded capsules. Subsequently the nano capsules begin to associate to form spheres of spheres that ultimately fuse to form larger capsules. The larger capsules continue to fuse and grow to more than micron diameter structures. Fusion kinetics were followed by observing the dilution of the encapsulated self-quenching eosin Y dye, as dye labeled capsules combined with an excess of water containing capsules. The capsules are easily resized to form homogeneous populations in the 20-30 nm range by extruding them through polycarbonate filters with controlled pore sizes. In addition, dropping the temperature to 4° C suspends the fusion process allowing the production of uniform and stable peptide capsules that could be used in vivo.

2.5 Abbreviations

TFA, Trifluoroacetic acid; Na-TFA, Sodium Trifluoroacetate; TFE, 2,2,2 – Trifluoroethanol; S/TEM, Scanning Transmission Electron Microscopy; FTIR, Fourier Transform Infrared Spectroscopy; MWCO, Molecular Weight Cut Off; MD, Molecular Dynamics; SEM, Standard Error of Mean.

2.6 Acknowledgement

This is publication 14-071-J from the Kansas Agricultural Experiment Station. Partial support for this project was provided by PHS-NIH grant # RO1 074096 (to J.M.T) and the Terry Johnson Cancer Center for summer support (for P.S. and S.G.)

2.7 References

1. Couvreur, P. Nanoparticles in drug delivery: Past, present and future. *Advanced Drug Delivery Reviews **2013***, 65 (1), 21–23.

2. Gudlur, S., Sukthankar, P., Gao, J. Avila, L.A., Hiromasa, Y., Chen, J., Iwamoto, T., Tomich, J.M. Peptide Nanovesicles Formed by the Self-Assembly of Branched Amphiphilic Peptides. *PLOS ONE*. **2012 7** (9) e45374.

3. Kempe M. and Barany G. CLEAR: A Novel Family of Highly Cross-Linked Polymeric Supports for Solid Phase Synthesis, *J. Am. Chem. Soc.* **1996** 118,7083-7093.

4. Iwamoto, T., Grove, A., Montal, M.O., Montal, M. and Tomich, J.M. Chemical synthesis and characterization of peptides and oligomeric proteins designed to form transmembrane ion channels. *Int. J. Pept. Protein Res.* **1994** 43:597-607.

5. Gruen, L.C. Stoichiometry of the reaction between methyl mercury (II) iodide and soluble sulphides. *Anal. Chim. Acta.* **1970** 50: 299-303.

6. Forbes W.F., Hamlin C.R. Determination of –SS and –SH groups in proteins. I. A reassessment of the use of methylmercuric iodide. *Canadian Journal of Chemistry*. **1968** 46, 3033-3040.

7. Anderson, W.L., Wetlaufer, D.B. A new method for the disulfide analysis of peptides. *Analyt. Biochem.* **1975** 67, 493-502

8. Chen, R. F. Measurements of absolute values in biochemical fluorescence spectroscopy. *J. Research National Bureau Standards.* **1972** 76A (6), 593-606.

9. Sponer H. Remarks on the Absorption Spectra of Phenylalanine and Tyrosine in Connection with the Absorption in Toluene and Paracresol. J. *Chem. Phys*. **1942** 10, 672.

10. Aebi, U. and Pollard, T.D. A glow discharge unit to render electron microscope grids and other surfaces hydrophilic. *J. Electron Microsc. Tech.* **1987** 7, 29-33.

11. Utsunomiya, S. and Ewing, R.C. Application of High-Angle Annular Dark Field Scanning Transmission Electron Microscopy, Scanning Transmission Electron Microscopy-Energy Dispersive X-ray Spectrometry, and Energy-Filtered Transmission Electron Microscopy to the Characterization of Nanoparticles in the Environment. *Environ. Sci. Technol.* **2003** 37, 786-791.

12. Monticelli L, Kandasamy SK, Periole X, Larson RG, Tieleman DP, and Marrink SJ. The MARTINI coarse-grained force field: Extension to proteins. *J. Chem. Theory. and Comput.* **2008** 4 (5),819–834.

13. LeVine, H., 3rd. Thioflavine T interaction with synthetic Alzheimer's disease β - amyloidpeptides: Detection of amyloid aggregation in solution Protein Science. **1993** 2, 404-410.

14. Brooks BR, Bruccoleri RE, Olafson BD, States DJ, Swaminathan S, Karplus M. CHARMM - A program for macromolecular energy, minimization, and dynamics calculations. *J. Comput. Chem.* **1983** 4 (2), 187–217.

15. Brooks BR, Brooks CL, Mackerell AD, Nilsson L, Petrella RJ, Roux B, Won Y, Archontis G, Bartels C, Boresch S, Caflisch A, Caves L, Cui Q, Dinner AR, Feig M, Fischer S, Gao J, Hodoscek M, Im W, Kuczera K, Lazaridis T, Ma J, Ovchinnikov V, Paci E, Pastor RW, Post CB, Pu JZ, Schaefer M, Tidor B, Venable RM, Woodcock HL, Wu X, Yang W, York DM, Karplus M. CHARMM: The biomolecular simulation program. *J Comput Chem.* **2009** 30 (10), 1545–1614.

16. Humphrey W, Dalke A, Schulten K. VMD: Visual molecular dynamics. *J Mol Graph* **1996** 14 (1), 33–38.

17. Bellin, J.S. and Oster, G. Photoreduction of Eosin in the Bound State. *J. Am. Chem. Soc.* **1957** 79, 2461-2464.

18. LeVine, H., 3rd. Thioflavine T interaction with synthetic Alzheimer's disease β - amyloidpeptides: Detection of amyloid aggregation in solution Protein Science. **1993** 2, 404-410.

19. Sun X, Rossin R, Turner JL, Becker ML, Joralemon MJ, Welch MJ, Wooley KL. An Assessment of the Effects of Shell Cross-linked Nanoparticle Size, Core Composition, and Surface PEGylation on in Vivo Biodistribution. *Biomacromolecules.* **2005** 6(5), 2541–2554.

20. Stolnik S, Illum L, Davis SS. Long circulating microparticulate drug carriers. *Adv Drug Deliv Rev*. **1995** 16 (2–3), 195–214.

21. Huang S-D. Stealth nanoparticles: high density but sheddable PEG is a key for tumor targeting. *J Control Release.* **2010** 145(3), 178–181.

22. Decuzzi P, Godin B, Tanaka T, Lee SY, Chiappini C, Liu X, Ferrari M. Size and shape effects in the biodistribution of intravascularly injected particles. *J Control Release*. **2010** 141(3), 320–327.

23. Groenning, M. Binding mode of Thioflavin T and other molecular probes in the context of amyloid fibrils—current status *J Chem Biol*. **2010** 3(1),1-18.

24. Marrink SJ, Risselada HJ, Yefimov S, Tieleman DP, de Vries AH. The MARTINI force field: Coarse grained model for biomolecular simulations. *J Phys Chem B.* **2007** 111 (27),7812–7824

Chapter 3 - Branched Amphiphilic Peptide Capsules: Cellular Uptake and Retention of Encapsulated Solutes

This chapter has been reproduced in its current format with permission from 'Sukthankar, P., Avila, LA; Whitaker, S.K; Iwamoto, T; Morgenstern, A; Apostolidis, C; Liu, K; Hanzlik, R.P., Dadachova, E; Tomich, J.M. (2014) Branched Amphiphilic Peptide Capsules: Cellular Uptake and Retention of Encapsulated Solutes. Biochimica et Biophysica Acta – Biomembranes. 1838 (9), 2296-305 © 2014 Elsevier.

3.1 Introduction

There is a great deal of interest in the area of nanoparticle-mediated therapies. Nano-carrier mediated targeted cellular therapy is a rapidly growing area of research for the treatment of malignant and infectious diseases. Particle emitting radioisotopes complemented with a targeting moiety are being recognized as some of the most promising cytotoxic candidates for the treatment of cancerous tumors. Nano-particles enjoy distinct advantages in the delivery of drug payloads. Their nano sizes enable them to be directly injected into systemic circulation[1,2] and afford them longer circulating times.[3,4] Furthermore, the circulating time can be increased by the surface modification of nanoparticles with hydrophilic moieties such as polyethylene glycol,[5,6,7] and nanoparticles composed of biodegradable polymers can be tuned to release their drug payload in a controlled fashion; either by micelle dissociation, polymer degradation, diffusion or in combination.[8,9,10] Mechanisms of nanoparticle internalization into cells are influenced by their physiochemical properties. Biocompatible nanocomposites such as lipid based carriers (liposomes and micelles); polymeric vesicles designed from amphiphilic block co-polymers[11] such as polyethylene glycol-polylactic acid (PEG-PLA) and PEG-polycaprolactone (PEG-PCL);[12] nanocapsules;[13,14] Bola-amphiphiles (amphiphilic molecules possessing two polar heads

on both sides of an aliphatic chain) such as aminoundecyltriethoxysilane (AUT);[15,16] and carbon nanotubes[17] have been studied for their efficacy as delivery systems.

Liposomes are preferred over other delivery systems due to their ability to encapsulate both hydrophobic and hydrophilic contents. They can also be modified with respect to their fatty acid and head group composition, and surface alterations to modulate drug release and target affinity. Some of the issues associated with liposomes such as degradation by hydrolysis, oxidation, sedimentation, aggregation, or fusion during storage are being addressed with the development of niosomes[18] and proniosomes,[19,20] however further testing is need to fully establish safety and efficacy.

The selection of any nanoparticle for a specific pharmacological use is contingent on its mechanism of cellular uptake and intracellular trafficking.[21] In addition, concerns relating to the successful encapsulation of cargo, stability, specificity, bio-reactivity, biodegradability and toxicity are also relevant. The ability to release their contents is not necessarily a requirement for certain cargos. In the case of Targeted Alpha particle Therapy (TAT) - a treatment modality for metastatic cancer and infectious diseases - the advantageous properties of ^{225}Ac [22] are partially offset by its systemic toxicity[23] due to the potential accumulation of its daughter nuclides in off-target sites. Utilization of alpha-emitters requires containment systems that allow the high-energy alpha particles to penetrate target tissues while retaining the radionuclide and its daughter isotopes. This poses a considerable challenge since the energy (5 to 8 MeV / ^{225}Ac α-particle) released is sufficient to disrupt the integrity of most traditional nano-carriers. This property has hampered the development of ^{225}Ac as a viable radio-therapeutic agent.[24,25] The current use of chelating agents for ^{225}Ac radioimmunotherapy has been challenging as a consequence of the poorly defined coordination chemistry of Ac(III), owing to the lack of stable isotopes to enable

routine chemical analysis.[26] Chelators like EDTA, DTPA, DOTA and PEPA[27,28] have been used to complex with ^{225}Ac with varying degrees of success. On the other hand the potential of the otherwise promising ^{225}Ac -HEHA macrocylic complex in radiotherapy[29] has been marred by instability, due to the coordinated ^{225}Ac radionuclide decaying into its daughter isotopes.[26]

Efforts to develop bifunctional chelators capable of stably binding ^{225}Ac to antibodies as well as competently containing resulting daughter nuclides at target sites, has not been successful. This has forced the development of sterically stabilized pegylated liposomes[30] and stable pegylated phosphatidylcholine-cholesterol liposomes[31] for radioimmunotherapeutic

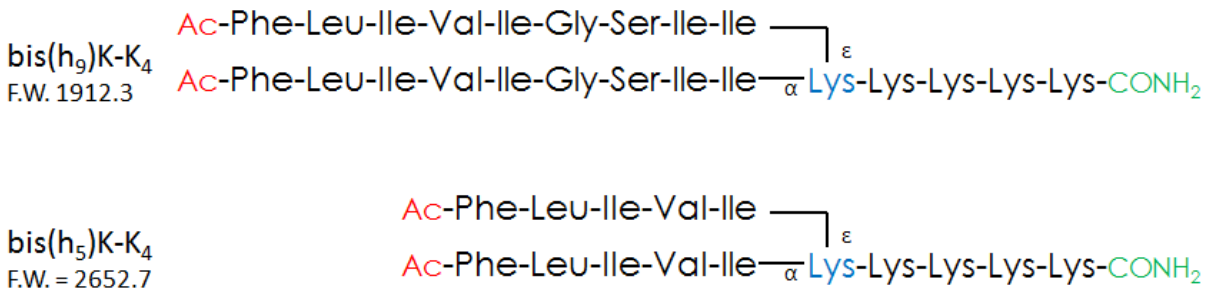

Figure 3.1 Bilayer Forming Branched Amphiphilic Peptide Sequences

applications despite the inherent instability and retention based limitations associated with traditional liposomal systems. Moreover, novel liposomal carriers such as MUVELs (Multivesicular liposomes) - involving the passive entrapment of small vesicles into large liposomes - have been designed to enhance the targeting capabilities and the retention of alpha particle emitting daughters of ^{225}Ac, in an effort to better utilize their positive cytotoxic potential.[32] All these liposome directed encapsulation techniques are however lengthy and tedious;[30-32] and involve considerable preparation times that include complex formation of ^{225}Ac with a chelate, annealing procedures, extended waiting periods, extrusions and centrifugation; apart from addressing various issues to counter physiochemical problems such as possible

oxidation due to alpha emissions[33,34] and beta[35] and gamma[36] radiation. The work presented herein presents an alternative and flexible means of radionuclide encapsulation that is easy to perform and generates stable in vivo constructs.

Peptide based nano-assemblies show promise as nano-delivery vehicles for the safe, targeted transport of drugs to specific tissues and organs, with minimal off target accumulation[37] by overcoming some of the problems associated with traditional lipid and viral based delivery systems. BAPCs (Branched Amphiphilic Peptide Capsules) are a new class of self-assembling peptide nano-capsular spheres[38,39] formed during the cooperative association of a mixture of two (15-23 residue) poly-cationic branched amphiphilic peptides (**Fig 3.1**). The hydrophobic core sequences are derived from an internal fragment of CaIVS3, the human dihydropyridine sensitive L-type calcium channel segment.[40] The ability of the BAPCs to form bilayer-delimited spheres (**Fig. 2**) capable of trapping solutes is a consequence of the unique characteristics of its constituent peptides - bis(FLIVI)-K-K_4 and bis(FLIVIGSII)-K-K_4, which reversibly transition from an alpha helical conformation in 2,2,2-Trifluoroethanol, to a beta sheet in water.[38,39] The branch point lysine in the sequence orients the two peptide segments at ~90˚ angle, mimicking the geometry of diacyl phospholipids. Coarse grain molecular dynamic simulations, [38] consistent with S/TEM analysis, indicate the presence of a single capsular bilayer (3 - 4 nm) comparable to that of a phospholipid system, which is below the discerning resolution of electron microscopy.

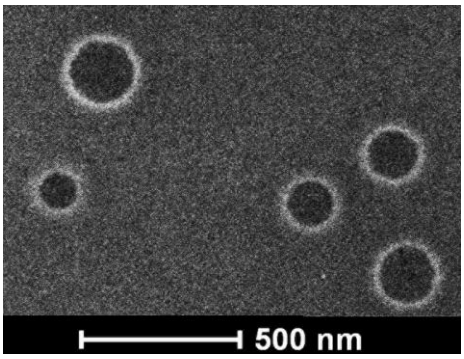

Figure 3.2 S/TEM image of BAPCs. They containing 30% Hg label and imaged at 2 h post hydration w/ negative glow discharge and uranyl acetate staining prepared as previously described.[39]

Recently, we described how the flexible BAPCs possess many of the properties of phospholipid vesicles, such as fusion, solute encapsulation and an ability to be resized by membrane extrusion through polycarbonate filters with defined pore sizes.[39] We also demonstrated several biophysical characteristics including, their mode of assembly, high thermodynamic stability, and their kinetics of fusion. The BAPCs can – like their lipid counterparts – be both resized, and maintained there by placing them at 4° C. The versatility of these peptides to self-assemble enables us to tag individual monomers with ligands and molecular markers for a variety of analytical and functional assays, making these constructs particularly suited as biocompatible vehicles for the targeted delivery of cargo into the cells. In this report, we study the stability, cellular uptake, load capacity, retention within biological environments for extended periods of time, tolerance to a radionuclide load, biodistribution and capacity to maintain their structural integrity even when subjected to alpha particle emissions.

3.2 Materials and Methods

3.2.1 Peptide Synthesis

3.2.1.1 Synthesis of bis(FLIVI)-K-K$_4$ and bis(FLIVIGSII)-K-K$_4$ variants

Peptides were synthesized using solid phase peptide chemistry on 4-(2,4-dimethoxyphenyl-Fmoc-aminomethyl) phenoxyacetyl-norleucyl-cross-Linked Ethoxylate Acrylate Resin[41] (Peptides International Inc; Louisville, Kentucky) on a 0.1 mmol scale using Fmoc (N-(9-fluorenyl) methoxycarbonyl)/tert-butyl chemistry on an ABI Model 431 peptide synthesizer (Applied Biosystems; Foster City, CA). This resin yields the carboxyamide at the C-terminus upon cleavage. The Fmoc amino acids were obtained from Anaspec, Inc (Fremont, CA). The branch point was introduced by incorporating $N^{\alpha,\varepsilon}$ di-Fmoc-L-Lysine in the fifth position from the C-terminus. Deprotection of the two Fmoc protecting groups leads to the generation of two reactive sites that allow for the generation of the bifurcated peptide branch point. This enables the simultaneous addition of either of the hydrophobic tail segments, FLIVI and FLIVIGSII to the common hydrophilic oligo-Lysine segment by the stepwise addition of Fmoc amino acids.[42] The N-termini of the peptide were acetylated on the resin using Acetic Anhydride / N, N-Diisopropylethylamine / 1-Hydroxybenzotriazole prior to cleavage. The peptide was cleaved from the resin using Trifluoroacetic acid (TFA)/H_2O (98:2, v/v) for 90 min at RT. The released peptide product was washed 3× with diethyl ether and re-dissolved in water prior to lyophilization. The water used throughout this study is deionized, reverse osmosis treated and then distilled. The RP-HPLC purified peptides were dried in vacuo and characterized on a Bruker Ultraflex III matrix-assisted laser desorption ionization time of flight mass

spectrometer (MALDI TOF/TOF) (Bruker Daltonics, Billerica, MA) using 2,5-dihydroxybenzoic acid matrix (Sigma-Aldrich Corp., St. Louis, MO). The dried peptides were stored at RT.

3.2.1.2 Synthesis of Rhodamine labeled Peptide bis(FLIVI)-K-K_4

'Dye labeled peptides' were synthesized by solid phase peptide chemistry on a 0.1 mmol scale on MBHA[43] (4-methylbenzhydrylamine) resin (Anaspec, Inc., Fremont, CA). After coupling the first amino acid (N^{α} - Fmoc - N^{ε} -*t*- Boc - L – lysine), the resin was treated with TFA/Dichloromethane/ H_2O (80:18:2, v/v/v) for 30 min to remove the side chain *t*-butoxycarbonyl protecting group; exposing the lysyl ε amine. This was then manually reacted with the N-Hydroxysuccinimide ester of Rhodamine B (Sigma-Aldrich Corp., St. Louis, MO) in presence of N-N-Diisopropylethylamine to generate the label on the C-terminal Lysine. The N^{α} - Fmoc was de-protected and the remainder of the synthesis was carried out as indicated earlier. The labeled peptide was cleaved from the resin using standard HF cleavage protocol.[44,45] The concentrations of all peptides were calculated using the molar extinction coefficient (ε) of phenylalanine residues (two per sequence) at 257.5 nm (195 cm^{-1} M^{-1})[46,47] on a CARY 50 Bio UV/Vis spectrophotometer (Varian Inc., Palo Alto, CA) using a 0.3 cm path length quartz cuvette (Starna Cells Inc., Atascadero, CA). The Rhodamine B adducted sequences were incorporated at a prescribed mole percentage along with the unlabeled bis(FLIVI)-K-K_4 sequence of the BAPCs and utilized in fluorescence experiments.

3.2.1.3 Synthesis of Pep-1

Pep-1 (Ac-KETWWETWWTEWSQPKKKRKV-CONH-$(CH_2)_2$-SH) was synthesized by solid phase peptide synthesis using Fmoc-Cysteamine-SASRIN™ resin, 0.6 meq/gm, (Bachem,

Torrance, CA) on an Applied Biosystems 431A Peptide Synthesizer at a 0.1 mmol scale using standard Fmoc(N-(9-Fluorenyl)methoxycarbonyl)/tert-butyl chemistry as described.[42] The Fmoc amino acids used for the synthesis were obtained from Anaspec, Inc (Fremont, CA). The N-terminal amino group was acetylated and the peptide was cleaved from the resin using TFA/water/triisopropylsilane (94:4:2, v/v/v) for 90 min at RT to generate the C-terminal thiol. The peptide product was washed 3× with diethylether and redissolved in water prior to lyophilization. This was then purified using Reversed Phase - HPLC with 0.1% TFA / H_2O and 0.1%TFA / 90% Acetonitrile, as the binary solvent system. The purified peptide was dried in vacuo and characterized on a Bruker Ultraflex III matrix-assisted laser desorption ionization time of flight mass spectrometer (MALDI TOF/TOF) (Bruker Daltonics, Billerica, MA) using α-Cyano-4-hydroxycinnamic acid matrix (Sigma-Aldrich Corp., St. Louis, MO). The dried peptides were stored at RT.

3.2.2 Capsule Formation and Encapsulation

The bis(FLIVI)-K-KKKK and bis(FLIVIGSII)-K-KKKK peptides were dissolved individually in neat 2,2,2-Trifluoroethanol (TFE, Sigma-Aldrich Corp, St. Louis MO). In this solvent the peptides are helical and monomeric thereby ensuring complete mixing when combined. Concentrations were determined as diluted samples in water using the absorbance of phenylalanine as described in **section 3.2.1.2**. The bis(FLIVI)-K-KKKK and bis(FLIVIGSII)-K-KKKK peptide samples were mixed in equimolar ratios to generate a fixed calculated concentration of 0.1 mM in the final volume(s), then dried *in vacuo*. The dried peptide samples were then hydrated to form capsules of desired concentration by the drop-wise addition of water.

3.2.3 HeLa Cell Culture

HeLa cells were obtained from Dr. Stella Y. Lee's laboratory (Division of Biology, Kansas State University) and grown in Dulbecco's minimum essential medium (Life Technologies, Grand Island, NY) with 10 % fetal bovine serum. Cell cultures were passaged every 3rd-4th day by trypsinizing them using TrypLETM Express (Life Technologies, Grand Island, NY) and were kept in a humidified incubator at 37°C and 5% CO_2. The medium was replaced every 72 h with no addition of antibiotics.

3.2.4 Cellular uptake of Branched Amphiphilic Peptide Capsules

3.2.4.1 Cellular Uptake and Lysosomal co-localization of BAPCs

HeLa cells were seeded on confocal 35 mm clear petri-dishes at a density of$1x10^4$ cells/mL and grown to ~ 80% confluence and washed twice with PBS. Thereafter, 750 µl of fresh medium was added along with a 250 µl aqueous suspension of BAPCs incorporating 30% Rhodamine B label on the bis(FLIVI)-K-K4 peptide. The final concentration of BAPCs was 50 µM. The cells were incubated for 4 h at 37°C at 5% CO_2 . After a PBS wash, the cells were then incubated for 5 min with LysoTracker® Green DND-26 probe (Molecular Probes, Carlsbad, CA) at a final concentration of 75 nM and washed again with PBS. Cells were observed and images acquired using a Zeiss LSM 510 Meta Confocal Microscope (Carl Zeiss, Gottingen, Germany).

3.2.4.2 Cellular Uptake of BAPCs at different Temperatures

HeLa cells were seeded on 12 mm culture dishes at a density of $1x10^4$ cells/mL and grown to ~60% confluence. Fresh media at 4°C and 37°C respectively was added to the cells. Immediately thereafter, 100 µL of media was replaced by a solution of BAPCs prepared with 30

% Rhodamine B label on the bis(FLIVI)-K-K_4 peptide. The final peptide concentration was 100 µM and cells were incubated for 2 h at 4 °C and 37 °C respectively. Cells were fixed with 3.7% formaldehyde at RT for 2 h, followed by a wash in PBS-T (PBS solution containing 1% Triton X-100) (Fisher Scientific LLC, Pittsburgh, PA). Subsequently, cells were incubated with Mouse Anti-β-tubulin mAb antibody,[48] 2G7D4 (Gen Script USA Inc., Piscataway, NJ) at dilutions of 1:1000 for 6 h. After three washes with PBS-T, the tissues were incubated 3 h with secondary antibody, Alexa Fluor® 488 goat anti-mouse IgG (Molecular Probes, Carlsbad, CA). Stained tissues were washed again with PBS-T and mounted in glycerol containing the nuclear stain DAPI (2 µg mL^{-1}; Sigma-Aldrich Corp., St. Louis, MO). Cells were observed and images acquired using a Zeiss LSM 510 Meta Confocal Microscope (Carl Zeiss, Gottingen, Germany).

3.2.5 Fluorescence and confocal microscopy

Images for **Figure 3.2** were taken using a LSM 700 laser scanning confocal microscope (Carl Zeiss, Gottingen, Germany) and for **Figure 3. 3** were taken using a Zeiss LSM 510 Meta Confocal Microscope (Carl Zeiss, Gottingen, Germany). The cell boundary and structure was visualized using "Differential interference contrast microscopy (DIC)". All measurements, except where stated, were performed with un-fixed, live cells.

3.2.6 Protein Uptake Studies

HeLa cells were seeded into 11 mm wells (48-well plate) at a density of $1x10^4$ cells/well and grown to roughly 60% confluence. Immediately thereafter, fresh media was added to the cells and 100 µL of the same was replaced by a solution of BAPCs containing Tcytc (5(6)-TAMRA labeled cytochrome c) and TRNaseA ((5(6)-TAMRA labeled RNase A) respectively. A

parallel experiment was performed following the same protocol, but with Pep-1 + Tcytc and Pep-1 + TRNaseA respectively, as positive controls for protein uptake. The final concentrations of peptides in each well were; 50 μM for BAPCs and for 5 μM for Pep-1. Cells were incubated for 3 h, washed twice with pre-warmed PBS prior to taking epifluorescence images. Subsequently, cells were trypsinized and allowed to re-attach for 18 h and images re-acquired.

3.2.7 Long term cellular uptake study

HeLa cells were seeded on 11 mm culture dishes at a density of $1x10^4$ cells/well and grown to ~60% confluence. Immediately thereafter, 100 μL of media was replaced by a solution of BAPCs containing 30 % Rhodamine B adducted bis(FLIVI)-K-K_4; with a final BAPC concentration of 100 μM. The cells were incubated at 37°C in an atmosphere of 5% CO_2 in air. The culture was kept for 14 days after which confocal microscopy images were acquired as previously detailed. Cells were trypsinized twice during this period and the media was replaced every 72 h.

3.2.8 Encapsulation and retention of ^{225}Ac in BAPCs.

The bis (FLIVIGSII)-K-K_4 and bis (FLIVI)-K-K_4 peptides (100 μM ea.) were mixed in their monomeric conformation in 50% TFE/H_2O to ensure proper mixing and then dried. The dried peptides were rehydrated using a 0.15 M ammonium acetate buffer containing 100 μCi ^{225}Ac with ligand DOTA (tetraazacyclododecane-1,4,7,10-tetraacetic acid; Macrocyclics, Dallas, TX) and allowed to incubate for 2 h. Non-encapsulated radionuclide was removed by spin filtering the mixture with a 30-kDa cut-off membrane filter followed by several buffer washes. At the indicated time points, aliquots of BAPCs were withdrawn, separated from supernatant on

the 30-kDa cut-off membrane filter and the ^{225}Ac activity remaining in the BAPCs was quantified immediately and afterwards at 4 h to account for the daughters decay, on a 1282 Compugamma CS, Universal Gamma Counter (LKB Wallac, Geithersburg, MD) equipped with the multi-channel analyzer using 150-600 keV energy window for ^{225}Ac and its daughters.

3.2.9 Cellular uptake of the BAPC-encapsulated ^{225}Ac into CasKi cells.

CasKi cells (human metastatic cervical cancer cell line) were obtained from ATCC and grown as previously described.[49] BAPCs carrying ^{225}Ac were then used immediately to treat cells, to ensure that the BAPCs diameters remain within the 50-200 nm range. Samples of 10^6 cells in triplicate were mixed with BAPC encapsulated ^{225}Ac; the cells were spun into pellet at 0, 1, 2, 4, 6 and 24 h, and the ^{225}Ac in the cellular pellet was quantified in the gamma counter as described in **section 3.2.8**.

3.2.10 Biodistribution of ^{225}Ac and its daughter ^{213}Bi

All animal experiments were conducted with the permission of the Albert Einstein College of Medicine Institute for Animal Studies. ^{225}Ac was encapsulated into BAPCs by addition of 500 µL 0.15 M ammonium acetate buffer with pH of 6.5 containing 60 µCi ^{225}Ac chloride, to 1 mM lyophilized peptides for 30 min at room temperature. After incubation the non-incorporated ^{225}Ac was removed by centrifugation on a micro-concentrator with a 30 kDa MW cut off filter. The degree of ^{225}Ac incorporation into the BAPCs was calculated to be approximately 30% of the starting amount of 60 µCi. The ^{225}Ac-BAPCs were then diluted with sterile 0.15 M ammonium acetate buffer and eight CD-1 male mice were injected intraperitoneally (IP) with 2 µCi ^{225}Ac-BAPCs/100 µL. As controls eight CD-1 male mice were IP injected with 2 µCi free $^{225}AcCl_3$/100 µL. At 1 and 24 hrs post-injection, four mice from each

group were humanely sacrificed and their blood, liver, kidneys and bone were removed, weighed and counted for radioactivity in a gamma counter as described previously in **section 3.2.8**.

3.3 Results and Discussion

3.3.1 Cellular Uptake of Branched Amphiphilic Peptide Capsules

In our earlier studies we noted that synthetic branched amphiphilic peptides self-assembled to form solvent filled bilayer delimited spheres (BAPCs) that had characteristic qualities (e.g., thermal, proteolytic and chaotrope stability, cellular uptake, and low cytotoxicity) that made them potential candidates for drug delivery; and as such they might provide certain advantages over conventional lipid and/or viral based drug delivery systems.[38] Apart from carrying out a number of biophysical studies we also carried out studies that characterized the initial assembly and subsequent fusion of the BAPCs. The ability to re-size and then maintain the BAPCs at fixed sizes allowed for the generation of stable capsules that could exploit cellular fenestration and transport processes.[39]

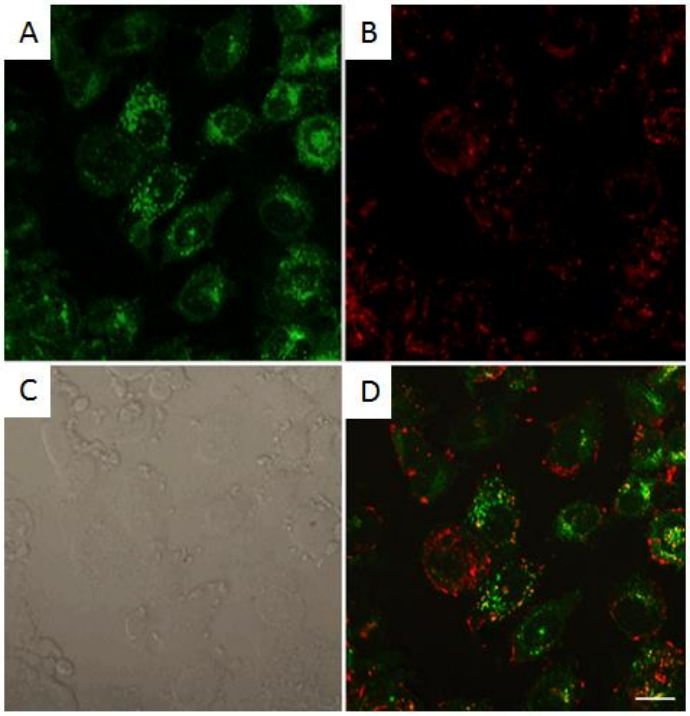

Figure 3.3 Lysosomal co-localization of BAPCs
Confocal microscopy analysis of HeLa cells incubated at 37°C with 50 μM 30% Rhodamine B labeled BAPCs for 4 h. **A)** HeLa cells with lysosomal stain (green) **B)** Rhodamine B labeled BAPCs (red) **C)** Bright field Image **D)** Merge image showing co-localization of BAPCs and the lysosomes (yellow). Scale bar = 20 μm.

These results prompted our current studies on the cellular uptake and release capabilities of these

nano-capsules. We hypothesized that cellular degradative processes would eventually cause release of the encapsulated solutes within the BAPCs. Realizing that BAPCs initially form as 20-30 nm (diameter) capsules, we also wanted to determine the maximum size of a solute that could be entrapped, as well as determine the limits of percent solute encapsulation from solution during the formation of the BAPCs. Initial studies demonstrated the loading, solute retention and cellular uptake capabilities of the BAPCs by observing the in vitro cellular co-localization of two-color fluorescence from Rhodamine B labeled BAPCs incorporating 5(6)-Carboxyfluorescein solution encapsulate.

To examine cellular uptake and intra-cellular localization of BAPCs (**Fig 3.3**); 50 μM BAPCs prepared with a 30% Rhodamine B labeled bis(FLIVI)-K-K_4 were incubated with HeLa cells for 4 h; with the Lysomes stained using LysoTracker Green DND-26, as described in **section 3.2.4.1.** As can be seen, the stained lysosomes (green) as well as the Rhodamine B labeled BAPCs (red) are visualized in the HeLa cells, in **Fig 3.3A** and **Fig 3.3B** respectively. Upon merging the two images (**Fig 3.3D)** both co-localized and non co-localized BAPCs are observed, with non co-localized particles predominating. At 2 h incubation most the BAPCs seem to be co-localized with the lysosomes (data not shown). These results indicate that BAPCs enter cells through the endosomal route yet rapidly escape the late endosomes; most like due to lysis caused by the proposed *proton-sponge effect*, commonly observed for cationic particles.[50]

In another experiment (**Fig 3.4**) HeLa cells were treated with the Rhodamine labeled BAPCs followed by immune-fluorescence labeling prior to fixation; to monitor uptake at two different temperatures, 4°C and 37°C. The cell nuclei were stained with DAPI (blue) and cellular β-Tubulin was stained with Alexa Fluor® 488 goat anti-mouse IgG (green) as previously described in **section 2.4.2** Cells incubated at 37°C (**Fig 3.4B**) readily took up the BAPCs while

those incubated at 4°C did not; instead the BAPCs appeared to accumulate at the cell surface (**Fig 3.4A**), presumably outside the cell.

These results indicate that cellular uptake is energy dependent. Endocytosis is a general mechanism of cellular uptake that is associated with receptor binding and/or attachment to the cellular membrane prior to internalization.[51] Non-endocytotic membrane fusion based uptake is known to be a function of the phase transition of the cellular lipid bilayer,[52] whereas penetration

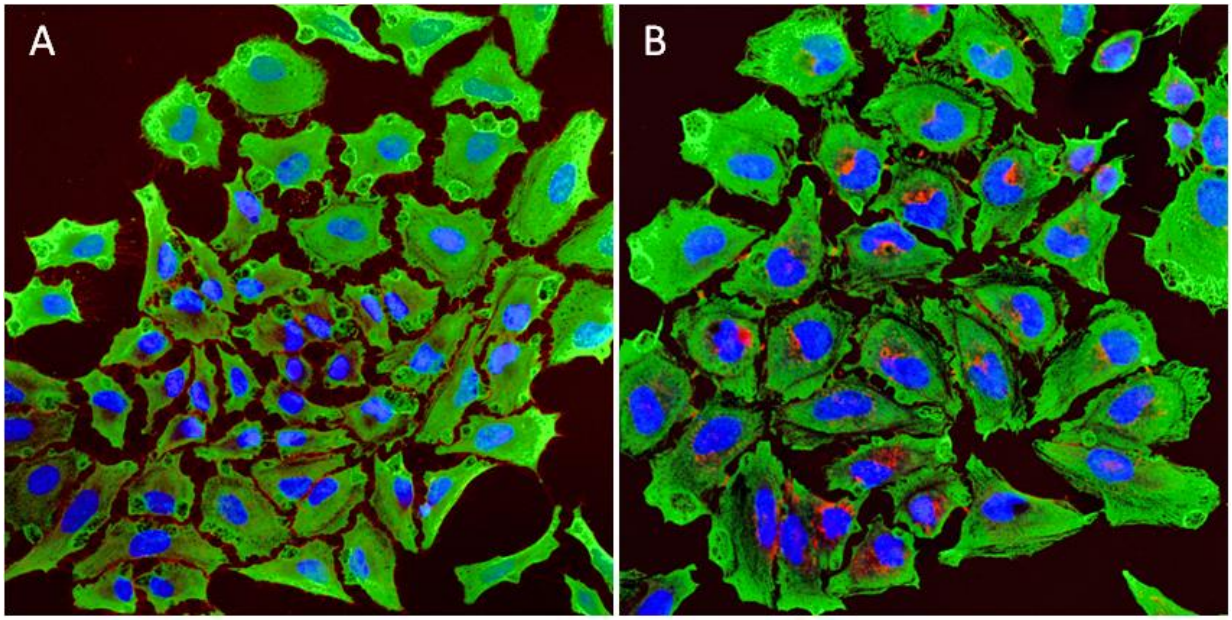

Figure 3.4 Temperature Dependence of Cellular Uptake.

Confocal microscopy analysis of HeLa cells incubated with 100 μM 30% Rhodamine B labeled BAPCs for 2 h. **A)** HeLa cells at 4 ˚C and **B)** at 37 ˚C.

through the cellular membrane - observed with certain poly-cationic cell penetrating peptides - appears to proceed in an energy independent manner.[53,54] The exact mechanism of BAPC uptake is not fully understood and might proceed via any of the above-mentioned mechanisms; however it seems conceivable based on lysosomal co-localization and temperature dependent uptake data, that BAPCs are internalized by the cellular machinery via an energy dependent endocytotic pathway, The mechanistic studies of BAPC uptake were however not the main thrust of this work.

3.3.2 Encapsulation and retention.

Early in our work with BAPCs, we tried to encapsulate several small proteins, namely TAMRA-labeled RNase A (TRNaseA,13.7 kDa), and TAMRA-labeled cytochrome c (Tcytc,

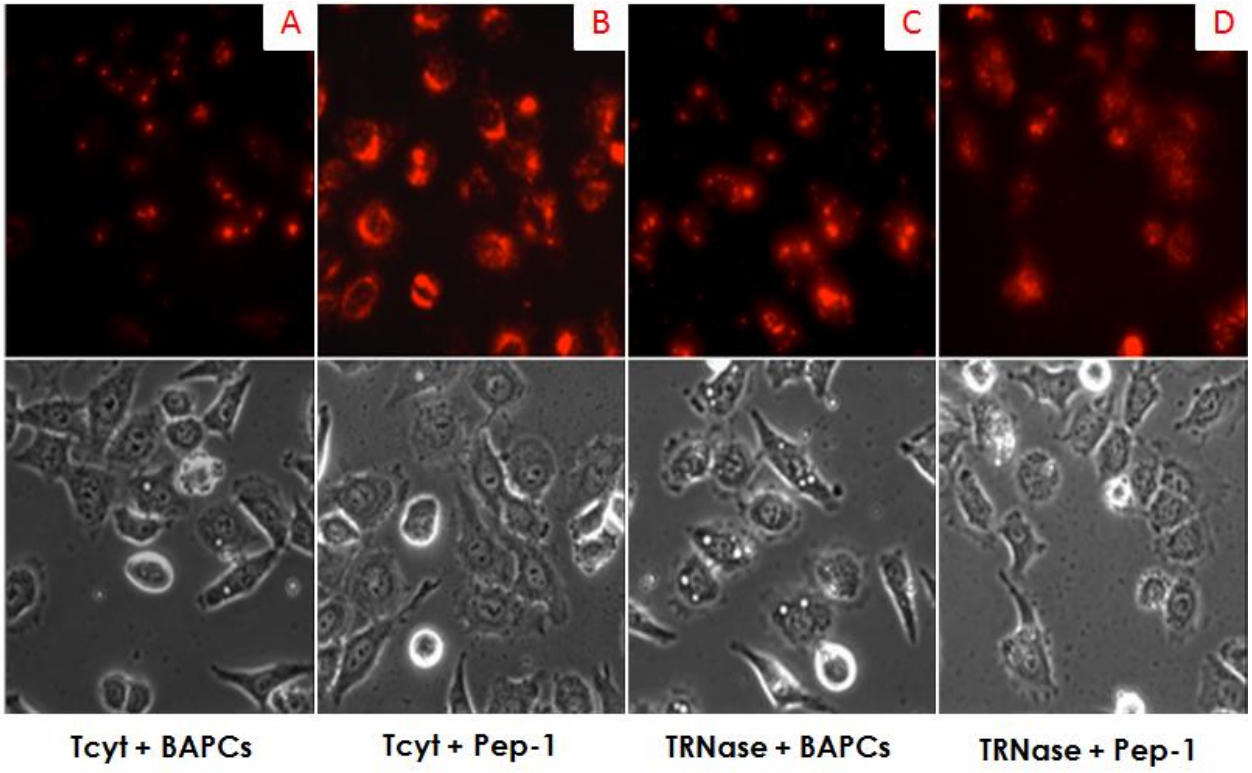

Figure 3.5 TAMRA Labeled Protein Uptake in HeLa Cells.
Fluoresence microscopy images of HeLa cells after 3 h of incubation. The lower panel shows DIC images. **A)** BAPCs with Tcytc **B)** Tcytc with Pep-1 **C)** BAPCs with TRNAse A **D)** TRNase A with Pep-1.

~12kDa), as well as the intrisically fluorescent GFP (26.9 kDa). These experiments were designed to test whether the BAPCs could deliver and then release the TAMRA-labeled proteins to induce a measurable cytotoxic effect. Both cytochrome c and RNaseA were successfully encapsulated in the BAPCs while the EGFP which has a tendency to aggregate in water was not. In Sukthankar et al., S/TEM studies with BAPCs adducted with methymercury showed that

nascent BAPCs are formed with an average diameter of 20 - 22 nm and a calculated internal volume of 4000 nm^3.[39] The larger molal volume of GFP may interfere with its encapsulation. Thus, we postulate that the small internal volume of the initial capsule limits the size of molecules that can be entrapped. That size limit is somewhere between 13.7 and 26.9 kDa. BAPCs individually loaded with Tcytc or TRNaseA were incubated with HeLa cells for 3 h. Pep-1, an amphipathic cell penetrating peptide carrier capable of inducing cellular uptake of a variety of proteins and peptides into cell lines with a high degree of efficiency,[55] was employed as a control delivery agent for Tcytc[56] and TRNaseA.

Figure 3.5 demonstrates the ability of the BAPCs to encapsulate and deliver both Tcytc and TRNaseA into HeLa cells. In these representative images, the efficiency of Tcytc transport with BAPCs (**Fig 3.5A**) is slightly less than that with Pep-1 (**Fig 3.5B**); however in case of TRNaseA there is no significant difference between the carrying capacity of the BAPCs (**Fig 3.5C**) versus Pep-1 (**Fig 3.5D**). Cytochrome c[57] and RNase A[58] are both known to effect cellular apoptosis. Interestingly enough, no significant cellular apoptosis was observed in the case of either of the proteins taken up by HeLa cells using BAPCs; while Pep-1 mediated transport led to

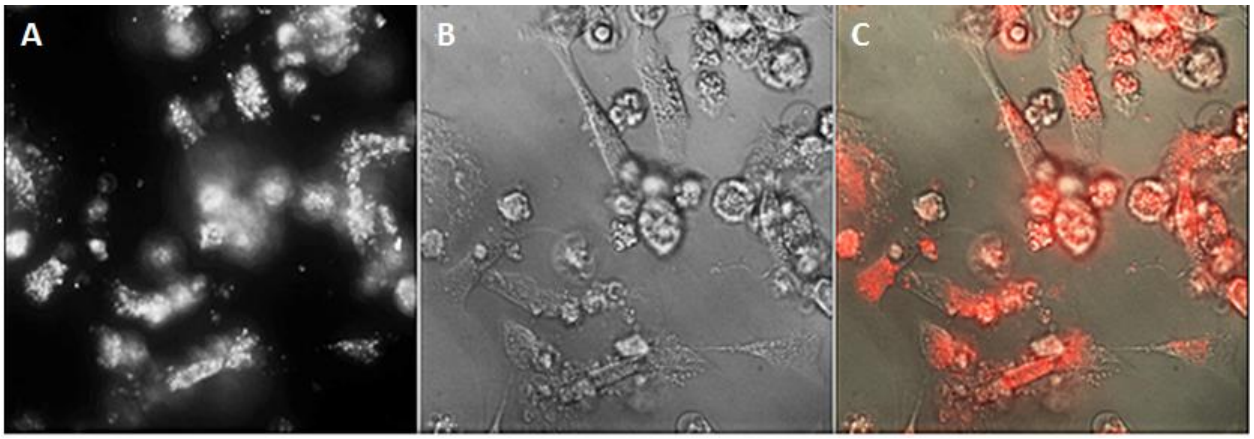

Figure 3.6 Long Term Cell Uptake Study

HeLa cells incubated with BAPCs with a 30% Rhodamine B label on bis(FLIVI)-K-K_4, observed after 2 weeks using confocal microscopy through two trypsinizations **A)** Dark field image with channel selected for the excitation of Rhodamine **B)** Bright-field image **C)** Overlap of the bright-field image and channel for Rhodamine.

frank cytotoxicity in the expected manner (data not shown). The ability of the BAPCs to persist within HeLa cells was then examined over a longer time period. A confocal microscopy based study conducted using HeLa cells treated with Rhodamine B labeled BAPCs (**Fig 3.6**) revealed that even after 14 days, the BAPCs persist within the cells and are transferred to daughter cells during mitosis without any apparent degradation. The degradation of the BAPCs labeled with Rhodamine B would tend to proceed with a dispersion of the dye / dye-peptide fragments and/or an increase in the fluorescence intensity of Rhodamine B due to a change in its local environment.[59] None of these characteristics indicative of nanoparticles degrading within the cell were observed. This would - in retrospect - be consistent with expectation as cationic nano-particles, especially those containing poly-lysine tend to escape and/or evade lysosomal degradation by charge destabilizing the endo-lysosomal membranes.[60] It seems that the cellular machinery is unable to breakdown the BAPCs. In designing the BAPCs, we anticipated that they would be able to release cargo within the cytoplasm or a cellular compartment. However, the inability of the peptide capsules to do so make our constructs, in their current design, too stable for conventional targeted drug delivery. The peptides that constitute the BAPCs were designed to mimic diacyl phospholipids in molecular architecture. However, unlike liposomes where the non-solvated tail groups are held together primarily by hydrophobic interactions, BAPCs have the additional component of hydrogen bonding; as well as inter- and intra-molecular pi-stacking (π-π) between the Phenylalanine aromatic rings of peptide sequences that apparently imbues the capsules with remarkable stability.

3.3.3 Encapsulation of Radionuclides using BAPCs

Given the ability of BAPCs to take up but not release cargo, and their persistence in cells for extended periods of time suggested a potential application — α-particle therapy. Targeted α-particle therapy, using particle-emitting radionuclides holds promise as therapeutic agents in treating micrometastases.[61] The effectiveness of this therapy is a function of the α-particle's properties. They are emitted with energies in the MeV range, with Linear Energy Transfer (LET) having a mean energy deposition of 100 keV/μm, enabling them to produce more lethal DNA breaks per radiation track as compared to β^--particles in the cell nucleus. It has been estimated that a few α-particle transversals are sufficient to kill a cell.[62] The limited range of α-particles (50-100 μm) confines their toxicity to a small radius from the site of the isotope decay, enabling more specific tumor killing capability without damage to the surrounding normal tissue; as opposed to β^--particles, which have a much longer range.[26] Furthermore the cytocidal effectiveness of α-particles has been shown to be independent of oxygen concentration,[63] dose rate and cell cycle position.[64] Additionally, studies performed on a leukemia model indicated that α-emitter radionuclides exhibited cytotoxicity superior to that of β^--radiation or γ-radiation and are capable of killing cancer cells which are resistant to chemotherapeutic drugs such as doxorubicin.[65]

3.3.4 Targeted Alpha Particle Therapy

There are a number of α-emitter radionuclides, one of which, ^{213}Bi ($t_{1/2}$ = 46 min), has been proposed for therapeutic use and clinically evaluated. However, ^{213}Bi is generator produced and has a relatively short half-life requiring very rapid tumor targeting. An alternative then involves utilizing ^{225}Ac, which is the parent nuclide of ^{213}Bi. A single ^{225}Ac ($t_{1/2}$ = 9.9 days) generates four alpha and three beta particles during its disintegration, along with two useful gamma emissions, including the 221 keV of ^{221}Fr and the 440 keV of ^{213}Bi (**Figure 3.7**), that can be used for in vivo imaging.[66,67] The enhanced potency of ^{225}Ac as opposed to ^{213}Bi has been demonstrated in several pre-clinical studies.[65,68] Ongoing research has focused on harnessing the cell-killing power of these radionuclides by directing them to metastatic cells via appropriate targeting vectors.

^{225}Ac decay proceeds via a succession of daughter isotopes. This decay releases 28 MeV of energy in the form of α-particles. However, for the sake of optimal killing efficiency, the α-emissions and therefore the ^{225}Ac atom, must be delivered precisely and only to the region of interest. A problem closely associated with the 'targeting nanogenerator approach'[69] which involves stably chelating the ^{225}Ac for delivery in vivo is that, after the initial ^{225}Ac decay to ^{221}Fr, the co-ordinate bonds from the chelating ligand to the central metal atom are not retained. Thus the daughter isotopes distribute freely within the body causing unwanted cytotoxicity.

Therefore it is desirable to confine the daughter isotopes of ^{225}Ac within the carrier during circulation and targeting. This problem is compounded by the fact that the high kinetic energy of the α-particle emissions penetrates the phospholipid membrane in liposomes, which could otherwise be considered as suitable candidates for encapsulated delivery. Moreover, the recoil trajectory of the daughter nuclides (80-90 nm) penetrates the phospholipid membranes causing rupture and leakage[31] leading to escape and redistribution within the body, increasing

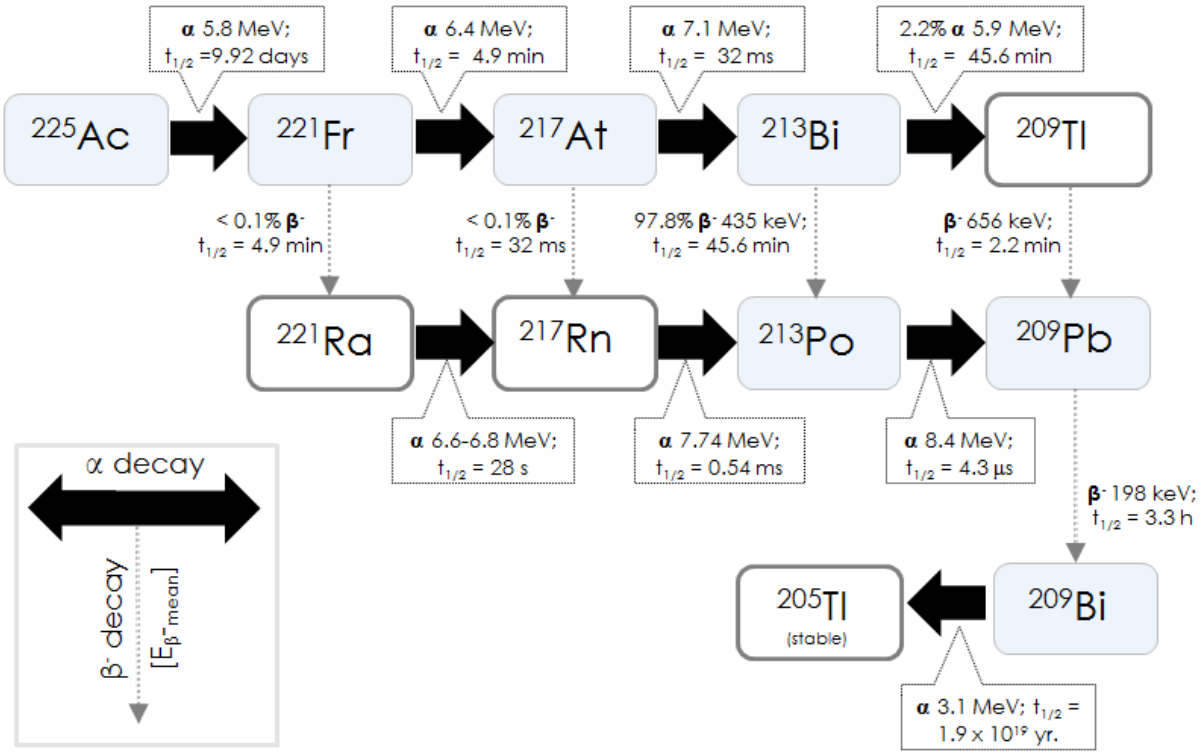

Figure 3.7 The proposed decay scheme for 225Ac based on the recently published studies[63, 64]

toxicity. Retention of daughter isotopes is size dependent. Theoretical calculations by Sofou et. al.[33] suggest negligible (<0.001%) daughter retention for the last isotope for 100 nm diameter liposomes and 50% retention of the same for liposomes with a diameter larger than 650 nm. Even for giant liposomes (1 µm diameter), retention does not exceed 65%. The measured last daughter retention for the 650 nm liposomes was found to be substantially lower (11%) than

what was calculated, owing to the tendency of ^{225}Ac to bind to the negatively charged phospholipid membrane leading to non-uniform distribution within the liposome causing daughter loss after recoil. The large size of such liposomes required to carry effective loads have serious limitations with regard to fenestration and cellular uptake. This coupled with low daughter retention capabilities - makes them a cumbersome system for efficient targeted radiotherapy. Considering the stability, uptake and retentive capabilities of the BAPCs; they were tested as a potential ^{225}Ac carrier for targeted alpha particle therapy applications.

3.3.5 Radio-therapeutic Potential of BAPCs

Experiments were performed to monitor encapsulation of ^{225}Ac into BAPCs, as well as its retention within them over 7 days. Uptake of BAPC-encapsulated ^{225}Ac was then tested in vitro using human metastatic cervical cancer (CasKi) cells. The ^{225}Ac was well contained by the BAPCs, with retention being ≥ 95% of the original activity for the period of 7 days (**Fig 3.8A**). The cellular uptake of encapsulated ^{225}Ac increased in a time dependent manner and reached

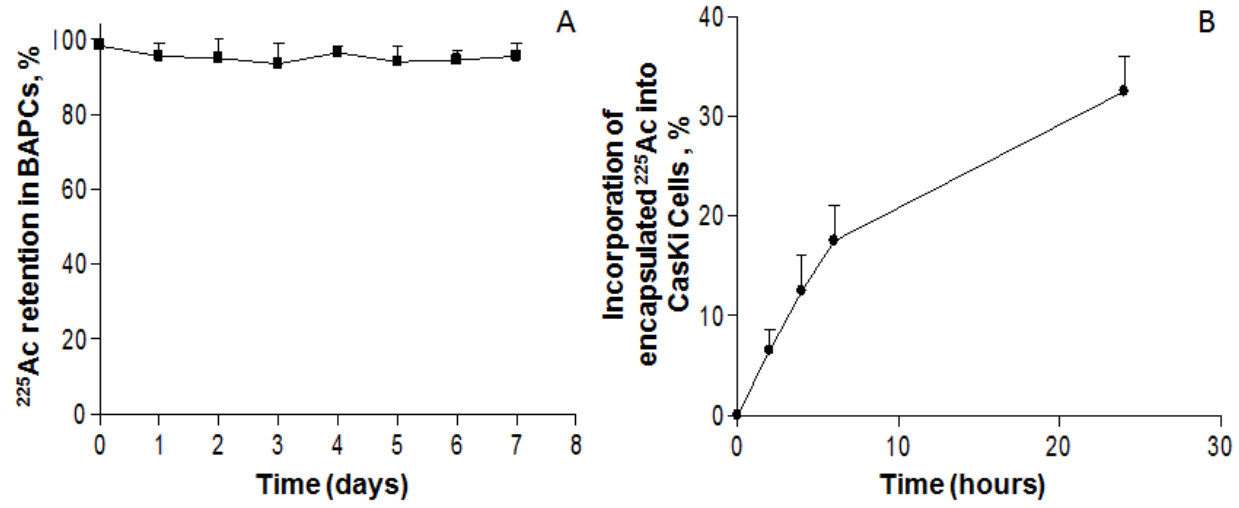

Figure 3.8 Cellular Uptake and Retention of BAPCs encapsulated with ^{225}Ac.

A) Encapsulation and retention of ^{225}Ac within BAPCs over 7 days and **B)** Cellular uptake of the BAPC-encapsulated ^{225}Ac into CasKi cells over 24 h.

33% at 24 h post incubation (**Fig 3.8B**). It is important to note that a much lower dose of ^{225}Ac (0.1 μCi) was used for this uptake experiment to avoid any cytocidal effects on the cells that could cloud the cellular uptake results. These findings were encouraging as they demonstrated the potential of BAPCs as candidates for ^{225}Ac encapsulation and cellular uptake.

3.3.6 Biodistribution of BAPCs encapsulating ^{225}Ac

To investigate the behavior of BAPCs *in vivo* we studied the distribution of BAPC encapsulated ^{225}Ac and its daughter ^{213}Bi (along with a control of free $^{225}AcCl_3$ and ^{213}Bi), in CD1 mice at 1 and 24 h post IP administration. Tissues were collected and analyzed at the indicated times. The 440 keV γ-emission of ^{213}Bi was used to calculate the percentage of the injected dose per gram of organ (ID/g organ, %) as described in **section 3.2.10**. In **Figure 3.9** we

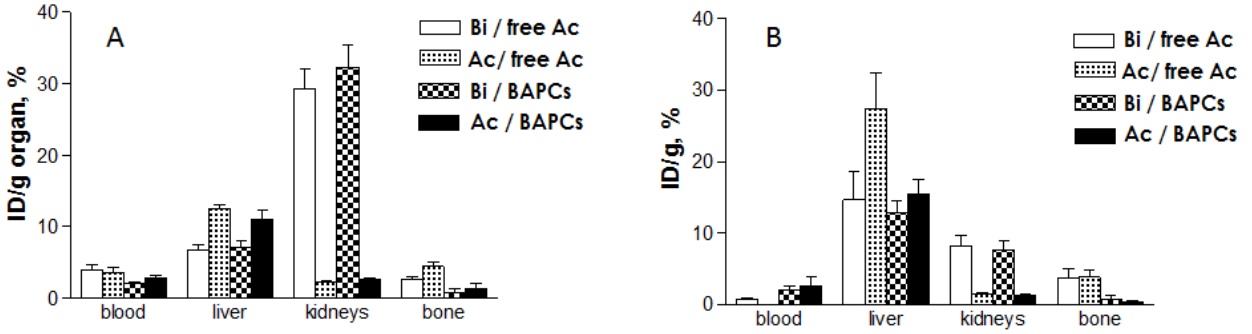

Figure 3.9 Biodistribution of free and BAPC-encapsulated, ^{225}Ac and its daughter ^{213}Bi, in CD1 mice.
A) 1 h time point; **B)** 24 h time point.

see the results of the in vivo distribution in mice for free $^{213}Bi/^{225}Ac$ *versus* encapsulated material. At 1 h post injection, when both 'BAPC encapsulated ^{225}Ac' and 'free ^{225}Ac' were still in the process of exiting the peritoneal cavity, there was no significant difference in organ uptake between BAPC encapsulated ^{225}Ac and free ^{225}Ac (except for bone, where free ^{225}Ac is known to accumulate). The uptake of ^{225}Ac daughter ^{213}Bi into the kidneys was higher than that of ^{225}Ac, as free ^{213}Bi targets kidneys. The differences between BAPC encapsulated ^{225}Ac, and free ^{225}Ac became more pronounced at 24 h post injection. The free ^{225}Ac is completely cleared from the blood via binding to the plasma proteins and being delivered to various organs. BAPC encapsulated ^{225}Ac stayed in circulation due to the small size of the BAPCs, consistent with nanomaterials in the 10-20 nm size range that tend to stay in circulation. Free ^{225}Ac accumulated

significantly more in the liver (P=0.03) and in the bone (P=0.02) than the BAPC encapsulated ^{225}Ac. This confirms the tight retention of ^{225}Ac within the vesicles. ^{213}Bi daughter was present together with ^{225}Ac pointing to retention of the daughters by the BAPCs as well. The only organ where there was more ^{213}Bi present in comparison with ^{225}Ac was the kidneys - which serve as the 'sink' for ^{213}Bi that has been released from any organ in the body. Overall, encapsulated ^{225}Ac cleared much more from the body than 'free ^{225}Ac' through the combination of renal, hepatobilliary and intestinal goblet cell (GC) secretion (IGCSP) pathways[70]. Taken together, these results point to the ability of BAPCs to incorporate and retain ^{225}Ac and its daughter isotopes through ^{213}Bi.

3.4 Conclusion

It is evident that the extraordinary stability of the BAPCs, in their current design, limits their use as a drug delivery modality. However, this same characteristic makes them appear ideal for targeted alpha particle therapy for the treatment of metastatic and infectious diseases. Our results show that the alpha emitting radionuclide ^{225}Ac, and its radioactive daughters, can be sequestered within the lumen of the BAPCs and then retained for days (and through multiple cell divisions), just outside the nucleus of the cell. This portends well for cytocidal effects.

The fact that BAPCs withstand rupture from the ejected high energy alpha particles and the resulting recoil of the daughter isotope, suggests a self-annealing property for BAPCs. It is likely that BAPCs are taken up by cells through a non-selective internalization process, possibly proceeding via transient pore formation, analogous to that observed with some polycationic lipids[71] and polymers.[72] Should this assessment be accurate, the BAPCs would be able to find utility as nano-carriers in cellular systems. The poly-lysine cationic surface of the BAPCs provides a convenient synthetic pathway for the modification and conjugation of ligands, antibodies and molecular markers to achieve cellular targeting. This could greatly reduce the whole body load required to kill desired cells as well as reduce deleterious off-target side effects. The fact that the capsules also remain in circulation for an extended period most like reflects their small size and flexibility. The ability of the BAPCs to persist in cells through cell division(s) suggests a potential use as cell lineage tracers and probes. BAPCs could be conjugated to quantum dots in an effort to resolve some of the biocompatibility issues associated with the latter.[73] The BAPCs constitute a unique and exciting new class of biomaterial, which

while portending promise as a convenient agent for targeted alpha particle therapy, could find application in many other areas as well.

3.5 Abbreviations

BAPCs, Branched Amphiphilic Peptide Capsules; DMEM, Dulbecco's minimum essential medium; FBS, Fetal Bovine Serum; TFE, 2,2,2 - Trifluoroethanol; DAPI, 2-(4-amidinophenyl)-1H -indole-6-carboxamidine; CD, Circular Dichroism Spectroscopy; DLS, Dynamic Light Scattering or photon correlation spectroscopy; S/TEM, Scanning Transmission Electron Microscopy; EM, Electron Microscopy; Tcytc, 5(6)-TAMRA labeled cytochrome c; TRNase A, 5(6)-TAMRA labeled RNase A; EDTA, 2-({2-[bis(carboxymethyl)amino]ethyl}(carboxymethyl)amino)acetic acid; DTPA, 2-({2-[bis(carboxymethyl)amino]ethyl}(carboxymethyl)amino)acetic acid; DOTA, 2-[4-nitrobenzyl]-1, 4, 7, 10-tetraazacyclododecane-N,N',N'',N'''-tetraacetic acid; HEHA, 1,4,7,10,13,16-hexaazacyclohexadecane- N,N',N'',N ''',N'''', N'''''–hexa-acetic acid; PEPA, 2-[4-nitrobenzyl]-1,4,7,10,13-pentaazacyclopentadecane-N,N',N'',N ''',N''''-pentaacetic acid; TETA, 2-[4-nitrobenzyl]-1, 4, 8, 11-tetraazacyclotetradecane N,N',N'',N'''-tetraacetic acid.

3.6 Acknowledgement

This is publication 14-166-J from the Kansas Agricultural Experiment Station. We would like to thank Dr. Stella Y Lee, Division of Biology, Kansas State University, for providing us with HeLa cell lines and, Dr. David Moore and Heather Shinogle at the University of Kansas Microscopy and Analytical Imaging Laboratory, for long term cellular uptake studies.

3.7 References

1. Douglas, S.J., Davis, S.S. and Illum, L. (1987) Nanoparticles in drug delivery. *Crit Rev Ther Drug Carrier Syst.* **3,** 233-261.

2. Gref, R., Domb, A., Quellec, P., Blunk, T., Müller, R.H., Verbavatz, J.M. and Langer, R. (1995) The controlled intravenous delivery of drugs using PEG-coated sterically stabilized nanospheres. *Adv Drug Deliv Rev.* **16,** 215-233.

[3]. Harashima, H., Sakata, K., Funato, K. and Kiwada, H. (1994) Enhanced hepatic uptake of liposomes through complement activation depending on the size of liposomes. *Pharm Res.* **11,** 402-406.

[4]. Devine, D.V., Wong, K., Serrano, K., Chonn, A. and Cullis, P.R. (1994) Liposome-complement interactions in rat serum: implications for liposome survival studies. *Biochim Biophys Acta.* **1191,** 43-51.

[5]. Dunn, S.E., Brindley, A., Davis, S.S., Davies, M.C. and Illum, L. (1994) Polystyrene-poly (ethylene glycol) (PS-PEG2000) particles as model systems for site specific drug delivery. 2. The effect of PEG surface density on the in vitro cell interaction and in vivo biodistribution. *Pharm Res.* **11,** 1016-1022.

[6]. Gref, R., Minamitake, Y., Peracchia, M., Trubetskoy, V., Torchilin, V. and Langer, R. (1994) Biodegradable long-circulating polymeric nanospheres. *Science.* **263,** 1600-1603.

[7]. Alexis, F., Pridgen, E., Molnar, L.K. and Farokhzad, O.C. (2008) Factors affecting the clearance and biodistribution of polymeric nanoparticles. *Mol Pharm*. **5**, 505-515.

[8]. Kim, S.Y., Shin, I.G., Lee, Y.M., Cho, C.S. and Sung, Y.K. (1998) Methoxy poly(ethylene glycol) and epsilon-caprolactone amphiphilic block copolymeric micelle containing indomethacin. II. Micelle formation and drug release behaviours. *J Control Release.* **51,** 13-22.

[9]. Kim, S.Y., Shin, I.G. and Lee, Y.M. (1999) Amphiphilic diblock copolymeric nanospheres composed of methoxy poly(ethylene glycol) and glycolide: properties, cytotoxicity and drug release behaviour. *Biomaterials.* **20,** 1033-1042.

[10]. Liu, J., Xiao, Y. and Allen, C. (2004) Polymer-drug compatibility: a guide to the development of delivery systems for the anticancer agent, ellipticine. *J Pharm Sci.* **93,** 132-143.

[11]. Letchford, K. and Burt, H. (2007) A review of the formation and classification of amphiphilic block copolymer nanoparticulate structures: micelles, nanospheres, nanocapsules and polymersomes. *Eur J Pharm and Biopharm.* **65,** 259-269.

[12]. Discher, D.E. and Ahmed, F. (2006) Polymersomes. *Annu Rev Biomed Eng.* **8,** 323-341.

[13]. Soppimath, K.S., Aminabhavi, T.M., Kulkarni, A.R. and Rudzinski, W.E. (2001) Biodegradable polymeric nanoparticles as drug delivery devices. *J Controlled Release*. **70**, 1-20.

[14]. Mora-Huertas, C.E., Fessi, H. and Elaissari, A. (2010) Polymer-based nanocapsules for drug delivery. *Int J Pharm.* **385,** 113-142.

[15]. Besnard, R., Cambedouzou, J., Arrachart, G., Diat, O. and Pellet-Rostaing, S. (2013) Self-Assembly of Condensable Bola-Amphiphiles in Water/Tetraethoxysilane Mixtures for the Elaboration of Mesostructured Hybrid Materials. *Langmuir* **29,** 10368-10375.

[16]. Yan, Y., Lu, T. and Huang, J. (2009) Recent advances in the mixed systems of bolaamphiphiles and oppositely charged conventional surfactants. *J Colloid Interface Sci.* **337,** 1-10.

[17]. Bianco, A., Kostarelos, K. and Prato, M. (2005) Applications of carbon nanotubes in drug delivery. *Curr Opin Chem Biol.* **9,** 674-679.

[18]. Kazi, K.M., Mandal, A.S., Biswas, N., Guha, A., Chatterjee, S., Behera, M. and Kuotsu, K. (2010) Niosome: A future of targeted drug delivery systems. *J Adv Pharm Technol Res.* **1,** 374-380.

[19]. Yasam, V.R., Jakki, S.L., Natarajan, J. and Kuppusamy, G. (2013) A review on novel vesicular drug delivery: proniosomes. *Drug Deliv.* [Epub ahead of print] DOI:10.3109/10717544.2013.].

[20]. Hu, C. and Rhodes, D.G. (1999) Proniosomes: a novel drug carrier preparation. *Int J Pharm.* **185,** 23-35.

[21]. Hillaireau, H. and Couvreur, P. (2009) Nanocarriers' entry into the cell: relevance to drug delivery. *Cell Mol Life Sci.* **66,** 2873-2896.

[22] Imam, S.K. (2001) Advancements in cancer therapy with alpha-emitters: a review. *Int J Radiation Oncology Biol Phys.* **51,** 271-278.

[23]. Davis, I.A., Glowienka, K.A., Boll, R.A., Deal, K.A., Brechbiel, M.W., Stabin, M., Bochsler, P.N., Mirzadeh, S. and Kennel, S.J. (1999) Comparison of ^{225}actinium chelates: tissue distribution and radiotoxicity. *Nucl Med Biol.* **26,** 581-589.

[24]. Schwartz, J., Jaggi, J.S., O'Donoghue, J.A., Ruan, S., McDevitt, M., Larson, S.M., Scheinberg, D.A. and Humm, J.L. (2011) Renal uptake of ^{213}bismuth and its contribution to kidney radiation dose following administration of ^{225}actinium—labeled antibody. *Phys. Med. Biol.* **56,** 721-733.

[25]. Jaggi, J.S., Seshan, S.V., McDevitt, M.R., LaPerle, K., Sgouros, G. and Scheinberg, D.A. (2005) Renal tubulointerstitial changes after internal irradiation with alpha-particle-emitting actinium daughters. *J Am. Soc. Nephrol.* **16,** 2677-2689.

[26.] Kim, Y.S. and Brechbiel, M.W. (2012) An overview of targeted alpha therapy. *Tumour Biol.* **33**, 573-590.

[27]. Deal, K.A., Davis, I.A., Mirzadeh, S., Kennel, S.J. and Brechbiel, M.W. (1999) Improved in vivo stability of actinium-225 macrocyclic complexes. *J Med Chem.* **42**, 2988-2992.

[28]. Hider, R.C. and Hall, A.D. (1991) Clinically useful chelators of tripositive elements. *Prog Med Chem.* **28**, 41-173.

[29]. Chappell, L.L., Deal, K.A., Dadachova, E. and Brechbiel, M.W. (2000) Synthesis, conjugation, and radiolabeling of a novel bifunctional chelating agent for ^{225}Ac radioimmunotherapy applications. *Bioconjug Chem.* **11**, 510-519.

[30]. Henriksen, G., Schoultz, B.W., Michaelsen, T.E., Bruland, Ø.S. and Larsen, R.H. (2004) Sterically stabilized liposomes as a carrier for α-emitting radium and actinium radionuclides. *Nucl Med Biol.* **31**, 441-449.

[31]. Sofou, S., Thomas, J.L., Lin, H.Y., McDevitt, M.R., Scheinberg, D.A. and Sgouros, G. (2004) Engineered liposomes for potential alpha-particle therapy of metastatic cancer. *J Nucl Med.* **45**, 253-260.

[32]. Sofou, S., Kappel, B.J., Jaggi, J.S., McDevitt, M.R., Scheinberg, D.A. and Sgouros, G. (2007) Enhanced retention of the alpha-particle-emitting daughters of ^{225}Actinium by liposome carriers. *Bioconjug Chem*. **18**, 2061-2067.

[33]. McDevitt, M.R., Finn, R.D., Sgouros, G., Ma, D. and Scheinberg, D.A. (1999) An ^{225}Ac/^{213}Bi generator system for therapeutic clinical applications: construction and operation. *Applied Radiation and Isotopes.* **50,** 895-904.

[34]. Nikula, T.K., McDevitt, M.R., Finn, R.D., Wu, C., Kozak, R.W., Garmestani, K., Brechbiel, M.W., Curcio, M.J., Pippin, C.G., Tiffany-Jones, L., Geerlings MW, S., Apostolidis, C., Molinet, R., Geerlings, M.W.,Jr, Gansow, O.A. and Scheinberg, D.A. (1999) Alpha-emitting bismuth cyclohexylbenzyl DTPA constructs of recombinant humanized anti-CD33 antibodies: pharmacokinetics, bioactivity, toxicity and chemistry. *J Nucl Med.* **40**, 166-176.

[35]. Chakrabarti, M.C., Le, N., Paik, C.H., De Graff, W.G. and Carrasquillo, J.A. (1996) Prevention of radiolysis of monoclonal antibody during labeling. *J Nucl Med.* **37,** 1384-1388.

[36]. Stensrud, G., Redford, K., Smistad, G. and Karlsen, J. (1999) Effects of gamma irradiation on solid and lyophilised phospholipids. *Radiat Phys Chem.* **56,** 611-622.

[37]. Couvreur, P. (2013) Nanoparticles in drug delivery: Past, present and future. *Adv Drug Deliv Rev.* **65**, 21-23.

[38]. Gudlur, S., Sukthankar, P., Gao, J., Avila, L.A., Hiromasa, Y., Chen, J., Iwamoto, T. and Tomich, J.M. (2012) Peptide nanovesicles formed by the self-assembly of branched amphiphilic peptides. *PLoS One.* **7,** e45374.

[39]. Sukthankar, P., Gudlur, S., Avila Flores, L.A., Whitaker, S.K., Katz, B.B., Hiromasa, Y., Gao, J., Thapa, P.S., Moore, D.S., Iwamoto, T., Chen, J. and Tomich, J.M. (2013) Branched Oligopeptides Form Nano-Capsules with Lipid Vesicle Characteristics. Langmuir Nov 18. [Epub ahead of print] DOI: 10.1021/la403492n

[40]. Grove, A., Tomich, J.M., Iwamoto, T. and Montal, M. (1993) Design of a functional calcium channel protein: inferences about an ion channel-forming motif derived from the primary structure of voltage-gated calcium channels. *Protein Sci.* **2,** 1918-1930.

[41]. Kempe M. and Barany G. (1996) CLEAR: A Novel Family of Highly Cross-Linked Polymeric Supports for Solid Phase Synthesis, *J. Am. Chem. Soc.* **118**, 7083-7093.

[42]. Iwamoto, T., Grove, A., Montal, M.O., Montal, M. and Tomich, J.M. (1994) Chemical synthesis and characterization of peptides and oligomeric proteins designed to form transmembrane ion channels. *Int. J. Pept Protein Res.* **43**, 597-607.

[43]. Pietta, P.G., Cavallo, P.F., Takahashi, K. and Marshall, G.R. (1974) Preparation and use of benzhydrylamine polymers in peptide synthesis. II. Synthesis of thyrotropin releasing hormone, thyrocalcitonin 26-32, and eledoisin. *J Org Chem*. **39**, 44-48.

[44]. Pennington, M.W. (1994) HF Cleavage and Deprotection Procedures for Peptides Synthesized Using a Boc/Bzl Strategy in Peptide Synthesis Protocols (Pennington, M.W. and Dunn, BM, eds.) Vol. **35**, pp.41-62, Humana Press.

[45]. Tomich, J.M., Carson, L.W., Kanes, K.J., Vogelaar, N.J., Emerling, M.R. and Richards, J.H. (1988) Prevention of aggregation of synthetic membrane-spanning peptides by addition of detergent. *Anal Biochem* **174**, 197-203.

[46]. Chen, R. F. (1972) Measurements of absolute values in biochemical fluorescence spectroscopy. *J Res National Bureau Standards* **76A**(6), 593-606.

[47]. Sponer H. (1942) Remarks on the Absorption Spectra of Phenylalanine and Tyrosine in Connection with the Absorption in Toluene and Paracresol. *J Chem Phys*. **10**, 672.

[48]. Geisert Jr., E.E. and Frankfurter, A. (1989) The neuronal response to injury as visualized by immunostaining of class III β-tubulin in the rat. *Neurosci Lett.* **102,** 137-141.

[49]. Harris M, Wang XG, Jiang Z, Phaeton R, Koba W, Goldberg GL, Casadevall A, Dadachova E. (2013) Combined treatment of the experimental human papilloma virus-16-positive cervical and head and neck cancers with cisplatin and radioimmunotherapy targeting viral E6 oncoprotein. *Br J Cancer.* **108**(4), 859-865.

[50]. Midoux P, Pichon C, Yaouanc JJ, Jaffrès PA. (2009) Chemical vectors for gene delivery: a current review on polymers, peptides and lipids containing histidine or imidazole as nucleic acids carriers. *Br J Pharmacol*.**157**(2):166-178.

[51]. Xiang, S., Tong, H., Shi, Q., Fernandes, J.C., Jin, T., Dai, K. and Zhang, X. (2012) Uptake mechanisms of non-viral gene delivery. *J Control Release.* **158**, 371-378.

[52]. Melchior, D.L., Morowitz, H.J., Sturtevant, J.M. and Tsong, T.Y. (1970) Characterization of the plasma membrane of Mycoplasma laidlawii. VII. Phase transitions of membrane lipids. *Biochim Biophys Acta - Biomembranes.* **219,** 114-122.

[53]. Madani F, Lindberg S, Langel Ü, Futaki S, Gräslund A (2011) Mechanisms of Cellular Uptake of Cell-Penetrating Peptides. *J Biophys* DOI: 10.1155/2011/414729.

[54]. Gupta, B., Levchenko, T.S. and Torchilin, V.P. (2005) Intracellular delivery of large molecules and small particles by cell-penetrating proteins and peptides. *Adv Drug Deliv Rev.* **57**, 637-651.

[55]. Morris, M.C., Depollier, J., Mery, J., Heitz, F. and Divita, G. (2001) A peptide carrier for the delivery of biologically active proteins into mammalian cells. *Nat.Biotechnol.* **19**, 1173-1176.

[56]. Fawell, S., Seery, J., Daikh, Y., Moore, C., Chen, L.L., Pepinsky, B. and Barsoum, J. (1994) Tat-mediated delivery of heterologous proteins into cells. *Proc Natl Acad Sci. U.S.A.* **91**, 664-668.

[57]. Zhivotovsky, B., Orrenius, S., Brustugun, O.T. and Doskeland, S.O. (1998) Injected cytochrome c induces apoptosis. *Nature.* **391,** 449-450.

[58]. Kim, J.S., Soucek, J., Matousek, J. and Raines, R.T. (1995) Mechanism of ribonuclease cytotoxicity. *J Biol Chem.* **270**, 31097-31102.

[59] Romero, G., Echeverria, M., Qiu, Y., Murray, R.A. and Moya, S.E. (2014) A novel approach to monitor intracellular degradation kinetics of poly(lactide-co-glycolide) nanoparticles by means of flow cytometry. J.Mater.Chem.B.

[60] Panyam, J., Zhou, W.Z., Prabha, S., Sahoo, S.K. and Labhasetwar, V. (2002) Rapid endo-lysosomal escape of poly(DL-lactide-co-glycolide) nanoparticles: implications for drug and gene delivery. *FASEB J.* United States **16,** 1217-1226

[61]. Couturier, O., Supiot, S., Degraef-Mougin, M., Faivre-Chauvet, A., Carlier, T., Chatal, J.F., Davodeau, F. and Cherel, M. (2005) Cancer radioimmunotherapy with alpha-emitting nuclides. *Eur J Nucl Med Mol Imaging* **32**, 601-614.

[62]. Sgouros, G., Roeske, J.C., McDevitt, M.R., Palm, S., Allen, B.J., Fisher, D.R., Brill, A.B., Song, H., Howell, R.W., Akabani, G., SNM MIRD Committee, Bolch, W.E., Brill, A.B., Fisher, D.R., Howell, R.W., Meredith, R.F., Sgouros, G., Wessels, B.W. and Zanzonico, P.B. (2010) MIRD Pamphlet No. 22 (abridged): radiobiology and dosimetry of alpha-particle emitters for targeted radionuclide therapy. *J Nucl Med.* **51,** 311-328.

[63]. Wulbrand, C., Seidl, C., Gaertner, F.C., Bruchertseifer, F., Morgenstern, A., Essler, M., Senekowitsch-Schmidtke, R. (2013) Alpha-particle emitting ^{213}Bi-anti-EGFR

immunoconjugates eradicate tumor cells independent of oxygenation. *PLOS One*. **8**(5), e64730.

[64]. Miederer, M., Scheinberg, D.A. and McDevitt, M.R. (2008) Realizing the potential of the Actinium-225 radionuclide generator in targeted alpha particle therapy applications. *Adv Drug Deliv Rev.* **60**, 1371-1382.

[65]. Friesen, C., Glatting, G., Koop, B., Schwarz, K., Morgenstern, A., Apostolidis, C., Debatin, K.M. and Reske, S.N. (2007) Breaking chemoresistance and radioresistance with [213Bi]anti-CD45 antibodies in leukemia cells. *Cancer Res.* **67**, 1950-1958.

[66]. Suliman G, Pommé S, Marouli M, Van Ammel R, Stroh H, Jobbágy V, Paepen J, Dirican A, Bruchertseifer F, Apostolidis C, Morgenstern A. (2013) Half-lives of ^{221}Fr, ^{217}At, ^{213}Bi, ^{213}Po and ^{209}Pb from the ^{225}Ac decay series. *Appl Radiat Isot*. **77**, 32-37.

[67]. Pommé S, Marouli M, Suliman G, Dikmen H, Van Ammel R, Jobbágy V, Dirican A, Stroh H, Paepen J, Bruchertseifer F, Apostolidis C, Morgenstern A. (2012) Measurement of the ^{225}Ac half-life. *Appl Radiat Isot.* **70**(11), 2608-2614.

[68]. McDevitt, M.R., Barendswaard, E., Ma, D., Lai, L., Curcio, M.J., Sgouros, G., Ballangrud, A.M., Yang, W.H., Finn, R.D., Pellegrini, V., Geerlings, M.W.,Jr, Lee, M., Brechbiel, M.W., Bander, N.H., Cordon-Cardo, C. and Scheinberg, D.A. (2000) An alpha-particle emitting antibody ([^{213}Bi]J591) for radioimmunotherapy of prostate cancer. *Cancer Res.* **60**, 6095-6100.

[69]. McDevitt, M.R., Ma, D., Lai, L.T., Simon, J., Borchardt, P., Frank, R.K., Wu, K., Pellegrini, V., Curcio, M.J., Miederer, M., Bander, N.H. and Scheinberg, D.A. (2001) Tumor therapy with targeted atomic nanogenerators. *Science.* **294**, 1537-1540.

[70] Zhao, B., Sun, L., Zhang, W., Wang, Y., Zhu, Z., Zhu, X., Yang, L., Li, C., Zhang, Z. and Zhang, Y. Secretion of intestinal goblet cells: A novel excretion pathway of nanoparticles. Nanomedicine: Nanotechnology, Biology and Medicine.

[71]. Hafez, I.M., Maurer, N. and Cullis, P.R. (2001) On the mechanism whereby cationic lipids promote intracellular delivery of polynucleic acids. *Gene Ther*. **8,** 1188-1196.

[72]. Hong, S., Bielinska, A.U., Mecke, A., Keszler, B., Beals, J.L., Shi, X., Balogh, L., Orr, B.G., Baker, J.R.,Jr and Banaszak Holl, M.M. (2004) Interaction of poly(amidoamine) dendrimers with supported lipid bilayers and cells: hole formation and the relation to transport. *Bioconjug Chem* **15,** 774-782.

[73]. Alivisatos, A.P., Gu, W. and Larabell, C. (2005) Quantum dots as cellular probes. *Annu Rev Biomed Eng*. **7,** 55-76.

Chapter 4 - Thermally Induced Conformational Transitions in Branched Amphiphilic Peptide Capsules

4.1 Introduction

Branched Amphiphilic Peptide Capsules (BAPCs) constitute a new class of self-assembling nano-delivery vehicles, made exclusively from two, 15-23 amino acid poly-cationic branched amphiphilic peptide sequences.[1] The ability of the BAPCs to form bilayer delimited spheres capable of trapping solutes is due to the unique properties of their constituent peptides. These peptide sequences bis(FLIVI)-K-K_4 and bis(FLIVIGSII)-K-K_4 (**Figure 4.1**) - incorporated in equimolar proportions for BAPC formation - are designed to mimic diacyl phospholipids in molecular architecture, with the branch point lysine orienting the two peptide segments at a ~ 90˚ angles. The hydrophobic segments of these peptides are derived from the internal fragment of the human dihydropyridine sensitive L-type calcium channel segment CaIVS3.[2] It is this characteristic of the sequence to reversibly transition from an alpha helical conformation in 2,2,2- Trifluoroethanol (TFE) to a beta sheet in water that enables the self-assembly of the BAPCs when the constituent peptide mixture is hydrated from its monomeric state.

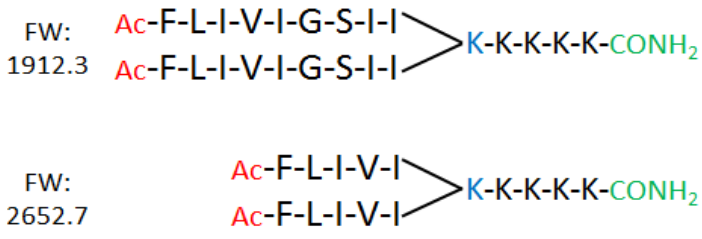

Figure 4.1 Bilayer forming peptide sequences

In a recent publication[3] (**Chapter 3**) we described the stability, cellular uptake capabilities, load capacity and retention in biological environments for extended periods of time. We observed that the BAPCs are readily taken up by cells through the endocytotic pathway, escape

the late endosomes, and accumulate in the peri-nuclear region where they persist without apparent degradation for at least two weeks. This extraordinary stability of the BAPCs enabled us to study their tolerance to a radioactive load, cellular uptake and biodistribution. This suggests a potential application for BAPCs in targeted alpha particle therapy.

The versatility of the self-assembling peptides enables us to tag individual monomers with ligands and molecular markers prior to assembly, making BAPCs particularly suited as biocompatible vehicles for the purposes of targeted drug delivery to cells. However the inability of the BAPCs to release their cargo makes these constructs in their current form unsuitable for the purposes of general drug delivery. A better comprehension of the parameters that contribute BAPC stability would enable us to develop variants that would be better suited for the purposes of efficient drug delivery into cells.

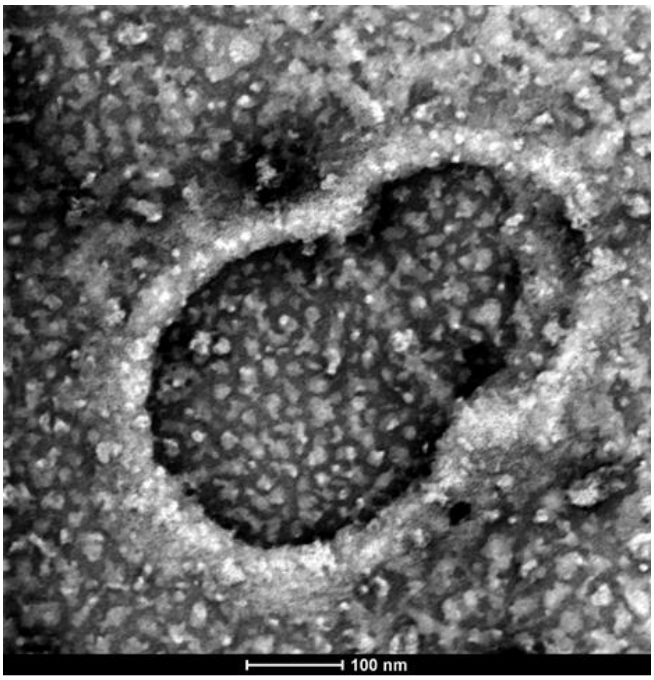

Figure 4.2 S/TEM Image BAPCs in the process of fusion. BAPCS with 30% MeHg label were incubated for 30 min at RT and then spotted on a negatively glow discharged Cu-C grid as described in section 4.2.6. No staining was employed for the purposes of this image

In contrast to liposomes, where hydrophobic tail groups are held together primarily by hydrophobic interactions, BAPCs incorporate the additional components of hydrogen bonding, as well as inter- and intra-molecular pi-stacking (π-π) between the phenylalanine aromatic rings of peptide sequences. This apparently imbues the capsules with remarkable stability. In Sukthankar et al.,[4] (**Chapter 2**) we carried out investigations into some of the biophysical characteristics of the

BAPCs; where we examined the mode of assembly, kinetics of fusion, high thermodynamic stability as well as our ability to re-size the BAPCs by passage through membrane extrusion filters with defined pore sizes. All of these experiments where carried out at 25 ˚C. It was however during the process of studying the kinetics of BAPC fusion that we made the observation that fusion did not occur, and therefore small size was maintained, by incubating the BAPCs at 4 ˚C. This suggested the presence of a temperature effect, either kinetic or structural that needed to be factored into our understanding of BAPC behavior.

In this study, we examined the temperature induced conformational changes in BAPCs and delineated the primary structural parameters within the sequences that contribute to these transitions. Biophysical studies were conducted to explore the assembly, encapsulation and fusion characteristics of bis(FLIVI)-K-K_4 and bis(FLIVIGSII)-K-K_4 along with two experimentally designed variants, at various temperatures.

4.2 Materials and Methods

4.2.1 Peptide Synthesis

All Peptides were synthesized using solid phase peptide chemistry on 4-(2,4-dimethoxyphenyl-Fmoc-aminomethyl) phenoxyacetyl-norleucyl-cross-linked Ethoxylate Acrylate Resin[5] (Peptides International Inc; Louisville, Kentucky) using Fmoc (N-(9-fluorenyl) methoxycarbonyl)/tert-butyl chemistry on an ABI Model 431 peptide synthesizer (Applied Biosystems; Foster City, CA) on a 0.1 mmol scale. Fmoc amino acids were obtained from Anaspec, Inc (Fremont, CA). The resin yielded the carboxyamide at the C-terminus upon cleavage. The branch point was incorporated by introducing $N^{\alpha,\varepsilon}$ di-Fmoc-L-lysine in the fifth position from the C-terminus. De-protection of the two Fmoc protecting groups led to the

generation of two reactive sites allowing for the generation of the bifurcated peptide branch point. The hydrophobic tail segments, FLIVI, FLIVIGSII, FLIVIGGII and FLIVIAAII were simultaneous coupled to the common hydrophilic oligo-lysine backbone by the stepwise addition of Fmoc amino acids to generate the respective variants.[6] The N-termini of the peptides were acetylated using Acetic anhydride / N, N-Diisopropylethylamine / 1-Hydroxybenzotriazole prior to cleavage. The peptides were cleaved from the resin using 2,2,2-Trifluoroacetic acid (TFA)/H_2O (98:2, v/v) for 90 min at RT. Each cleaved peptide product was thrice washed with diethyl ether and re-dissolved in water prior to lyophilization. The water used throughout this study is deionized, reverse osmosis treated and distilled. The RP-HPLC purified peptides were dried in vacuo and characterized using a Bruker Ultraflex III matrix-assisted laser desorption ionization time of flight mass spectrometer (MALDI TOF/TOF) (Bruker Daltonics, Billerica, MA) using 2,5-dihydroxybenzoic acid matrix (Sigma-Aldrich Corp., St. Louis, MO). The dried peptides were stored at RT.

4.2.2 Synthesis of Cysteine-Hg-Me variants for Electron Microscopy Analysis

C-terminal cysteine adducted peptides were synthesized on a 0.1mmol scale with standard Fmoc(N-(9-fluorenyl)methoxycarbonyl)/tert-butyl chemistry upon a CLEAR-Amide Resin (Peptides International Inc; Louisville, Kentucky) support. An additional N-α-Fmoc-S-p-methoxytrityl-L–cysteine (Anaspec, Inc; Fremont, CA) was coupled to the resin at C-terminus and the remainder of the synthesis, cleavage, post cleavage processing and characterization was performed as previously described (**section 4.2.1**), to generate bis(FLIVI)-K- K_4 -C-$CONH_2$ and bis(FLIVIGSII)-K- K_4-C-$CONH_2$ respectively. Both cysteine adducted peptides were solubilized in water and reacted with 1 equivalent of Methylmercury(II) iodide (Sigma-Aldrich Corp., St.

Louis, MO) at pH 9.8 for 6 h at RT[7,8]. The resulting solution was reduced using vacuum evaporation and subsequently lyophilized to generate the product. The percent methyl mercury incorporated was determined by measuring the concentration of free cysteine present after the coupling reaction. Unlabeled peptides of equal concentration served as the control. Samples were treated with 4 mg/mL Ellman's reagent (5, 5'-Dithiobis-(2-nitrobenzoic acid)) (Sigma-Aldrich Corp., St. Louis, MO) in a pH of 8.2 in 0.1 M phosphate buffer. The absorbance values of the fully reacted sample were measured at 412 nm on a CARY 50 Bio UV/Vis spectrophotometer (Varian Inc., Palo Alto, CA) using a 0.3 cm path length quartz cuvette (Starna Cells Inc., Atascadero, CA)[9]. The concentrations of the peptides were calculated using the molar extinction coefficient (ε) of phenylalanine residues (two per sequence) at 257.5 nm (195 cm^{-1} M^{-1}).[10,11]

4.2.3 BAPC formation and Encapsulation

The bis(FLIVI)-K- K_4 and bis(FLIVIGSII)-K- K_4 peptides were dissolved individually in neat 2,2,2-Trifluoroethanol. In this solvent the peptides are helical and monomeric thereby ensuring complete mixing when combined. The concentrations of all peptides were calculated using the molar extinction coefficient (ε) of phenylalanine residues (two per sequence) at 257.5 nm (195 cm^{-1} M^{-1})[10,11] on a CARY 50 Bio UV/Vis spectrophotometer (Varian Inc., Palo Alto, CA) using a 0.3 cm path length quartz cuvette (Starna Cells Inc., Atascadero, CA). The bis(FLIVI)-K- K_4 and bis(FLIVIGSII)-K- K_4 peptide samples were mixed in equimolar ratios to generate a final concentration of 0.1 mM, then dried in vacuo. The dried peptide samples were then hydrated to form capsules at desired concentration by the drop-wise addition of water. In case of BAPC formation using the bis(FLIVIGGII)-K-K_4 and bis(FLIVIAAII)-K-K_4 , the respective peptides

were used in conjunction with bis(FLIVI)-K-K_4 using the same mixing protocol outlined above. For the purposes of BAPC hydration at 4 ˚C and 37 ˚C; dried peptide samples were prepared as previously noted, and hydrated with water or eosin Y maintained at the indicated temperatures using a Heating/Cooling Fluid Circulator (IBM Corp., Armonk, New York); during the course of the experiment.

4.2.4 Sample preparation for Electron Microscopy

The 30 mole% Me-Hg capsules were prepared in a manner similar to that previously detailed, by co-dissolving 0.7 mole equivalents of bis(FLIVI)-K- K_4 and bis(FLIVIGSII)-K- K_4 with 0.3 mole equivalents of their respective cysteine containing Me-Hg labeled variants in water, to a final concentration containing 0.1 mM for each of bis(FLIVI)-K- K_4 and bis(FLIVIGSII)-K- K_4 peptides. The dried mixture was hydrated and allowed to stand for the indicated time intervals. Carbon Type A (15-25 nm) on 300-mesh support film grids with removable Formvar (Ted Pella Inc., Redding, CA) were immersed in chloroform to strip off the Formvar. These were subsequently negatively (hydrophilic) glow discharged[12] at 5 mA for 20 s using a EMS 150 ES Turbo-Pumped Sputter Coater/Carbon Coater (Electron Microscopy Sciences, Hatfield, PA) - the carbon end of the grids being exposed to the plasma discharge making the carbon film hydrophilic and negatively charged, thus allowing easy spreading of aqueous suspensions. Capsule sample solutions (6 μL) were spotted on to grids and allowed to stand for 5 min, after which excess solution was wicked off the grid with a Kimwipe™ tissue (Kimberly-Clark Worldwide Inc., Roswell, GA) and allowed to air dry before loading it into the FEI Tecnai F20XT Field Emission Transmission Electron Microscope (FEI North America, Hillsboro, Oregon) with a 0.18 nm STEM HAADF resolution and a 150X – 2306 x 106 X range of

magnification[13]. Scanning transmission electron microscopy was carried out in the annular dark field mode with a single tilt of 17°. For S/TEM analysis of BAPCs prepared using bis(FLIVIGGII)-K-K_4 and bis(FLIVIAAII)-K-K_4 peptides; the peptides were studied with 0.3 mole equivalents label of bis(FLIVI)-K- K_4-Cys-MeHg and 0.7 mole equivalents of bis(FLIVI)-K- K_4.

4.2.5 Circular Dichroism Experiments

Circular Dichroism (CD) experiments were conducted to analyze conformational changes in secondary structures formed by the BAPCs as well as individual peptides in water or 50% TFE. Data was collected on a Jasco J-815 CD spectrophotometer (Jasco Analytical Instruments, Easton, MD) using a 0.2 mm path-length jacketed cylindrical quartz cuvette (Starna Cells Inc., Atascadero, CA). Spectra were scanned from 260 nm to 190 nm at scan rate of 50 nm / min with 1 nm step intervals. Temperatures required for the experiments were maintained using a Heating/Cooling Fluid Circulator (IBM Corp., Armonk, New York) connected to the jacketed cuvette. Circular Dichrosim was measured in 'mdeg' with the final spectrum representing an average of five scans recorded. The raw data was subtracted from blank at the appropriate temperature and smoothed using a Savitsky-Golay filter[14] using Spectra Analysis® software provided by the manufacturer (Jasco Analytical Instruments, Easton, MD).

Peptide concentrations were determined using the absorbance of Phenylalanine as previously described. For experiments related to the study of capsule structure at different temperatures; 1 mM each of the individual 15mer and 23mer peptides were used for BAPC generation; whereas for the measurement of individual peptides, peptide concentration was kept at 2 mM to ensure internal consistency of all the protein samples. The analytic parameters, and total peptide

concentrations for all samples measured have been kept identical across the board for the purposes of comparison.

4.2.6 Dye Encapsulation and Measurement

1mM BAPC samples were prepared by the solvation of a dried monomeric mixture of the constituent peptides with aqueous 2.13 mM eosin Y and then allowed to stand for 30 min. Centrifugation was carried out at 14,000 x g in Amicon ultra- 0.5 mL 30 kDa molecular weight cut-off centrifugal cellulose filters (Millipore, Billerica, MA) using a Thermo Electron Legend 14 personal micro-centrifuge (Thermo Fisher Scientific Inc., Waltham, MA).Samples were subjected to three centrifugation process cycles starting with a 5 min incubation with 200 mM Na-TFA salt, and then spin filtered. The TFA^- counter-ion is successfully able to strip Eosin Y extraneously associated with the capsule surface.[4] For the second and third centrifugation cycles, the eosin encapsulating capsules were washed with water prior to centrifugation. At the conclusion of the third spin, the removable-filter unit was inverted and placed in a fresh tube and spun at 2000 x g for 5 min to recover the remaining volume containing the capsules which are then suspended in water.

Fluorescence measurement of the encapsulated content was carried out by the excitation of eosin Y (Sigma-Aldrich Corp., St. Louis, MO) at 490 nm and scanning for observed emissions from 495-800 nm with a CARY Eclipse Fluorescence spectrophotometer (Varian Inc., Palo Alto, CA) (Scan rate: 600 nm/min; PMT detector voltage: 600 V; Excitation slit: 10 nm; Emission slit: 10 nm) using a 0.3 cm path length quartz cuvette.

4.3. Results and Discussion

In a previously conducted experiment titled 'Capsule fusion study'[4] (**Chapter 2**); we employed the self-quenching fluorescence property of Eosin Y to spectroscopically study the fusion kinetics of our peptide capsules. 1 mM BAPCs encapsulating 2 mM eosin Y, were allowed to fuse with 20 mM BAPCs containing water. The fluorescence emissions were recorded as a function of time using excitation of eosin Y. The eosin concentration becomes diluted, as the few

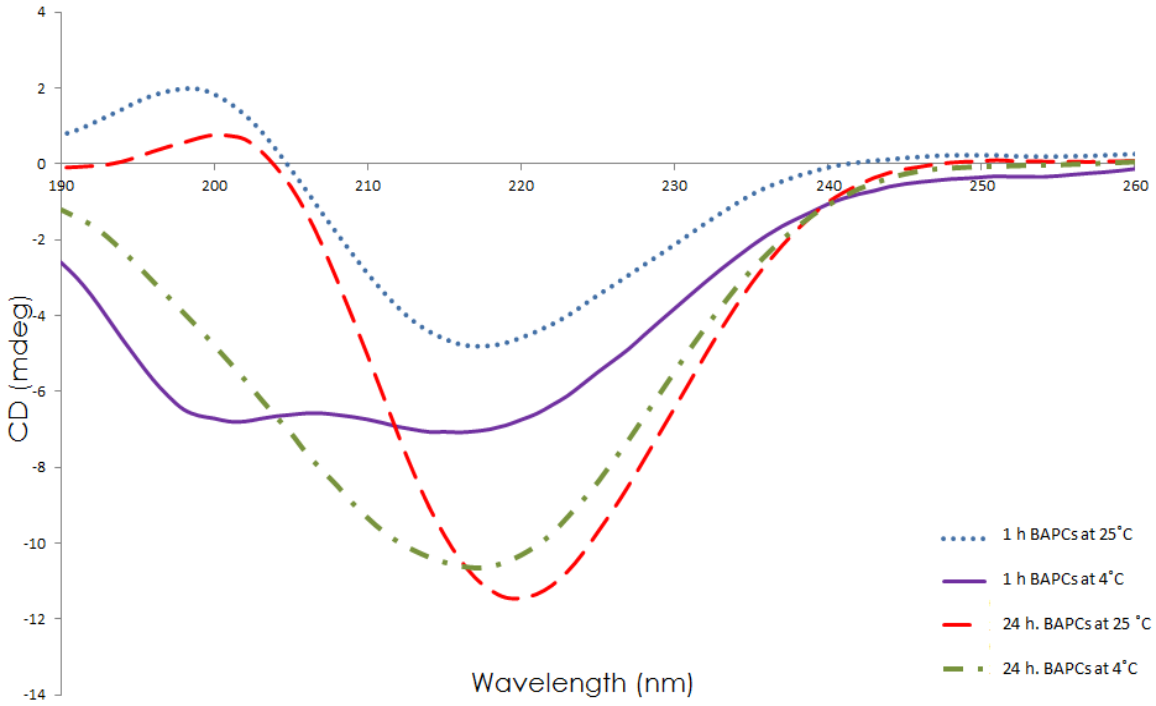

Figure 4.3 Circular Dichosim Spectra of 1 h and 24 h BAPCs at 25 ˚C and 4 ˚C.
1mM BAPCs were incubated for 1 h and 24 h respectively and then analyzed by CD at RT, before and after retaining them at 4˚C for 5 h.

eosin containing capsules fuse with the many water containing ones. Accordingly, the fluorescence intensity for eosin Y continued to rise with each fusion event as a consequence of the reduction in the dye quenching. Finally, at about 3 h from the time of commencing the experiment no further increase in the fluorescence intensity of eosin Y was observed. This was

not necessarily due to the cessation of fusion per se; but due to presence of dynamic equilibrium existing between the now normalized eosin concentrations amongst all BAPCs at that time point. However, an interesting phenomenon was observed when we tried to repeat the identical experiment a few hours later, using the same samples placed at 4 ˚C. On this occasion, the 1mM BAPCs encapsulating eosin Y kept at 4 ˚C, when mixed with 20 mM water containing BAPCs

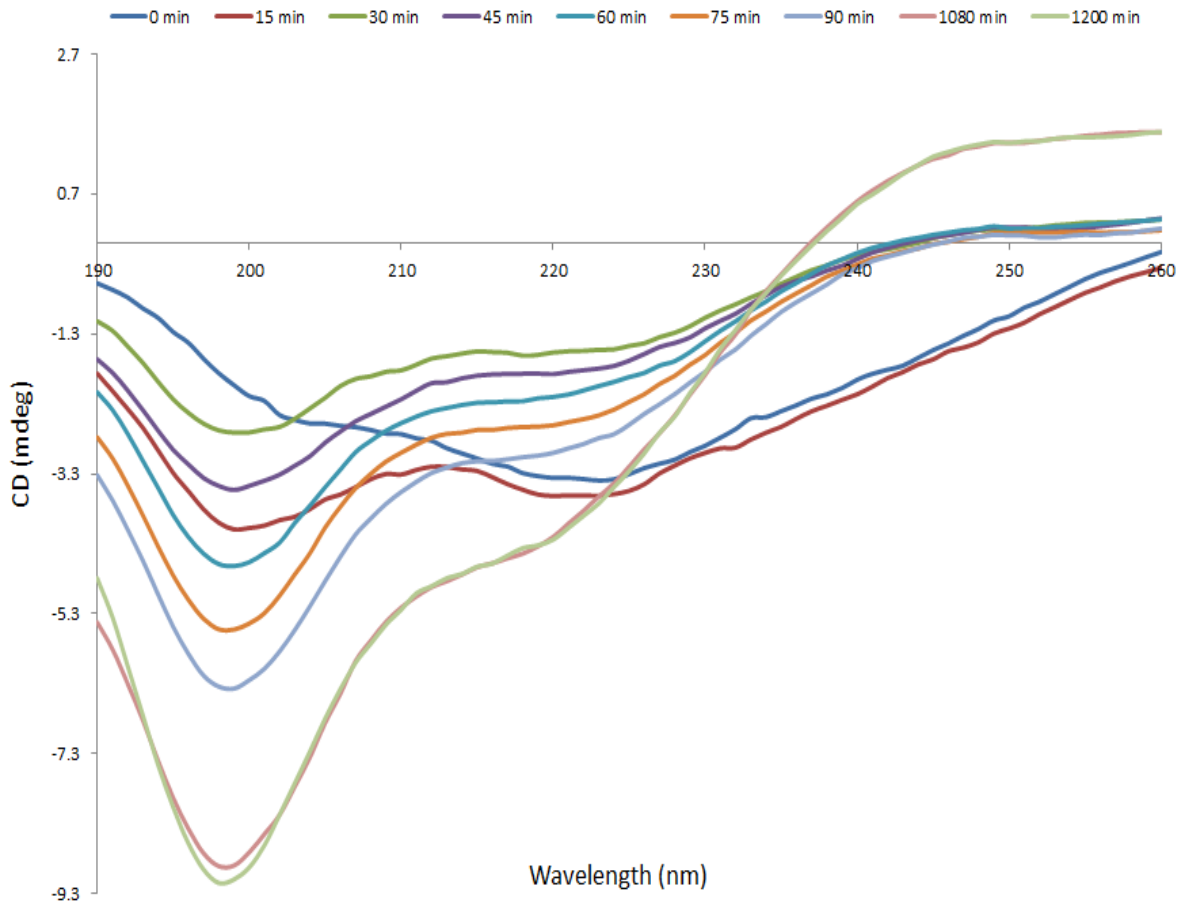

Figure 4.4 CD of BAPCs at 4 ˚C.

1mM BAPCs were hydrated at RT and incubated for 30 min prior to placing them at 4 ˚C in a jacketed cuvette and subjected to CD analysis at maintained temperature to study changes in secondary structure over a period of time.

showed no increase in fluorescence intensity. The intensity of fluorescence remained identical to that of that observed for the initial time point during the 25 ˚C experiment. Furthermore,

increasing the temperature of the system to up to 85 ˚C did not initiate the fusion process, nor did it lead to the release of the dye due to BAPC rupture - as would have been observed by a rapid increase in the fluorescence intensity due to the sudden dilution event. A Differential scanning experiment previously performed on BAPCs[1] had identified the BAPCs as constructs capable of maintaining their integrity till at least 95 ˚C. Therefore, it seems reasonable to hypothesize that the BAPCs possibly undergo some form of a temperature based conformational alteration that leads to a change in their behavioral characteristics.

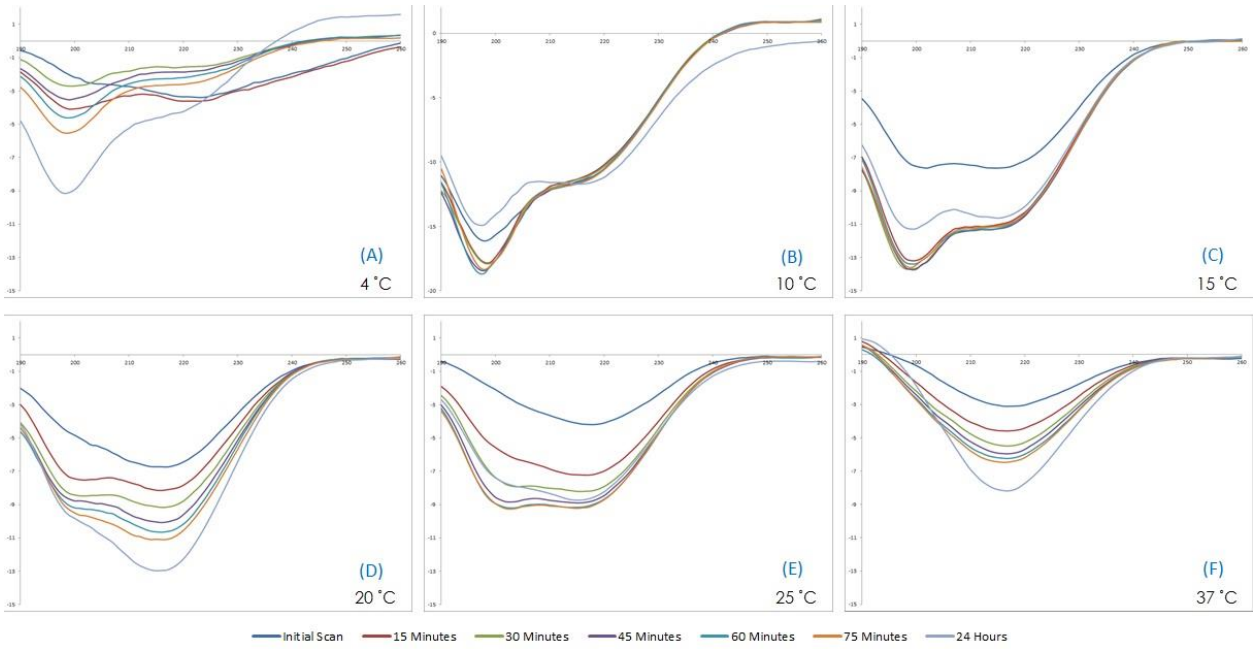

Figure 4.5 CD Spectra Scans of BAPCs at various Temperatures.

1mM BAPCs were hydrated at 25 ˚C for 30 min and CD spectra scanned after placing them at **(A)** 4 ˚C **(B)** 10 ˚C **(C)** 15 ˚C **(D)** 20 ˚C **(E)** 25 ˚C and **(F)** 37 ˚C respectively for a period of 24 h. Initial scans were recorded at 0 min, and then at 15 min, 30 min, 45 min, 60 min, 75 min and 24 h. All cans were carried out at temperatures appropriate for the respective experiment.

In an effort to verify this, we conducted a preliminary experiment where 1mM BAPCs incubated for 1 h and 24 h were analyzed for their CD spectra before and after placing them at 4 ˚C for a period of 5 h. As can be seen in **Figure 4.3** the CD spectrum for the 1 h BAPCs at 25 ˚C show a negative band at 218 nm and a positive band a 196 nm, indicative of beta structure[15,16]; a trait consistent with the behavioral characteristics of our constituent

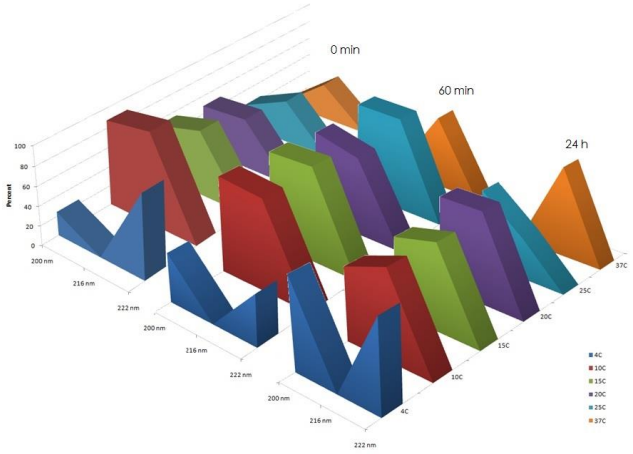

Figure 4.6 Graphical Representation of Change in CD of BAPCs at different temperatures as a function of time. Absolute values at 200, 216 & 222 nm for different temperature scans taken as a percent of the global absolute minima values for the respective wavelengths.

peptides. However, when these capsules were subjected to 4 ˚C we observed a substantial change in the CD spectra. Apart from the negative band at 218 nm, there emerged another negative band at 200 nm coupled with the disappearance of the positive band at 196 nm. In case of the 24 h BAPCs at 25 ˚C, the beta character was retained albeit with a decrease in the value of the negative band and a slight shift of the minima from 218 nm to 217 nm. The 24 h BAPCs at 4 ˚C closely followed the spectral pattern of that of the 1 h BAPCs at 25 ˚C; however with decreased minima at 218 nm accompanied by the disappearance of the positive band at 196 nm. This clearly indicated the presence of a temperature based conformational variation within the BAPCs. Eosin Y encapsulation experiments with BAPCs conducted under this set of conditions (data not shown) showed no release of dye, indicating that the BAPCs retained their structural integrity during this process. Since some of the more drastic alterations were seen with BAPCs incubated for shorter periods of time we postulated that the propensity for conformational alteration is more prevalent in early BAPCs. Consequently, BAPCs incubated for 30 min at 25 ˚C were used for carrying out temperature secondary structure analysis.

A CD experiment was conducted to observe the changes in the secondary structure of BAPCs over a period of time after placing them at 4 ˚C. This revealed (**Figure 4.4**) the almost instantaneous generation of the 198 / 222 nm minima band, which within 30 min gave rise to a

spectral curve with a pronounced negative band at 198 nm coupled with a greatly diminished negative band at 222 nm. Thereafter, the intensity of the 198 nm negative band continued to increase throughout the course of the experiment until it more of less stabilized at the 20 h mark. It is important to note that within the first 30 min of the 4 ˚C treatment the spectral pattern had been defined and this did not vary throughout the remainder of the experiment. This trait remained consistent when we carried out a more comprehensive experiment where we assessed the changes in circular dichroism over a period of 24 h at 4, 10, 15, 20, 25 and 37 ˚C respectively. The results of that experiment are seen in **Figure 4.5**. As is seen, a decrease in temperature led to the shifting of the spectral minima bands towards lower wavelength suggesting perhaps a transition to a coil like intermediate. However the propensity of the minima bands to gravitate to a higher wavelength upon increase in temperature seemed to indicate the presence of a structure beyond the resolution capabilities of circular dichroism. The spectra were distinctive in that few or no positive bands were observed during the course of the experiments. Incubation at 37 ˚C generated a single negative band at 222 nm which, as seen consistently with all the other temperatures, continued to decrease with time until equilibrium was reached by 24 h. Since the CD spectral patterns of temperature based conformational changes did not suggest any one structural motif, a 3-D graphic representation was generated to aid in visualizing the changes observed at the different temperatures as a function of time. The representations show the absolute values of the spectral data points (no positive bands were seen), and the absorbance values at 200 nm, 216 nm and 222 nm (these being the ternary wavelengths where a spectral change, if any, was always seen) as a percentage of the absolute global minima seen at those values for the collective temperature experiments. The changes observed at 0 and 60 min and 24 h for all temperatures are shown in **Figure 4.6**. This figure illustrates that - within the range of

the temperatures scanned - changes observed at 4 ˚C and 37 ˚C represent distinct states, with the conformational spectra at the remaining temperatures being intermediary.

To find out if BAPC assembly is feasible at 4 ˚C and 37 ˚C, we decided to conduct dye encapsulation experiments. As before, 1 mM of bis(FLIVI)-K- K_4 and bis(FLIVIGSII)-K- K_4 were mixed in equimolar concentrations in 100% TFE, dried and then solvated with a 2 mM solution of Eosin Y at 4 ˚C and 37 ˚C respectively. The contents were then spin filtered and stripped of any external surface-bound dye and re-suspended in water (**section 4.2.6**) before measuring the extent of dye encapsulation using the fluorescence of eosin Y. BAPCs were

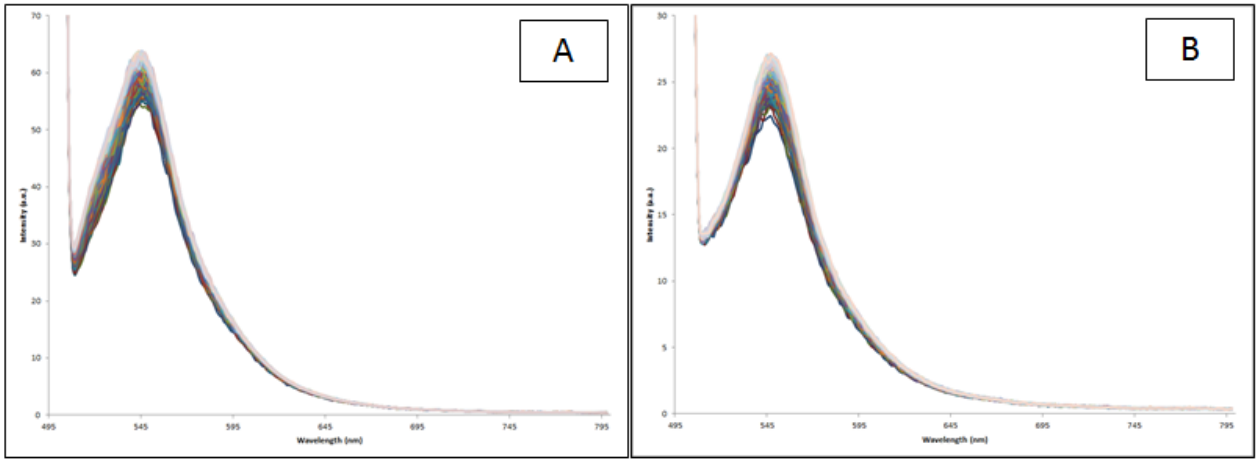

Figure 4.7 BAPC fusion study at 4 ˚C and 37 ˚C.

Salt washed eosin Y encapsulating BAPCs hydrated at 4 ˚C and 37 ˚C were mixed with water filled BAPCs in the ratio of 1:20 at 4 ˚C and 37 ˚C respectively. All BAPCs were prepared at their respective experimental temperatures which were maintained during the course of the experiment. **A)** BAPC fusion at 4 ˚C with each scan representing an interval of 10 min read over 8 h **B)** BAPC fusion at 37 ˚C with each scan representing an interval of 5 min over 4 h.

maintained at the respective experimental temperatures throughout the course of the experiment. The fluorescence intensity values obtained from BAPC encapsulation experiments at 4 and 37 ˚C were comparable to those obtained at 25 ˚C (data not shown) indicating that BAPCs do assemble at these particular temperatures although, as characterized by the CD data, they exist in different conformational states. We thought that an increase in temperature would kinetically drive the rate of BAPC fusion. We carried out fusion experiments to calculate the rate of fusion for

BAPCs hydrated at 4 and 37 ˚C, analogous to the ones carried out for BAPC fusion at 25 ˚C (**Chapter 2**). BAPCs (1 mM) encapsulating 2 mM Eosin Y at 4 ˚C and 37 ˚C were mixed with 20 mM water-filled BAPCs at 4 and 37 ˚C, respectively. Temperatures were maintained throughout the process of hydration, washing, assembly and fusion steps. Eosin excitation scans were carried out every 5 min for 37 ˚C experiments over 4 h and every 10 min for 4 ˚C for 8 h.

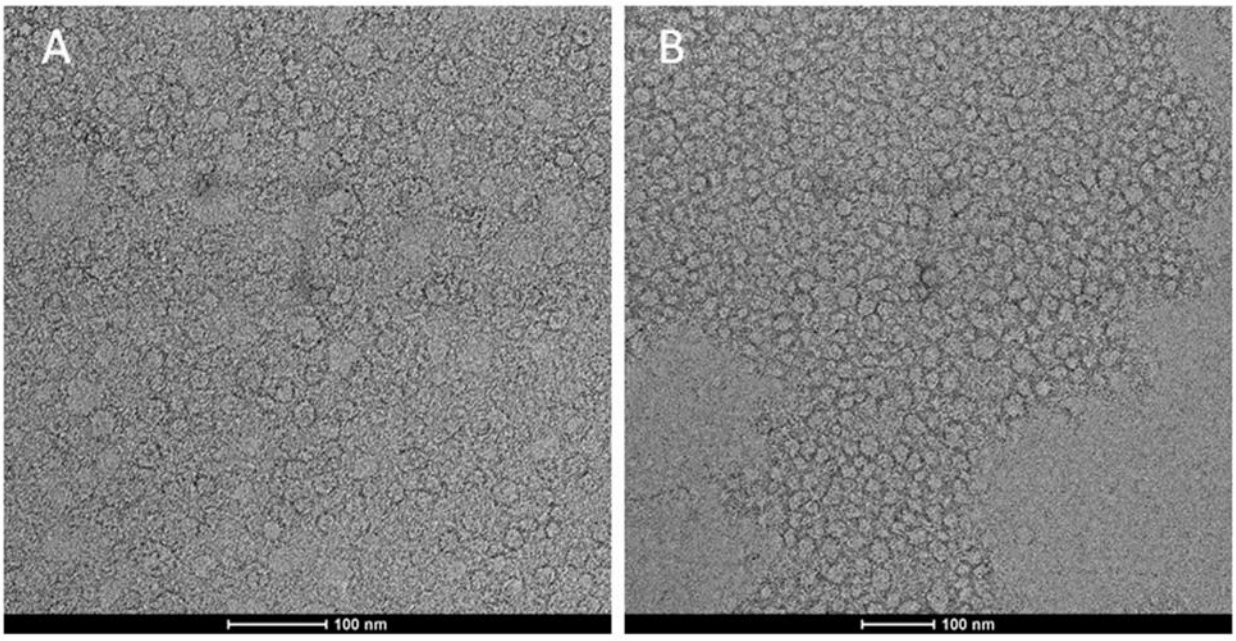

Figure 4.8 Transmission Electron Microscopy Images elucidating the Temperature Dependence on BAPC Fusion
0.1 mM BAPCs with 30% Hg label on bis(FLIVI)-K- K_4 were hydrated and incubated at 4 ˚C and 37 ˚C respectively for 30 min. Samples were spotted on grids and stained with 2% Uranyl Acetate prior to imaging. **A)** BAPCs hydrated at 4 ˚C and **B)** BAPCs hydrated at 37 ˚C. Scale bar represents 100 nm.

Eosin Y dilution as a consequence of fusion was expected to lead to an increase in fluorescence intensity over time. However, we found no significant change in the fluorescence intensity for either temperature (**Figure. 4.7**).

In order to visually determine these processes, we carried out electron microscopy analysis of these samples. For the purposes of these experiments, 0.1 mM BAPCs labeled with 30% Me-Hg on the bis(FLIVI)-K- K_4 were prepared at 4 and 37 ˚C respectively and spotted on sample grids

as described in Section 2.4. The representative TEM images of the experiment are shown in **Figure 4.8**. We discovered that both 4 and 37 ˚C BAPCs were seen to appear as uniform 20 - 30 nm diameter capsules at 30 min. If temperature induced kinetic factors were playing a role in BAPC fusion we should have seen larger BAPCs for the 37 ˚C experiment, as opposed to the 4 ˚C one. However, no such distinction was seen. On the contrary, the 4 ˚C BAPCs as a whole appeared to be slightly larger than those seen for the 37 ˚C experiment. Moreover, unlike BAPC fusion experiments carried out at 25 ˚C; no BAPCs were observed in the process of fusion.[4] This seemed to indicate that the fusogenic properties of BAPCs at these temperatures were not kinetically driven; but restricted by their conformation.

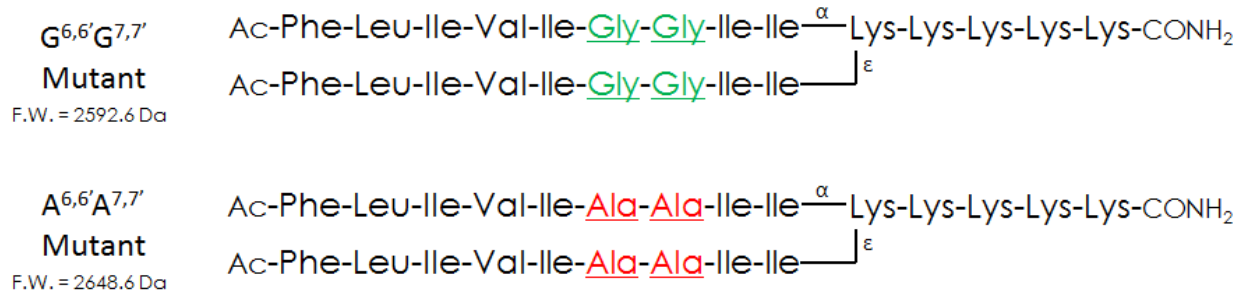

Figure 4.9 Mutant, branched amphiphilic peptide sequence variants.
$G^{6,6'}G^{7,7'}$ and $A^{6,6'}A^{7,7'}$ variants of bis(FLIVIGSII)-K-K_4 peptide were designed, where the Ser-Gly residues on the 6th and 7th positions of both the branches were substituted with Gly-Gly and Ala-Ala respectively, to generate stronger and weaker beta conformers of the parent sequence.

BAPCs are comprised of peptides that reversibly form beta sheets in water, and alpha helices in TFE.[1] The factors that contribute towards the formation of beta sheets are not fully understood. Consequently, there exist no well-defined rules to predict beta-sheet formation.[17] Nonetheless, like any other structural conformation in proteins beta sheet formation is governed by the intrinsic beta sheet propensities of the amino acids as well as by side chain-side chain interactions across the beta strands. Since, our objective was to understand the factors contributing to thermally induced conformation changes; it seemed obvious to assess the effect

of temperature on the peptide residues that contribute to its secondary structure. Preliminary IR analysis conducted on BAPCs at 4 ˚C showed absorption at 1634 cm^{-1} suggesting the presence of a β-hairpin.[18] Glycine is the most flexible amino acid in the peptide sequence and would therefore constitute a potential site to study for its contribution to beta sheet formation. Experiments carried out on polypeptide models have indicated that the 'Glycine-Serine' residues contribute to the stabilization of β-turn motifs.[19,20] In order to study the contribution of the 'Gly-Ser' residue to the conformational malleability bis(FLIVIGSII)-K-K_4 peptide, we designed two new mutant sequences - bis(FLIVIGGII)-K-K_4, a branched amphiphilic peptide that would exhibit a tighter beta turn, and bis(FLIVIAAII)-K-K_4, a peptide that would exhibit a weaker beta turn (**Figure 4.9**).[20,21,22]

The peptides bis(FLIVI)-K-K_4, bis(FLIVIGSII)-K-K_4 bis(FLIVIAAII)-K-K_4 and bis(FLIVIGGII)-K-K_4 were analyzed using Circular Dichroism, at 4, 25 and 37 ˚C to assess the effect of temperature on the secondary structure of these sequences as described previously. The spectrum in **Figure 4.10A** shows the least amount of thermal variability across all three temperatures and also the highest propensity towards a coil structure. This would be expected from the bis(FLIVI)-K-K_4 sequence as it is composed of only 15 residues and does not contain the Gly-Ser residues that we believe are responsible for generating the beta conformer. The contribution of temperature towards a beta structure is evident in **Figure 4.10B, 4.10C** and **4.10D** where the increase in beta character is evident in samples measured at 37 ˚C versus 25 ˚C. The bis(FLIVIGGII)-K-K_4 mutant (**Figure 4.10D**) shows the greatest degree of beta character at 25 and 37 ˚C , due to the presence of the turn inducing Gly-Gly residues.[23] The bis(FLIVIAAII)-K-K_4 mutant (**Figure 4.10C**) does shows beta character at 25 and 37 ˚C, but with broader negative minima bands. This is indicative of that fact that although the Ser-Gly residues in the

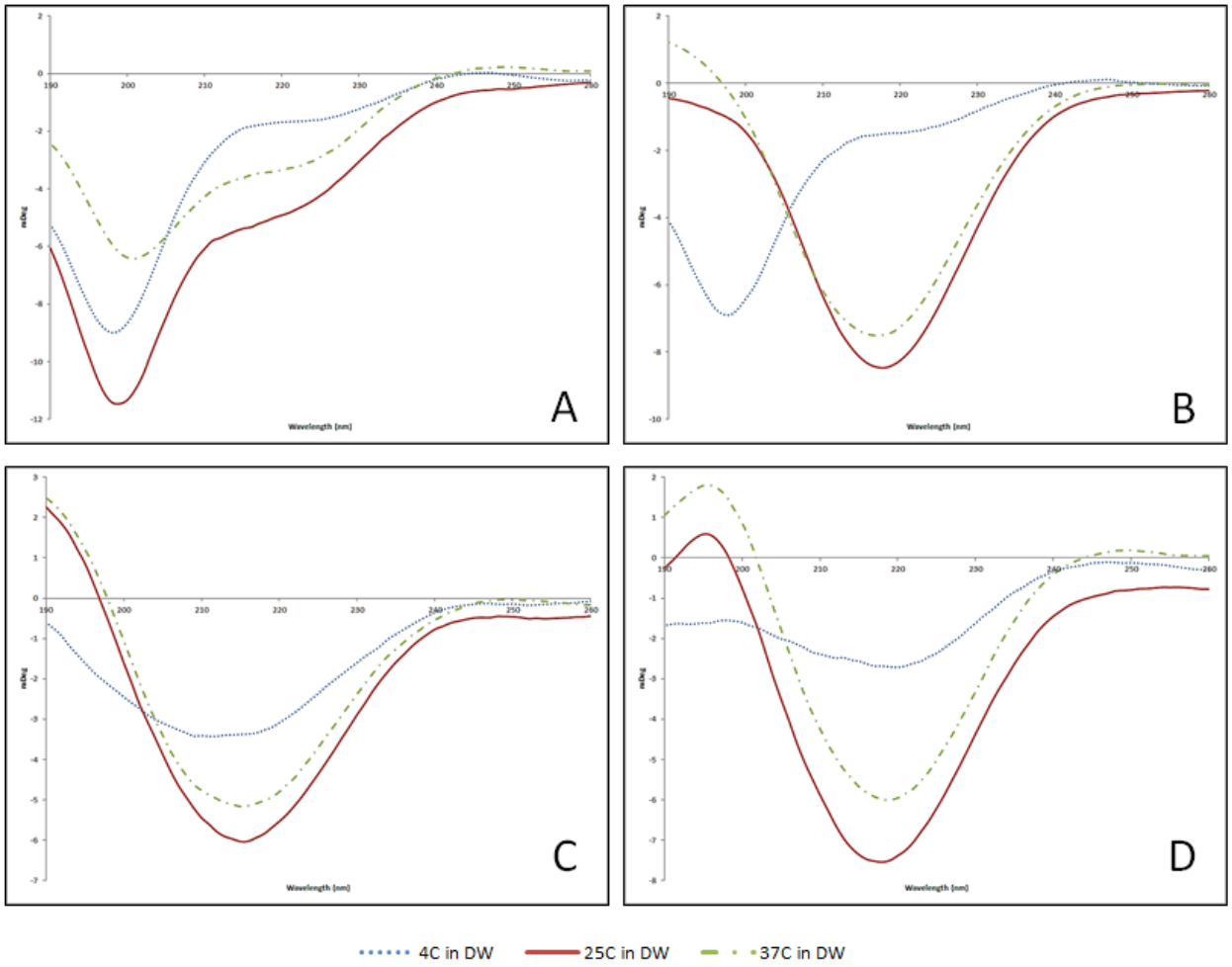

Figure 4.10 - CD Spectra of Branched Amphiphilic Peptides at 4, 25 and 37 ˚C.

2 mM concentrations of **A)** bis(FLIVI)-K-K_4 **B)** bis(FLIVIGSII)-K-K_4 **C)** bis(FLIVIAAI)-K-K_4 **D)** bis(FLIVIGGII)-K-K_4 in water at 4 ˚C, 25 ˚C and 37 ˚C

parent sequence do contribute to the formation of the beta conformers; there are undoubtedly other residual, steric and electrostatic forces within these branched sequences that enable the Ala-Ala mutant to form beta-like structures. The bis(FLIVIAAII)-K-K_4 mutant does however show the least amount of secondary structure variation between 25 and 37 ˚C suggesting the temperature based variations within this range have partly to do with the presence of turn forming residues in the 6^{th} and 7^{th} positions. The transition to 4 ˚C brings about a loss of β-structure in all studied sequences. This suggests that factors other than the turn forming residues contribute to this transition. For if the Ser-Gly turn residues exclusively dictated the beta

character, then the weaker Ala-Ala mutant should not have demonstrated a loss of beta conformation at 4 ˚C; and alternately the stronger Gly-Gly mutant should have retained its β-structure at all studied temperatures. Whereas a loss of beta-character is apparent in all three 23mer sequences (**Figure 4.10B**, **4.10C** and **4.10D**) at 4 ˚C; it is only the parent sequence - bis(FLIVIGSII)-K-K_4 that shows a transition from a classic beta, to a coil like structure almost identical to that observed with bis(FLIVI)-K-K_4 at the same temperature. This transition driven by the presence of the 'Ser-Gly; residues at the 6,6' and the 7,7' positions provides for a common conformational denominator to both the sequences. And it is this structural commonality that allows for synergistic association between the bis(FLIVIGSII)-K-K_4 and bis(FLIVI)-K-K_4 sequences which enables the BAPCs to seamlessly transition from one state to another. This might account for why bis(FLIVIGSII)-K-K_4 and bis(FLIVI)-K-K_4 make successful sequence pairs for BAPC formation. The transformation into a conformationally homogeneous random coil construct at low temperatures might account for the abrogation of fusion at 4 ˚C implying that it is the conformational characteristics of the bis(FLIVIGSII)-K-K_4 that are the fundamental driving force behind BAPC fusion.

4.4 Abbreviations

BAPCs, Branched Amphiphilic Peptide Capsules; TFE, 2,2,2 - Trifluoroethanol; CD, Circular Dichroism Spectroscopy; S/TEM, Scanning Transmission Electron Microscopy; EM, Electron Microscopy.

4.5 Acknowledgement

This is publication **xx-xxx-x** from the Kansas Agricultural Experiment Station. We would like to thank, Dr. David Moore and Dr. Prem Thapa at the University of Kansas Microscopy and Analytical Imaging Laboratory, for electron microscopy studies and Mark Boatwright Department of Biochemistry and Molecular Biophysics, Kansas State University for IR studies.

4.6 References

1 Gudlur, S., Sukthankar, P., Gao, J., Avila, L.A., Hiromasa, Y., Chen, J., Iwamoto, T. and Tomich, J.M. (2012) Peptide nanovesicles formed by the self-assembly of branched amphiphilic peptides. *PLoS One.* **7**, e45374

2 Grove, A., Tomich, J.M., Iwamoto, T. and Montal, M. (1993) Design of a functional calcium channel protein: inferences about an ion channel-forming motif derived from the primary structure of voltage-gated calcium channels. *Protein Sci.* **2**, 1918-1930

3 Sukthankar, P., Avila, L.A., Whitaker, S.K., Iwamoto, T., Morgenstern, A., Apostolidis, C., Liu, K., Hanzlik, R.P., Dadachova, E. and Tomich, J.M. (2014) Branched amphiphilic peptide capsules: Cellular uptake and retention of encapsulated solutes. *Biochim.Biophys.Acta.* **1838** (9), 2296-305

4 Sukthankar, P., Gudlur, S., Avila, L.A., Whitaker, S.K., Katz, B.B., Hiromasa, Y., Gao, J., Thapa, P., Moore, D., Iwamoto, T., Chen, J. and Tomich, J.M. (2013) Branched oligopeptides form nanocapsules with lipid vesicle characteristics. *Langmuir.* **29,** 14648-14654

5. Kempe M. and Barany G. (1996) CLEAR: A Novel Family of Highly Cross-Linked Polymeric Supports for Solid Phase Synthesis, *J. Am. Chem. Soc.* **118**, 7083-7093.

6. Iwamoto, T., Grove, A., Montal, M.O., Montal, M. and Tomich, J.M. (1994) Chemical synthesis and characterization of peptides and oligomeric proteins designed to form transmembrane ion channels. *Int. J. Pept Protein Res.* **43**, 597-607.

7 Gruen, L.C. (1970) Stoichiometry of the reaction between methyl mercury (II) iodide and soluble sulphides. *Anal. Chim. Acta.* **50**: 299-303.

8 Forbes W.F., Hamlin C.R. (1968) Determination of –SS and –SH groups in proteins. I. A reassessment of the use of methylmercuric iodide. *Canadian Journal of Chemistry*. **46**, 3033-3040.

9 Anderson, W.L., Wetlaufer, D.B. (1975) A new method for the disulfide analysis of peptides. *Analyt. Biochem.* **67**, 493-502

10 Chen, R. F. (1972) Measurements of absolute values in biochemical fluorescence spectroscopy. *J Res Natl. Bureau Standards* **76A**(6), 593-606.

11 Sponer H. (1942) Remarks on the Absorption Spectra of Phenylalanine and Tyrosine in Connection with the Absorption in Toluene and Paracresol. *J Chem Phys.* **10**,672.

12 Aebi, U. and Pollard, T.D. (1987) A glow discharge unit to render electron microscope grids and other surfaces hydrophilic. *J. Electron Microsc. Tech.* **7**, 29-33.

13 Utsunomiya, S. and Ewing, R.C. (2003) Application of High-Angle Annular Dark Field Scanning Transmission Electron Microscopy, Scanning Transmission Electron Microscopy-Energy Dispersive X-ray Spectrometry, and Energy-Filtered Transmission Electron Microscopy to the Characterization of Nanoparticles in the Environment. *Environ. Sci. Technol.* **37**, 786-791.

14 Savitzky, A. and Golay, M.J.E. (1964) Smoothing and Differentiation of Data by Simplified Least Squares *Procedures. Anal. Chem.* **36**, 1627-1639

15 Yang, J.T., Wu, C.C. and Martinez, H.M. [11] Calculation of protein conformation from circular dichroism in Methods in Enzymology. Vol.130, pp.208-269, Academic Press.

16 Woody, R.W. [4] Circular dichroism in Methods in Enzymology. Vol. 246, pp.34-71, Academic Press.

17 Hughes, R.M. and Waters, M.L. (2006) Model systems for β-hairpins and β-sheets. *Curr. Opin. Struct. Biol.* **16**, 514-524

18 Hollosi, M., Majer, Z., Ronai, A.Z., Magyar, A., Medzihradszky, K., Holly, S., Perczel, A. and Fasman, G.D. (1994) CD and Fourier transform ir spectroscopic studies of peptides. II. Detection of beta-turns in linear peptides. *Biopolymers*. **34**,177-185

19 Matsushima, N., Yoshida, H., Kumaki, Y., Kamiya, M., Tanaka, T., Izumi, Y. and Kretsinger, R.H. (2008) Flexible structures and ligand interactions of tandem repeats consisting of proline, glycine, asparagine, serine, and/or threonine rich oligopeptides in proteins. *Curr. Protein Pept. Sci.* **9**, 591-610

20 Blanco, F., Ramirez-Alvarado, M. and Serrano, L. (1998) Formation and stability of beta-hairpin structures in polypeptides. *Curr. Opin. Struct. Biol.* **8**, 107-111

21 Rose, G.D., Gierasch, L.M. and Smith, J.A. (1985) Turns in peptides and proteins. *Adv. Protein Chem*. **37**, 1-109

22 Chou, P.Y. and Fasman, G.D. (1977) Beta-turns in roteins. *J. Mol. Biol.* **115**, 135-175

23 Wilmot, C.M. and Thornton, J.M. (1988) Analysis and prediction of the different types of beta-turn in proteins. *J. Mol. Biol.* **203**, 221-232

Chapter 5 - Significance, Future Directive and Other Studies

The material that has gone into constituting this thesis is but a cohesive fraction of the research that I have undertaken into designing and understanding the nature of peptide based biomaterials.

BAPCs constitute a new and exciting class of nanocarriers constituted exclusively from peptides. The capabilities of these capsules stem from the unique properties of their constituent sequences that can transition from an alpha helix in trifluoroethanol to a beta sheet in water. BAPCs are non-immunogenic and biocompatible. They are analogous to liposomes in that they possess a bilayer and that they fuse and can be re-sized by membrane extrusion. Their flexibility and their ability to be re-sized and maintained at a desired size, makes them attractive candidates for drug delivery. *In vitro* and *in vivo* experiments described in this report indicate that BAPCs are readily taken up by cells, escape and/or evade the endocytotic pathways and accumulate in the peri-nuclear region of the cell for extended durations of time without apparent degradation.

We have demonstrated the capabilities of these constructs to encapsulate small solutes and proteins; and transport them into the cell. BAPCs - unlike liposomes - are remarkably stable and can maintain their integrity in the face of alpha particle bombardment. This portends potential applications in radionuclide based therapy, which is plagued by the lack of suitable stable carriers for encapsulating radioactive agents. However, it is this extraordinary stability of the BAPCs and their inability to extravasate their cargo limits them from being used as nano-carriers for conventional drug delivery, in their current configuration. We have conducted biophysical investigations and identified structural parameters within the sequence that contribute to some of the characteristics that imbue these peptide-capsules with their remarkable properties.

A better understanding into the nature of these BAPCs and their bilayer can enable us to design variants that could help us selectively de-stabilize these capsules in cells thus enhancing their cargo release potential. One of the unique properties of the BAPCs is their tune-ability. The incorporation of peptide variants into the capsular constitution could be another way to modulate BAPC behavior. We have designed a set of peptide sequences that have shown promise in their ability to form temperature sensitive capsules with varying stabilities, and further investigation is in progress. Work is also ongoing on the development of branched amphiphilic sequences with varying lengths to modulate the initial size of assembly that governs the maximum size of the cargo capable of encapsulation. Much needs to be understood about the nature of the BAPC bilayer. I have designed 'Fluorine and ^{13}C' incorporating variants of the BAPC sequences to make them suitable for the purposes of REDOR NMR analysis and collaborations to that effect are being pursued with Prof. Frances Separovic, Department of Chemistry, University of Melbourne.

The mode of BAPC cellular uptake and internalization is another area worthy of exhaustive investigation. The availability of ε-Lysine amino groups on the surface of these capsules makes BAPCs ideal for the purposes of functionalization. We have till date managed to attach small dye molecules as well as methyl-mercury on to some of these sites and see no reason why molecular markers, ligands and antibodies couldn't be attached for the purposes of targeted therapy. The self-assembling nature of BAPCs means that a selected mole percentage of sequences pre-ligated with targeting moieties could be incorporated into the capsule in a simple and efficient process prior to assembly. The fact that the constituent peptides can be made readily available in large quantities with high purity; and that BAPC assembly is spontaneous and easy, makes them suitable candidates for scalable therapeutic and pharmaceutical applications.

The peptides that make up the BAPCs also constitute a novel class of biomaterial. We have been able to develop a procedure to solubilize these peptides in toluene. This has widened the applications of these peptides by making them available to the diverse realm of non-aqueous organic chemistries. In collaboration with Prof. Christopher Sorensen, Department of Physics, Kansas State University, we have managed to coat a mono-layer of branched amphiphilic peptides onto gold nano-particles; in effect turning them into aqueous colloidal suspensions. BAPCs adumbrate great potential as singular, biologically inspired constructs with prospects for applications and scientific investigation. A lot remains to be asked and a lot remains to be done.

Apart from my work on BAPCs, I have also had the pleasure of working with numerous other investigators in the area of organic chemistry and peptide synthesis. I owe a lot to Prof. Stefan Bossmann, Department of Chemistry, Kansas State University for allowing me to work in his lab on the generation of NIPAM-AA co-polymers and for providing me valuable insight in the area of organic syntheses. In collaboration with Prof. Kanost, Department of Biochemistry and Molecular Biophysics, Kansas State University, I have managed to develop a *de novo* procedure for total chemical synthesis of a biotinylated glycolate ester used for isolating free N-termini proteins from serum; and developed variants thereof for the purposes of process efficiency. For Dr. Kristin Michel, Divison of Biology, Kansas State University; I have developed a gentle procedure to increase the yield efficiency of aromatic amino to nitro conversions of p-Phenylenediamines coupled to the C-terminus of peptides in solution, and have synthesized bacterial cyclic esters for Prof. Lynn Hancock, Department of Molecular Biosciences, University of Kansas, that have shown high activity *in vitro*. I hope that over time, some or more of these projects would yield valuable contributions to the field of scientific inquiry.